PB83-107482

Considerations in Selecting Conveyors for Solid Waste Applications

National Center for Resource Recovery, Inc.
Washington, DC

Prepared for

Municipal Environmental Research Lab.
Cincinnati, OH

Sep 82

U.S. Department of Commerce
National Technical Information Service
NTIS

EPA-600/2-82-082
September 1982

PB83-107482

CONSIDERATIONS IN SELECTING CONVEYORS FOR SOLID WASTE APPLICATIONS

by

Zahid Khan
Marc L. Renard
Jay Campbell
National Center for Resource Recovery, Inc.
Washington, D.C. 20036

6-1/2"
9-1/8"

Grant No. R806709

Project Officer

Carlton C. Wiles
Solid and Hazardous Waste Research Division
Municipal Environmental Research Laboratory
Cincinnati, Ohio 45268

MUNICIPAL ENVIRONMENTAL RESEARCH LABORATORY
OFFICE OF RESEARCH AND DEVELOPMENT
U.S. ENVIRONMENTAL PROTECTION AGENCY
CINCINNATI, OHIO 45268

BEGIN LAST LINE OF TEXT
BOTTOM OF IMAGE AREA; OUTSIDE DIMENSION FOR TABLES AND ILLUSTRATIONS
3/8"

REPRODUCED BY
NATIONAL TECHNICAL
INFORMATION SERVICE
U.S. DEPARTMENT OF COMMERCE
SPRINGFIELD, VA 22161

EPA-287 (Cin.)
(4-76)

TECHNICAL REPORT DATA
(Please read Instructions on the reverse before completing)

1. REPORT NO. EPA-600/2-82-082	2.	3. RECIPIENT'S ACCESSION NO. PB83 107482
4. TITLE AND SUBTITLE CONSIDERATIONS IN SELECTING CONVEYORS FOR SOLID WASTE APPLICATIONS		5. REPORT DATE September 1982 6. PERFORMING ORGANIZATION CODE
7. AUTHOR(S) Zahid Khan, Marc L. Renard, and Jay Campbell		8. PERFORMING ORGANIZATION REPORT NO.
9. PERFORMING ORGANIZATION NAME AND ADDRESS National Center for Resource Recovery, Inc. 1211 Connecticut Avenue, SW Washington, DC 20036		10. PROGRAM ELEMENT NO. 11. CONTRACT/GRANT NO. R806709
12. SPONSORING AGENCY NAME AND ADDRESS Municipal Environmental Research Lab-Cinti, OH Office of Research and Development U.S. Environmental Protection Agency Cincinnati, OH 45268		13. TYPE OF REPORT AND PERIOD COVERED 14. SPONSORING AGENCY CODE EPA/400/14

15. SUPPLEMENTARY NOTES

Project Officer: Carlton C. Wiles (513) 684-7871

16. ABSTRACT

An engineering evaluation and experimental program involving several types of conveyors applied to processed fractions of municipal solid wastes was conducted by the National Center for Resource Recovery. This final project report discusses the properties and characteristics of waste affecting conveyability and presents experimentally determined values or observed characteristics. A procedure is developed for the selection, assessment and operation of belt conveyors based on spillage rate. Corroborating experimental results from a recirculating test rig operated with six waste fractions over a range of belt configurations, velocities and flow rates are presented. Experiments conducted on a vibrating pan conveyor with six feedstocks and over a range of frequencies and stroke length, and on a small apron conveyor (batch basis on two feedstocks), are described and the test results analyzed.

The development of an approach, a test plan and preliminary test rig equipment, design and costing for a pneumatic conveying system were part of this project, but are reported in a separately bound report.

17. KEY WORDS AND DOCUMENT ANALYSIS

a. DESCRIPTORS	b. IDENTIFIERS/OPEN ENDED TERMS	c. COSATI Field/Group

18. DISTRIBUTION STATEMENT	19. SECURITY CLASS *(This Report)*	21. NO. OF PAGES 134
	20. SECURITY CLASS *(This page)*	22. PRICE

EPA Form 2220-1 (Rev. 4-77) PREVIOUS EDITION IS OBSOLETE

NOTICE

Mention of trade names or commercial products does not constitute endorsement or recommendation for use.

FOREWORD

The Environmental Protection Agency was created because of increasing public government concern about the dangers of pollution to the health and welfare of the American people. Noxious air, foul water and spoiled land are tragic testimony to the deterioration of our natural environment. The complexity of that environment and the interplay between its components require a concentrated and integrated attack on the problem.

Research and development is that necessary first step in problem solution and it involves defining the problem, measuring its impact, and searching for solutions. The Municipal Environmental Research Laboratory develops new and improved technology and systems for the prevention, treatment and management of wastewater and solid and hazardous waste pollutant discharges from municipal and community sources, for the preservation and treatment of public drinking water supplies, and to minimize the adverse economic social, health and aesthetic effects of pollution. This publication is one of the products of that research; a most vital communications link between the research and the user community.

A number of the new municipal waste processing facilities have experienced conveying and material handling problems during start-up and full operation. One reason is the lack of data on waste properties and interrelationships between equipment operating parameters. This publication reports on the first systematic investigation of conveyors applied to the municipal waste and its processed fractions. The approaches, procedures and data developed in this program should be of great interest to designers and operators of municipal waste processing plants.

The cooperation and support of the Engineering and Services Laboratory, Headquarters Air Force Engineering and Services Center, Tyndall Air Force Base, Florida, who participated with EPA in later portions of this program are acknowledged.

Francis T. Mayo, Director
Municipal Environmental
Research Laboratory

BEGIN LAST LINE OF TEXT
BOTTOM OF IMAGE AREA; OUTSIDE DIMENSION FOR TABLES AND ILLUSTRATIONS
3/8"

ABSTRACT

An engineering evaluation and experimental program involving several types of conveyors applied to processed fractions of municipal solid wastes was conducted by the National Center for Resource Recovery. This final project report discusses the properties and characteristics of waste affecting conveyability and presents experimentally determined values or observed characteristics. A procedure is developed for the selection, assessment and operation of belt conveyors based on spillage rate. Corroborating experimental results from a recirculating test rig operated with six waste fractions over a range of belt configurations, velocities and flow rates are presented. Experiments conducted on a vibrating pan conveyor with six feedstocks and over a range of frequencies and stroke length, and on a small apron conveyor (batch basis on two feedstocks), are described and the test results analyzed.

The development of an approach, a test plan and preliminary test rig equipment, design and costing for a pneumatic conveying system were part of this project, but are reported in a separately bound report.

These two reports were submitted in fulfillment of Grant No. R80679091 by the National Center for Resource Recovery, Inc., under sponsorship of the Environmental Protection Agency. These reports cover the period June 1979 through October 1980.

8-1/2"
9-1/8"
BEGIN LAST LINE OF TEXT
BOTTOM OF IMAGE AREA; OUTSIDE DIMENSION FOR TABLES AND ILLUSTRATIONS
3/8"

PAGE NUMBER
EPA-287 (Cin.)
(4-76)

BEGIN
FIRST
LINE OF
TEXT
HERE

TYPING GUIDE SHEET

CENTER
OF PAGE

TOP OF
IMAGE

CONTENTS

Foreword iii
Abstract iv
Figures viii
Tables xii
Acknowledgments xiii

1. Introduction 1
    Objectives 2
    Scope 3
    Facility and test rig description 4
    Organization of the report 5

2. Properties and Characteristics of Solid Waste Fractions Affecting Conveyability 9
    Measured properties and results 9
        Angle of maximum inclination 9
        Angle of repose 9
        Angle of slide 12
        Angle of surcharge and maximum surcharge 12
        Loose bulk density 15
        Vibrated bulk density 15
        Angle of external friction; angle of internal friction; cohesiveness; flowability; particle hardness; and abrasiveness 15
        Size and weight of lumps 18
        Moisture content 18
        Screen analysis and particle size distribution 18
        Sized and unsized materials 19
    Characteristics assessed 19

TYPING GUIDE SHEET
BEGIN FIRST LINE OF TEXT HERE
CENTER OF PAGE
TOP OF IMAGE AREA
DROPPED HEAD; BEGIN SECTIONS HERE
6-1/2"
9-1/8"
BEGIN LAST LINE OF TEXT
BOTTOM OF IMAGE AREA; OUTSIDE DIMENSION FOR TABLES AND ILLUSTRATIONS
3/8"

Contents (continued)

3. Belt Conveyors 24
  Introduction 24
  Analysis and development of a test plan 25
    Rationale: Designing for a rate of spillage 25
    Horizontal belt: Choice of test variables and parameters 26
    Inclined belt: Analysis of test procedures and variables 35
  Belt Conveyors: Summary of results 43
    Test belt conveyor and test procedures . . . 43
    Horizontal mode test results 43
    Inclined mode test results 62
    Dust generation 62
4. Vibrating Conveyors 75
  Introduction 75
  Test vibrating conveyor and test plan 75
  Test results 81
    Vibration frequency and stroke vs. maximum carrying capacity 81
    Vibration stroke and frequency vs. conveying speed for a given mass flow rate 81
    Energy consumption vs. vibrating frequency for a given mass flow rate 81
    Conveying speed vs. material burden depth for a given frequency 81
    Compaction of material along the length of pan 85
    Segregation of material 85
    Dust generation 87
5. Apron Conveyors 91
  Introduction 91
  Test results 91
  Maximum angle of surcharge 91
  Maximum carrying capacity vs. conveyor speed and inclination 92

PAGE NUMBER
EPA-287 (Cin.)
(4-76)

Contents (continued)

Maximum angle of inclination 92
References 98

Appendices

A. Methods for testing waste samples 99
B. Effect on spillage on proposed measurements 117

6-1/2"
9-1/8"
BEGIN LAST LINE OF TEXT
BOTTOM OF IMAGE AREA; OUTSIDE DIMENSION FOR TABLES AND ILLUSTRATIONS
3/8"

PAGE NUMBER
EPA-287 (Cin.)
(4-76)

BEGIN FIRST LINE OF TEXT HERE
TYPING GUIDE SHEET
CENTER OF PAGE
TOP OF IMAGE AREA
DROPPED HEAD; BEGIN SECTIO HERE

FIGURES

Number **Page**

1 Schematic of conveyor test rig 6

2 Conveyor test rig 7

3 Angle of surcharge for three types of conveyors 14

4 Particle size distribution of test samples . . . 20

5 Schematic of belt conveyor system 27

6 Choosing an operating point for lower spillage than maximum admissible 29

7 Cross-section of loaded belt (at rest) 30

8 Shape of curves of dynamic reduction coefficient vs. speed, and mass flow rate vs. speed (fixed spillage) 34

9 Curve of mass flow rates vs. belt speed for various spillage rates 36

10 Examples of use of $\mathcal{S}$ curves 37

11 Increase in vertical cross-section with inclination 38

12 Family of curves "$\mathcal{S}_\alpha$" 41

13 Optimum speed V_* and preferred operating range, at inclination α 42

14 MSW sample spillage vs. belt velocity and mass flow rate with horizontal belt and 20° idlers 44

15 MSW sample spillage vs. belt velocity and mass flow rate with horizontal belt and 35° idlers 45

BEGIN LAST LINI OF TEXT
OTTOM OF IAGE AREA; UTSIDE IMENSION OR TABLES ND ILLUS- IATIONS

EPA-287 (Cin.)
(4-76)

TYPING GUIDE SHEET
CENTER
BEGIN FIRST LINE OF TEXT HERE
TOP OF IMAGE AREA
DROPPED HEAD, BEGIN SECTIONS HERE

Figures (continued)

Number **Page**

16 RDF sample spillage vs. belt velocity and mass flow rate with horizontal belt and 20° idlers 46

17 RDF sample spillage vs. belt velocity and mass flow rate with horizontal belt and 35° idlers 47

18 Heavy fraction sample spillage vs. belt velocity and mass flow rate with horizontal belt and 20° idlers 48

19 Heavy fraction sample spillage vs. belt velocity and mass flow rate with horizontal belt and 35° idlers 49

20 Ferrous metal sample spillage vs. belt velocity and mass flow rate with horizontal belt and 35° idlers 50

21 d-RDF sample spillage vs. belt velocity and mass flow rate with horizontal belt and 35° idlers 51

22 Coal/d-RDF blend sample spillage vs. belt velocity and mass flow rate with horizontal belt and 35° idlers 52

23 Sub-division of the test belt conveyor for sectional spillage measurements 54

24 Trajectories for heavy fraction at 4.5 Mg/h (5 tph) and 20° idlers 58

25 Trajectories for ferrous metals fraction at 4.5 Mg/h (5 tph) and 20° idlers 59

26 Trajectories for RDF fraction at 0.9 Mg/h (1 tph) and 20° idlers 60

27 Trajectories for MSW fraction at 2.7 Mg/h (3 tph) and 20° idlers 61

28 MSW sample spillage vs. belt velocity and mass flow rate with inclined belt and 35° idlers 63

BEGIN LAST LINE OF TEXT
TTOM OF AGE AREA; TSIDE MENSION R TABLES D ILLUS- ATIONS

(4-76)

BEGIN FIRST LINE OF TEXT HERE
TYPING GUIDE SHEET
CENTER
TOP OF IMAGE AREA

Figures (continued)

DROPPED HEAD: BEGIN SECTION HERE

Number Page

29 Heavy fraction sample spillage vs. belt velocity with inclined belt and 35° idlers 64

30 RDF sample spillage vs. belt velocity with inclined belt and 35° idlers 65

31 d-RDF sample spillage vs. belt velocity with inclined belt and 35° idlers 66

32 Coal/d-RDF blend sample spillage vs. belt velocity with inclined belt and 35° idlers . . 67

33 MSW sample spillage vs. belt velocity for a fixed 0.9 Mg/h (1 tph) mass flow rate and 35° idlers 68

34 Magnitude of dust generated conveying RDF on test belt inclined at 14° and 20° 70

35 Magnitude of dust generated conveying MSW on test belt inclined at 14° and 20° 71

36 Magnitude of dust generated conveying d-RDF on test belt inclined at 14° 72

37 Magnitude of dust generated conveying d-RDF/coal blend on test belt inclined at 14° 73

38 Magnitude of dust generated conveying heavy fraction on test belt inclined at 14° 74

39 Vibrating conveyor principle of operation 76

40 Schematic of vibrating conveyor 77

41 Vibrating conveyor installation 78

42 Maximum carrying capacity of test vibrating conveyor vs. vibration frequency for 12.7 (1/2") stroke 82

43 Maximum carrying capacity of test vibrating conveyor vs. vibration frequency for 22.m (7/8") stroke 83

44 Material velocity vs. vibration frequency at the test vibrating conveyor 84

BEGIN LAST LIN OF TEXT
ITTOM OF IAGE AREA; UTSIDE IMENSION OR TABLES ND ILLUS- RATIONS

(4-76)

BEGIN FIRST LINE OF TEXT HERE
TYPING GUIDE SHEET
CENTER OF PAGE
TOP OF IMAGE AREA
DROPPED HEAD: BEGIN SECTION HERE

Figures (continued)

Number **Page**

45 Material velocity vs. material burden depth on the test vibrating conveyor 86

46 Particle size distribution and segregational effects between the conveyor - 13.7 mm (1/2") stroke 88

47 Particle size distribution and segregational effects between the conveyor - 22.2 mm (7/8") stroke 89

48 d-RDF maximum capacity vs. apron conveyor velocity 93

49 Coal/d-RDF maximum capacity vs. conveyor velocity 94

50 d-RDF maximum capacity vs. apron conveyor inclination 95

51 Coal/d-RDF maximum capacity vs. apron conveyor inclination 96

BEGIN LAST LINE OF TEXT
BOTTOM OF IMAGE AREA: OUTSIDE DIMENSION FOR TABLES AND ILLUSTRATIONS
3/8"

PAGE NUMBER
EPA-287 (Cin.)
(4-76)

BEGIN
FIRST
LINE OF
TEXT
HERE

TYPING GUIDE SHEET

CENTER
OF PAGE

TOP OF
IMAGE
AREA

DROPPED
HEAD;
BEGIN
SECTIONS
HERE

TABLES

Number		Page
1	Test Rig Conveyor Specification	8
2	Properties and Characteristics of Bulk Materials Affecting Conveyability	10
3	Angles of Maximum Inclination	11
4	Angle of Repose	13
5	Angle of Slide	13
6	Maximum Angle of Surcharge	16
7	Bulk Density (Loose)	16
8	Bulk Density (Maximum)	17
9	Moisture Contents	19
10	Material Class Description	22
11	Material Characteristics	23
12	Section Conveyor Spillage as a Percent of Total Spillage	55
13	Test Vibrating Conveyors Operating Range . . .	80
14	Comparison of Tendency for Compaction	85
15	Relationship between Dust Generation and Stroke Length	90

TTOM OF
AGE AREA;
JTSIDE
MENSION
R TABLES
JD ILLUS-
ATIONS

BEGIN
LAST LINE
OF TEXT

EPA-287 (Cin.)
(4-76)

ACKNOWLEDGMENTS

The contribution of NCRR colleagues, Harvey Alter, in establishing the program approach and scope, and Bill Schlag, Dave Mark and Sushant Kapur, in the equipment operation and testing are acknowledged.

Thanks to William Horton of Carman Industries for his cooperation in providing the test vibrating conveyor.

6-1/2"
9-1/8"
BEGIN LAST LINE OF TEXT
BOTTOM OF IMAGE AREA; OUTSIDE DIMENSION FOR TABLES AND ILLUSTRATIONS
3/8"

PAGE NUMBER
EPA-287 (Cin.)
(4-76)

SECTION 1

INTRODUCTION

Guidelines exist in the established literature for the selection, design, and operation of various types of conveyors for most bulk solids. From these sources, data are also available on the relevant physical and other descriptive properties for a large number of materials; these data are essential for proper application of conveyor design guidelines.

The Belt Conveyor Design Handbook, published by the Conveyor Equipment Manufacturer's Association (1), is an excellent example of such literature, with properties of more than 400 materials and detailed guidelines on belt conveyor design. Yet except for glass cullet, no information is available in this or any other single publication on the properties or conveyability of municipal solid waste (MSW) or its processed fractions.

Lacking such information on material properties, the design engineer or equipment vendor has been hampered in efforts to apply well founded engineering data and principles to the selection and construction of conveyors for solid wastes or to conduct proper evaluation and assessment at existing plants. As a result, problems with conveyors have been common to nearly all existing waste processing facilities. Extensive (and often innovative) efforts have been expended to remedy the problems in the field with varying success. But such treatment of the symptoms rather than the causes contributes little to guiding or improving future conveyor designs. Problems should be attacked and solved in the design phase rather than in the field.

In response to these expressed needs, the Municipal Environmental Research Laboratory of the U.S. Environmental Protection Agency (EPA) implemented a program to investigate engineering design considerations in selecting conveyors for resource recovery facilities. The proposed research program was broken into three phases. Phase I was entitled " Test Rig Evaluations," and

BEGIN LAST LINE OF TEXT
BOTTOM OF IMAGE AREA; OUTSIDE DIMENSION FOR TABLES AND ILLUSTRATIONS
3/8"

this document is the final report. Included are material characterization, establishment of evaluative criteria and experimental measurements and observation.*

Phase II ("Full-Scale Evaluation") and Phase III ("Optimization of Selected Conveyors") were intended as follow-on field evaluations using the rationale and experience from the first phase, but neither phase has been or is scheduled to be funded.

At the outset of the Phase I project, representatives of several conveyor equipment manufacturers were contacted to discuss the needs, goals, and approach. Out of these discussions came conclusions similar to those above. Notably, the design and operation of conveyors for resource recovery plants could be improved if there were (1) more complete data on material properties and material handling interactions; (2) indications of which of these factors were most significant to reliable operation of the systems; and (3) availability of criteria and techniques for the evaluation and field testing of conveyor equipment at existing facilities.

Pneumatic conveyor systems are found at nearly every waste processing facility and have been characterized by even greater operation and performance problems than experienced with mechanical conveyors. Because good information was lacking on test rig design, costing, and test rationale, the approach has been to engineer such a test rig, estimate the cost of its construction, and develop a test plan. The results of this part of the Phase I project are included in a separately bound report entitled "A Pneumatic Conveying Test Rig for Municipal Solid Waste Fractions" (EPAR806709).

OBJECTIVES

The objectives of Phase I of this project were to:

- Determine through engineering analysis and experimentation which properties and characteristics of MSW or processed waste fractions have significance in conveyor design, operation, and assessment.

---

*Note: Near the end of the 1-year grant, EPA, under an Interagency Agreement with, and funded by, the Engineering and Services Laboratory, Headquarters Air Force Engineering and Services Center, Tyndall Air Force Base, Florida, initiated a second-year continuation to cover further testing on densified, refuse-derived fuel (d-RDF) and d-RDF/coal blends. These results are incorporated in this report, as well as included in a separately bound report to the Air Force.

- Measure these significant properties.

- Establish criteria and methods for evaluation of conveyors at resource recovery plants.

- Provide reliable engineering data to be used in future conveyor design as well as currently operating plants.

SCOPE

Not all conveyor types or processed waste fractions could be modeled or evaluated within the schedule or funding limits established for Phase I. Belt conveyors (horizontal and inclined), vibrating pan conveyors and pan (or apron) conveyors (only in limited batch tests) were considered. Screw conveyors, drag chain conveyors, and bucket elevators were not included, and pneumatic conveyors, as mentioned earlier, were only considered to the extent of developing a test program for a pneumatic test rig. With few exceptions, screw conveyors are not generally applied to processed waste fraction due to susceptibility to binding and blockages. Drag chain conveyors are also not widely applied in solid waste processing (with the exception of conveying combustion residues and occasionally in storage retrieval applications). Bucket elevators are most often used in conveying dense, heavy fractions which offer less problems in conveying and are more analogous to established application in the minerals processing field. Pan (or apron) conveyors are frequently found in waste processing plants, but usually in application to raw, unprocessed refuse or as discharge conveyors from shredding equipment. To model and test with raw waste required a pan conveyor and other handling equipment of a size and capacity beyond the scope of this program. Testing on a pan conveyor was initiated in the later portion of the project and then only on a batch basis and on feedstocks of d-RDF and a d-RDF coal blend.*

There are a variety of other, often unique types or styles of conveyors which are available or have had applications in resource recovery plants. These conveyors include, as examples, compartmentalized belts, tubular belts, slider beds and vibrating tubes. In the interest of obtaining results that are general to the design of conveyors rather than to a specific type, and in consideration of the types of conveyor most frequently encountered in the field, full test rig evaluations were limited to the belt and vibrating pan types of conveyors.

---

*See footnote on page 2.

Note, however, that the concentration of these two conveyor types in this test program does not preclude application of the rationale, analytical techniques or evaluation procedures to other types of conveyors or feedstocks that will be encountered in resource recovery plants. The usefulness of this first phase program lies on the application and testing of the results on a variety of conveyor styles, sizes and applications in full-scale commercial facilities. Such evaluations are necessary to assess and understand impact of variation on feedrates and characteristics and to undermine scaling relationships.

There is a variety of solid waste and processed fractions that are produced and conveyed in resource recovery plants (e.g., raw waste, shredded waste, air-classified light and heavy fractions, ferrous metals, etc.). The variation in properties for a particular fraction from one plant to another and over time at a single facility may also be significant (e.g., density, moisture, particle size, etc.). For this test program, the fractions selected for evaluation on the test rig were shredded MSW, air-classified light fraction (RDF) and heavy fraction, and ferrous metals. These were felt to be the most frequently encountered and more difficult to handle fractions. In the later portion of the project, feedstocks of densified refuse-derived fuel and a blend of d-RDF and coal were added as part of the Air Force-initiated portion to the program.

The samples of processed waste fractions were obtained from the Baltimore County Resource Recovery Facility in Cockeysville, MD. In spite of the recognition that the properties of each fraction were likely to vary from sample to sample, and thus have some impact on conveyor performance, the scope of the program did not allow test rig evaluations on multiple samples of a single fraction. Rather, through careful sampling at the Baltimore County facility and monitoring of sample properties, the goal was to obtain and test material samples representative of the individual processed fractions and reasonably consistent from test to test.

FACILITY AND TEST RIG DESCRIPTION

The experimental activities in this program were conducted at the National Center's Resource Recovery Laboratory, a 3000-square-foot-unit process test facility located in Upper Marlboro, MD, southeast of Washington, Concurrent engineering and analytical activities were supported from the main NCRR offices in Washington.

The design of the test rig was based on several considerations:

- ability to fix mass flow rates

BEGIN FIRST LINE OF TEXT HERE
CENTER OF PAGE
TOP OF IMAGE AREA
DROPPED HEAD; BEGIN SECTIONS HERE
BEGIN LAST LINE OF TEXT
BOTTOM OF IMAGE AREA; OUTSIDE DIMENSION FOR TABLES AND ILLUSTRATIONS
3/8"
PAGE NUMBER
EPA Form 2350-4 (4-80)
(PREVIOUSLY CIN. EPA FORM 287)
☆ U.S. GOVERNMENT PRINTING OFFICE 1980-660-639
TYPING GUIDE SHEET

- accessibility for dynamic measurements and sampling
- flexibility to interchange, incline, or vary speeds of the test conveyors.

A continuous loop, recirculating flow configuration as shown in schematic in Figure 1 and pictured in Figure 2 was selected for the tests. A surge hopper with a variable speed pan conveyor to control feedrate was tried initially but found to result in surging and thus poor feedrate control. The second and successful approach was to fix conveyor speeds and charge a measured quantity of the test material into the system and thus obtain a constant mass flow rate throughout the loop. It was experimentally established that the mass flow rate could be held within a range of plus or minus 5% of the measured average.

Table 1 provides specifications for each of the conveyors in the test rig. Both the test belt conveyor and test vibrating conveyor required modifications to provide the ranges of operating conditions that are shown.

ORGANIZATION OF THE REPORT

The first section of this report provides a description of the test rig equipment. This is followed in Section 2 with data and discussion on the key properties and characteristics of solid waste fractions affecting conveyability. Section 3 develops the rationale and approach for design of the test program and judging belt conveyor performance. The experimental results for the best conveyor are presented in Section 3 as well. Sections 4 and 5 present the results of testing on belt conveyors, vibrating pan conveyors and apron conveyors, respectively.

The results of the investigation and development of a pneumatic test program are presented in a separately bound volume entitled "Evaluation of a Pneumatic Conveying Test Rig for MSW Waste Fractions."

BEGIN FIRST LINE OF TEXT HERE
CENTER OF PAGE
TOP OF IMAGE AREA
DROPPED HEAD: BEGIN SECTIONS HERE
BEGIN LAST LINE OF TEXT
3/8"
PAGE NUMBER
BOTTOM OF IMAGE AREA; OUTSIDE DIMENSION FOR TABLES AND ILLUSTRATIONS
EPA Form 2350-4 (4-80)
(PREVIOUSLY CIN. EPA FORM 287)
☆ U.S. GOVERNMENT PRINTING OFFICE 1980-660-639
TYPING GUIDE SHEET

BEGIN FIRST LINE OF TEXT HERE
CENTER OF PAGE
TOP OF IMAGE AREA
DROPPED HEAD; BEGIN SECTION HERE

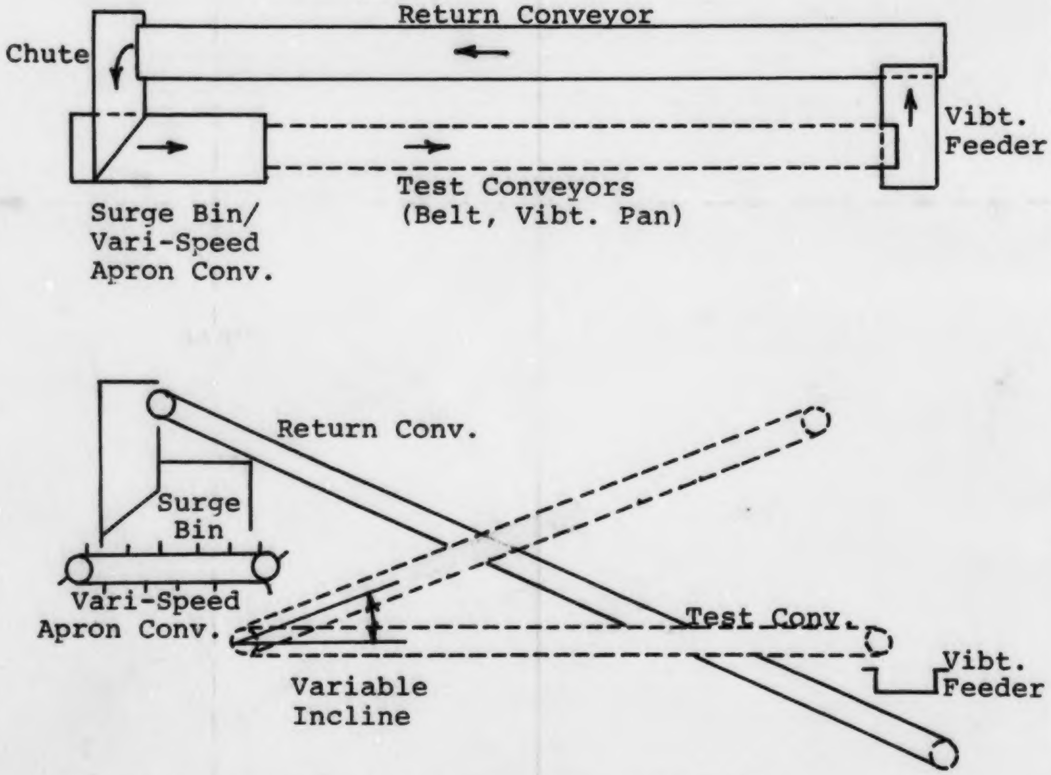
Return Conveyor
Chute
Vibt. Feeder
Test Conveyors
(Belt, Vibt. Pan)
Surge Bin/
Vari-Speed
Apron Conv.
Return Conv.
Surge Bin
Vari-Speed
Apron Conv.
Test Conv.
Vibt. Feeder
Variable Incline

Figure 1. Schematic of conveyor test rig.

BEGIN LAST LINE OF TEXT
BOTTOM OF IMAGE AREA; OUTSIDE DIMENSION FOR TABLES AND ILLUSTRATIONS
3/8"

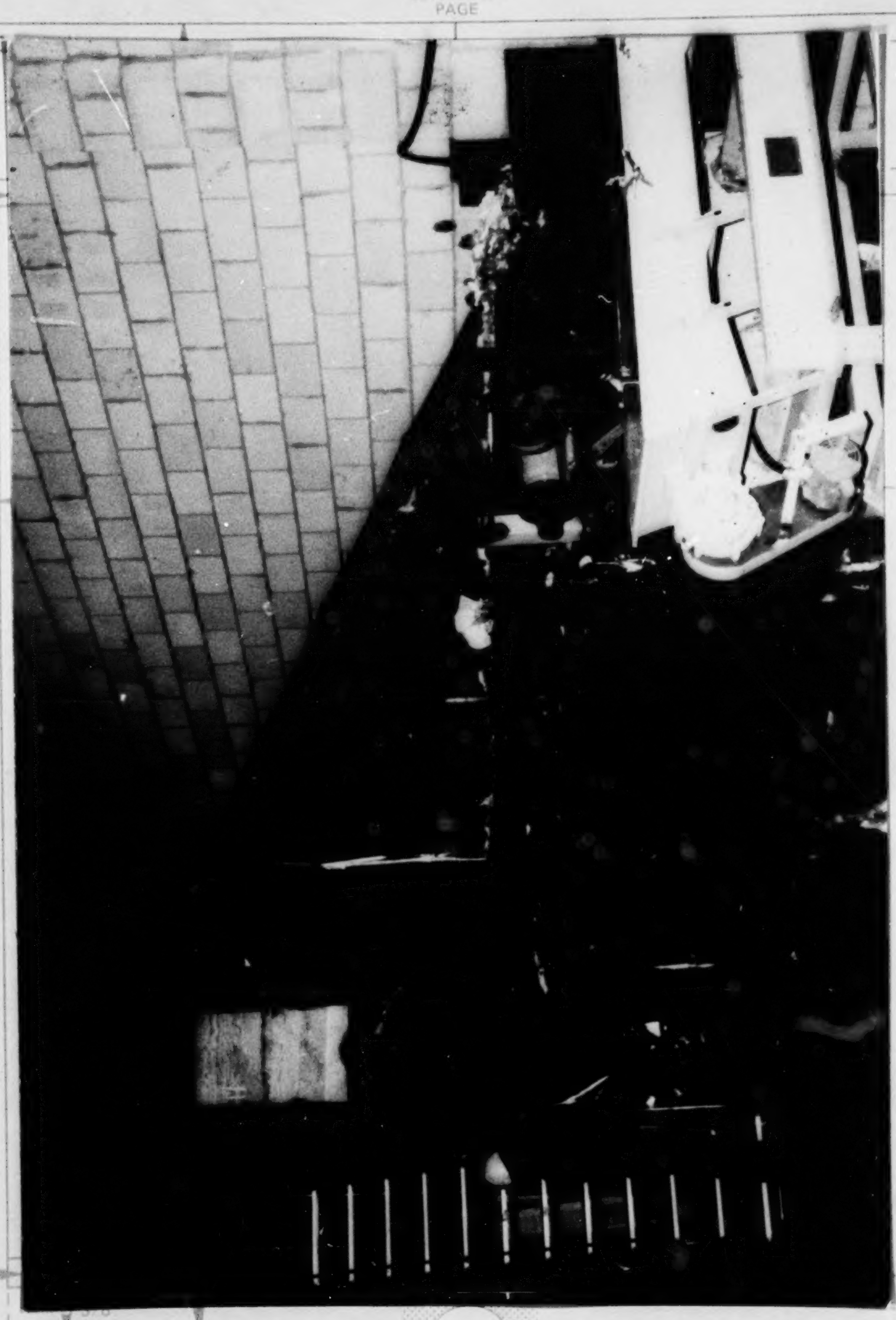

Figure 2. Conveyor test rig.

TABLE 1. TEST RIG CONVEYOR SPECIFICATION

Conveyor	Width m (in.)	Length m (ft)	Drive	Idlers angle	Stroke/ freq.	Incline	Speed	Manufacturer
Feed Apron	0.749 (29.5)	2.06 (6.75)	variable	N/A	N/A	0°	0.14 m/s (27 fpm)	Bonded Equipment
Test belt conveyor	0.457 (18)	7.63 (25)	variable	20°/ 35°	N/A	0°-32° max.	0.20-2.44 m/s (40-480 fpm)	Bonded Equipment
Vibrating conveyor	0.603 (23.75)	4.58 (15)	variable	N/A	12.7 mm (1/2 in.)/ 400-560 cpm 22.2 mm (7/8 in.)/ 470-545 cpm	0°	N/A	Carman Industries
Transfer vibrating conveyor	0.508 (20)	1.83 (6)	constant	N/A	4.8 mm (3/16 in.)/ 1300 cpm	0°	N/A	Meyer Machine Co.
Return conveyor	0.508 (20)	9.67 (31.7)	constant	35°	N/A	17°	1.04 m/s (205 fpm)	Bonded Equipment

SECTION 2

PROPERTIES AND CHARACTERISTICS OF SOLID WASTE FRACTIONS AFFECTING CONVEYABILITY

As discussed earlier, in conveyor design it is essential to have engineering data on material properties and material handling interactions. This information is available for most bulk solids but not for MSW or its processed fractions.

The properties and characteristics of bulk materials affecting conveyability and their test methods have been researched and published by the Conveyor Equipment Manufacturers Association (CEMA) (2). Table 2 shows a complete list of properties and characteristics that affect conveyability. The asterisks in Table 2 indicate those which were considered unrelated to the conveyability of solid waste fractions. The daggers rate properties for which test methods have yet to be developed.

MEASURED PROPERTIES AND RESULTS

The following are the results from reviews or measurements of the properties listed in Table 2. Test methods, as available or applied, are given in Appendix A.

Angle of Maximum Inclination

The angle of maximum inclination is defined for a belt conveyor to be that angle, in degrees to the horizontal, at which an empty conveyor belt will successfully transport the material fed to it. The results were observed to be dependent on belt configuration, belt speed and mass flow rate. Table 3 presents maximum angle of inclination for mid-range mass flow rates for each material and at a fixed belt velocity of 0.51 m/s (100 fpm). Angles are seen to be greater with feedstock with higher densities. The test procedure is given in Appendix A.1.

Angle of Repose

The angle of repose for a bulk material in a stockpile is the angle between the horizontal and a sloping line from the top of the pile to the base. The measurement procedure is

BEGIN LAST LINE OF TEXT
BOTTOM OF IMAGE AREA: OUTSIDE DIMENSION FOR TABLES AND ILLUSTRATIONS
3/8"

TABLE 2. PROPERTIES AND CHARACTERISTICS OF BULK MATERIALS AFFECTING CONVEYABILITY

Properties (measured)

1. Abrasiveness†
2. Angle of External Friction†
3. Angle of Internal Friction†
4. Angle of Maximum Inclination (of a belt)
5. Angle of repose
6. Angle of slide
7. Angle of surcharge
8. Bulk Density - loose
9. Bulk Density - vibrated
10. Cohesiveness†
11. Elevated Temperature*
12. Flowability - flow function†
13. Lumps - size - weight
14. Specific gravity*
15. Moisture Content
16. Particle Hardness†
17. Screen Analysis and particle size consist
18. Sized and unsized material

Characteristics (assessed)

1. Aeration - Fluidity*
2. Becomes plastic or tends to soften*
3. Builds up and hardens
4. Corrosive
5. Generates static electricity*
6. Degradable - size breakdown
7. Deteriorates in storage - decomposition
8. Dusty
9. Explosiveness
10. Flammability
11. Harmful dust, toxic gas or fumes
12. Hygroscopic*
13. Interlocks, mats and aggleomerates
14. Oils or fats present*
15. Packs under pressure
16. Particle shape
17. Stickiness - adhesion
18. Contaminable
19. Very light & fluffy - may be windswept

---

* Considered unrelated to conveyability of solid waste.

† Test methods for processed solid waste fractions yet to be developed.

TABLE 3. ANGLES OF MAXIMUM INCLINATION

SOLID WASTE FRACTION	Belt width mm (in.)	Belt idlers (°)	Belt speed m/s (ft/min)	Flow rate Mg/h (TPH)	Angle of maximum inclination (°)
MSW	457 (18)	35	0.51 (100)	0.9 (1.0)	19
RDF	457 (18)	35	0.51 (100)	0.9 (1.0)	21
d-RDF	457 (18)	35	0.51 (100)	4.5 (5.0)	30
HEAVY FRACTION	457 (18)	35	0.51 (100)	4.5 (5.0)	28
FERROUS FRACTION	457 (18)	35	0.51 (100)	4.5 (5.0)	28
d-RDF/COAL (1:1 volumetric basis)	457 (18)	35	0.51 (100)	9.1 (10.0)	27

Test Conditions:
(1) Belt width = 457 mm (18 in.)
(2) Belt idlers = 35°
(3) Belt velocity = 0.51 m/s (100 fpm)

provided in Appendix A.2. The results as a range for each material are shown in Table 4.

Angles of repose will vary due to irregularities in particle size, shape and concentrations. Also, the piles of waste materials were never observed to be uniformly conical, and thus several angles of repose were measured around the pile.

Angle of Slide

The angle of slide is that angle to the horizontal of an incline flat surface on which an amount of material will begin to slide downward due to its own weight. Such a measurement is of particular use in design of chutes or diverters.

Experimental determination of the angle of slide will be affected by the

- type and condition of the underlying surface
- state of compaction of the material
- rate of change in slope (controlled by the operator).

Tests were conducted both on a steel plate and rubber conveyor belting. For each test, approximately 14.2 dm^3 (0.5 ft^3) was utilized. The results in Table 5 indicate that all of the waste fractions will slide, under static conditions, at a lower angle on steel than conveyor belting. The test procedure is given in Appendix A.3.

Angle of Surcharge and Maximum Angle of Surcharge

The angle of surcharge is the angle to the horizontal which the surface of the material assumes while at rest on a moving conveyor belt. Figure 3 shows the angle of surcharge, α, for three types of conveyors. For bulk solids listed in the CEMA Handbook on belt conveyors, this angle is said to be observed to be 5° to 15° lower than the angle of repose (2).

The angle of surcharge as defined (on a moving belt) could not be experimentally determined because the available equipment and quantity of material was too small for the prescribed procedure.

In this program, a maximum angle of surcharge on a belt (α_{max}) has been defined as the experimentally determined angle at which the conveyor can be loaded to a maximum capacity (i.e., filling a maximum belt cross-section) under static conditions (i.e., with the belt at rest). These figures are shown for the six materials and two idler configurations in Table 6. The

TABLE 4. ANGLE OF REPOSE

SOLID WASTE FRACTION	ANGLE OF REPOSE	
	RANGE	AVERAGE
MSW	25° - 52°	39
RDF	29° - 49°	40
d-RDF	27° - 46°	38
HF	30° - 59°	40
Ferrous Fraction	N/A*	N/A*
d-RDF/coal	40° - 45°	42

* No measurement made as small sample size led to slumping to a monolayer.

TABLE 5. ANGLE OF SLIDE

SOLID WASTE FRACTION	ANGLE OF SLIDE	
	STEEL PLATE	CONVEYOR BELTING
MSW	29.3°	30.0
RDF	31.0°	35.0
d-RDF	32.8°	34.5
Heavy Fraction	27.5°	28.5
Ferrous Fraction	17.5°	32.0
d-RDF/coal	22.0°	24.0

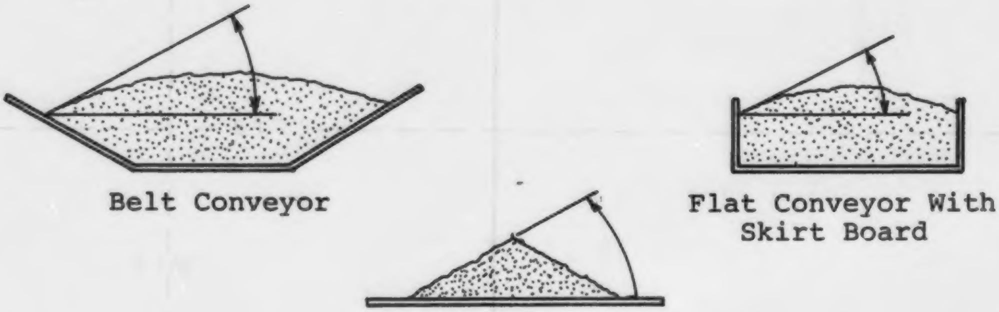

Belt Conveyor

Flat Conveyor With Skirt Board

Flat Apron Conveyor Without Skirtboard.
(Same As Angle of Repose)

Figure 3. Angle of surcharge for three types of conveyors.

BEGIN LAST LINE OF TEXT
BOTTOM OF IMAGE AREA; OUTSIDE DIMENSION FOR TABLES AND ILLUSTRATIONS
3/8"

procedure for this measurement of angle of surcharge is given in Appendix A.4.

Loose Bulk Density

While there are several published standards for determining bulk density, such as the American Society for Testing and Materials (ASTM) methods for aggregates and coal, they are not generally applicable to solid waste. The two methods to measure bulk density that were applied in this study, loose and vibrated, are described in Appendices A.5 and A.6, respectively.

The loose bulk density appears to be more representative of the two methods in representing the density of a material on a conveyor belt. Loose bulk density is the weight per unit volume of a sample discharged from a container into a pile or cone without any other compaction. The results are provided in Table 7. Note the wider ranges in loose bulk density for the more heterogeneous MSW and heavy fraction samples, due mainly to the presence of discrete heavy or larger-sized materials.

Vibrated Bulk Density

The vibrated bulk density is the weight per unit volume of a sample which is in a compacted condition as a result of vibrating or tapping of the test container as it is being filled.

The method (Appendix A.6) is comparable to a standard recently developed by The American Society for Testing Materials Committee on Resource Recovery (E-38) but substitutes the CEMA vibration method which is more applicable for coal and aggregates. The results are given in Table 8.

Comparing the results in Tables 7 and 8, it can be seen that the vibrated bulk densities are higher by about 20% than the loose bulk density. Whereas the vibrated bulk densities are generally utilized for determining volumetric flow rates, it is proposed that the loose bulk density value should be measured and used in conveyor design for MSW or its processed fractions as it is more representatives of the actual as-handled material conditions.

Angle of External Friction; Angle of Internal Friction; Cohesiveness; Flowability; Particle Hardness; and Abrasiveness

Brief definitions of these properties are as follows:

The Angles of External and Internal Friction are properties of a material related to shearing resistance between the material and a surface of another material (external) and resistance to sliding or rolling of particles in relation to themselves (internal). They are experimentally determined by a

BEGIN FIRST LINE OF TEXT HERE
CENTER OF PAGE
TOP OF IMAGE AREA
DROPPED HEAD; BEGIN SECTIONS HERE
BEGIN LAST LINE OF TEXT
BOTTOM OF IMAGE AREA; OUTSIDE DIMENSION FOR TABLES AND ILLUSTRATIONS
3/8"
PAGE NUMBER
EPA Form 2350-4 (4-80)
(PREVIOUSLY CIN. EPA FORM 287)
☆ U.S. GOVERNMENT PRINTING OFFICE 1980-660-539
TYPING GUIDE SHEET

TABLE 6. MAXIMUM ANGLE OF SURCHARGE

SOLID WASTE FRACTION	MAXIMUM ANGLE OF SURCHARGE 20° Idler	 35° Idler
MSW	55°	54°
RDF	51°	65°
d-RDF	not measured	49°
HEAVY FRACTION	48°	59°
FERROUS FRACTION	not measured	52°
d-RDF/COAL	not measured	40°

TABLE 7. BULK DENSITY (LOOSE)

SOLID WASTE FRACTION	BULK DENSITY (LOOSE) (kg/m^3) (lbs/ft^3) RANGE	 AVG.
MSW	61-152 (3.8 - 9.5)	106 (6.6)
RDF	34-50 (2.1 - 3.1)	43 (2.7)
d-RDF	361-387 (22.6 - 24.2)	374 (23.4)
FERROUS	N/A*	N/A*
HEAVY FRACTION	366-598 (22.9 - 37.4)	482 (30.1)
d-RDF/COAL	712 (44.5)	712 (44.5)

* No measurement made as sample size too small and material slumped to monolayer.

BEGIN FIRST LINE OF TEXT HERE
CENTER OF PAGE
TOP OF IMAGE AREA
DROPPED HEAD. BEGIN SECTIONS HERE
6-1/2"
9-1/8"
BEGIN LAST LINE OF TEXT
3/8"
PAGE NUMBER
BOTTOM OF IMAGE AREA; OUTSIDE DIMENSION FOR TABLES AND ILLUSTRATIONS
EPA Form 2350-4 (4-80)
(PREVIOUSLY CIN. EPA FORM 287)
☆ U.S. GOVERNMENT PRINTING OFFICE 1980-660-639
TYPING GUIDE SHEET

TABLE 8. BULK DENSITY (MAXIMUM)

Solid waste fraction	Bulk density kg/m^3 (lb/ft^3) Range		Average	
MSW	66 - 200	(4.1 - 12.5)	134	(8.4)
RDF	37 - 72	(2.3 - 4.5)	54	(3.4)
d-RDF	402-486	(25.1 - 30.4)	445	(27.8)
Heavy fraction	334 - 451	(20.9 - 28.2)	435	(27.2)
Ferrous fraction	194	(12.1)	194	(12.1)
d-RDF/coal	590	(36.9)	590	(36.9)

direct shear-controlled stress tester (3). Cohesiveness in bulk materials is characterized by the degree to which individual particles tend to cling together and is also measured in direct shear-controlled stress tests. Flowability (flow function) characterizes the freedom of constituent particles or groups of particles to move when the bulk material is put in motion and is determined in direct shear-controlled strain testing. Particle hardness is of interest in bulk material handling in relation to abrasiveness, and the potential for cracking or crumbles to smaller particles. Abrasiveness is a combination of physical characteristics of a material which enables it to abrade surfaces with which it comes in contact.

In the case of abrasiveness, a test to assess relative abrasiveness of the various waste fractions was developed but proved unsuccessful. A sheet of material - rubber belting and aluminum - was placed in the material trajectory at one of the right angle turns on the test rig. Measurements were made of the weight loss of the impact sheet related to mass flow and time for each waste fraction. Unfortunately, the results obtained during the test program were inconclusive. Much longer periods of time than were available and repetitive tests would appear to be required to provide meaningful results.

Although all of the other properties are likely to have importance in handling and conveying, the scope of the program did not allow for adopting existing procedures for these fractions or development of new, reliable procedures.

Size and Weight of Lumps

According to the CEMA definitions, lump size is the maximum linear dimension of a large particle or stable agglomeration thereof, in a bulk material. The lump weight is the weight of the maximum size lump. The measurements of the largest lump size were made in conjunction with the particle size distribution test outlined in Appendix A.8.

Whereas this definition might make sense for brittle, blocky and/or homogeneous material, it is thought to be largely inapplicable to solid waste fractions, and should not be retained as such. Particle size distribution, determined by sieving and weight distribution by component, are more indicative of how "large" the conveyed material is compared to the belt width. Yet, pliable materials such as textiles and plastics might be much larger than the nominal grate or sieve size and streams with significant amounts of these components are more prone to spillage. Considerable work remains to be done in characterizing MSW and its processed fractions as to the actual "size" of its components seen by the conveyor belt.

The small quantity of large lumps in the test samples and the need to remove occasional larger particles so as not to continually disrupt the recirculating tests precluded observations of the effect of lumps on performance. It is, however, a property of critical importance to design of conveyors, transfer points and chutes due to the potential for jams and bridging.

Moisture Content

The moisture content of a material reflects the absorbed and adsorbed water and is measured by evaporation through drying. The procedure used in this program is provided in Appendix A.7. Because of the wide variations in moisture content of MSW and its processed fractions, the results in Table 9 should be viewed only as general indicators.

Waste materials with higher moisture contents, although beneficial in limiting dust, may contribute to either operational or maintenance problems. Moisture will increase material stickiness and adhesion to belts or chutes and could lead to corrosion.

Screen Analysis and Particle Size Distribution

A screen analysis using a conventional shaker screen technique (see Appendix A.8) was conducted to obtain a particular size distribution (PSD) for four of the six solid waste fractions. No PSD analysis was performed for the d-RDF or coal/d-RDF blends because the fixed pellet shape (13 mm dia.) makes

TABLE 9. MOISTURE CONTENTS

Solid Waste Fraction	Moisture Content (% as-received)	
	Range	Avg.
MSW	18% - 30%	21.8%
RDF	9.1% - 19.0%	14.2%
d-RDF	20.5% - 22.7%	20.6%
Heavy Fraction	9.2% - 20.8%	15.9%
Ferrous Fraction	2.6%	2.6%
d-RDF/coal	-	9.3%

a screen size analysis meaningless. For reference, the coal specification size is 95% < 35 mm.

The results are presented in Figure 4. This information is of value in specifying conveyor parameters such as belt width, idler angles, conveyor skirting and in the design of conveyor loading and discharge configuration.

Sized and Unsized Materials

A sized material consists of particles which have been passed through some defined mesh screen and retained on some smaller mesh screen; a partially sized material is made of sized and unsized material.

Under those definitions, the solid waste fractions evaluated in this program are unsized, with the possible exception of the d-RDF which is produced by an extrusion process and thus effectively sized and uniform in physical dimensions. Processed waste fractions encountered in other waste processing plants may have undergone a screening process and thus be considered sized.

CHARACTERISTICS ASSESSED

Certain material characteristics do not have defined measurement techniques, but still must be addressed in designing a conveyor system. Several of the key characteristics and selected physical properties have been combined and coded in a

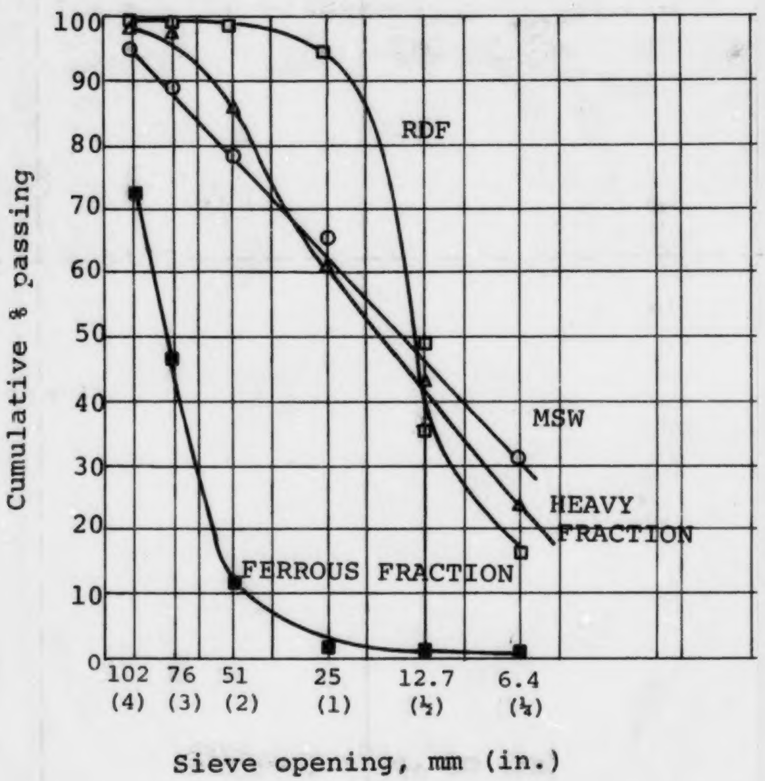

Figure 4. Particle size distribution of test samples.

BEGIN LAST LINE OF TEXT
3/8"
BOTTOM OF IMAGE AREA; OUTSIDE DIMENSION FOR TABLES AND ILLUSTRATIONS

material class description form shown in Table 10. Further discussion on these characteristics and their assessment are given by CEMA (1,2).

Using this CEMA classification approach, Table 11 provides coding for the six materials evaluated in this program. It is recommended that they be used with the awareness of their limitations due to the heterogeneity and variability of these types of material.

DROPPED HEAD: BEGIN SECTIONS HERE
6-1/2"
9-1/8"
BEGIN LAST LINE OF TEXT
BOTTOM OF IMAGE AREA; OUTSIDE DIMENSION FOR TABLES AND ILLUSTRATIONS
3/8"

TABLE 10. MATERIAL CLASS DESCRIPTION

	Material Characteristics	Code
Size	Very fine - less than 100 mesh	A_{100}
	fine -1/8 in. or less	B_6
	granular -3 in. or less	D_3
	lumpy - containing lumps 16 in. or less	D_{16}
	Irregular - stringy, interlocking	E
Flow-Ability	Very free flowing - angle of repose less than 19°	1
	Free flowing - angle of repose 20° to 29°	2
	Average flowing - angle of repose 30° to 39°	3
	Sluggish - angle of repose 40° and over	4
Abrasiveness	Non-abrasive	5
	Abrasive	6
	Very abrasive	7
	Very sharp - cuts or gouges belt conveyors	8
Characteristics (Assessed)	Builds up and hardens	F
	Deteriorates in storage	H
	Corrosive	T
	Degradable - Size Breakdown	Q
	Dusty	L
	Explosiveness	N
	Flammability	J
	Harmful dust, toxic gas or fumes	R
Characteristics	Interlocks, matts or agglomerates	V
	Packs under pressure	X
	Stickiness - Adhesion	O
	Very light fluffy	Y

TABLE 11. MATERIAL CHARACTERISTICS

Fraction	Avg. bulk kg/m^3	loose density (lbs/ft^3)	Angle of repose (degrees)	Angle of maximum inclination (degrees)	CEMA material code
MSW	106	(6.6)	25 - 52	19	E36HJVO
RDF	43	(2.7)	29 - 49	21	E35HJLXY
d-RDF	374	(23.4)	27 - 46	30	$D_3$35HJQL
Heavy Fraction	481	(30.1)	30 - 59	28	E47HQVO
Ferrous Fraction	192 (maximum B. D.)	(12.0)	N/A	28	D_{16}^{6}
d-RDF/coal	712	(44.5)	40 - 45	27	$D_3$46HQLJ

SECTION 3

BELT CONVEYORS

INTRODUCTION

Belt conveyors have wide applications in mining, construction and processing industries. Compared to other types of conveyors, they have advantages of being relatively simple and economical and suitable for conveying material of varying composition, size and moisture. They can be operated in the horizontal, inclined or declined mode. Belt conveyors are commonly present in resource recovery plants for transportation of MSW or the variety of its processed fractions.

Resource recovery plant operating experience has indicated that, in spite of simplicity in design and operation, numerous problems still beset belt conveyors such as spillage, jams, rollback, dusting and wear. Some of these problems are attributable to the properties and characteristics of the materials being conveyed as have been discussed in the previous section. But, others are related to operating variables over which a designer or operator has control such as belt size, speed and inclination; idler type and angles; and loading and discharge configuration. However, to understand or optimize design and operation, the influence of the conveyor configuration movement, shape and speed on these problems must first be understood.

The approach in this investigation was to explore the impact and interrelationship of these equipment and operating variables on conveyor performance though a systematic series of tests on a horizontal and inclined belt.

However, prior to the conduct of the tests, an analysis of the rationale and criteria for evaluating and judging conveyor performance had to be developed, and was published earlier in 1981 (4). This analysis and development of a test plan is described next and will be followed by the results and discussion of the tests.

BEGIN LAST LINE OF TEXT
BOTTOM OF IMAGE AREA: OUTSIDE DIMENSION FOR TABLES AND ILLUSTRATIONS
3/8"

ANALYSIS AND DEVELOPMENT OF A TEST PLAN

Rationale: Designing for a Rate of Spillage

In designing a series of tests to define the range of "good" or "best" operation of a belt conveyor carrying a given material, some thought should be given to the criteria by which such labels as "good" or "best" might be awarded.

As noted above, experience of observations gathered at a number of operating plants with systems to convey solid waste fractions strongly suggests that by far, the most undesirable feature in such systems is a high rate of spillage. Spillages on the sides of conveyor belts, or at transfer points, will fall on the floor, jam up rotating pieces of equipment and be a cause of constant problems in maintenance, odor, sanitation and clean-up. As an illustration, assume a rate of spillage of 1% of the mass flow rate on a conveyor belt 30.5 m (100 ft) long. The belt carries 1.8 Mg/h (2 ton/h) of light fraction (fluff RDF) having a bulk density of 54 kg/m^3 (3.4 lb/ft^3). After an 8-hour shift, 0.14 Mg (0.16 ton) will have accumulated along the belt, representing a total volume of 2.1 m^3 (94 ft^3). On each side of the belt, this would be the equivalent of a layer 30.5 cm (1 ft) wide and 15 cm (0.5 ft) high. Needless to say, such rate of spillage would be intolerable in steady operation.

Other desirable (but possibly less crucial) features of a belt conveyor system if known geometry, carrying a given material,

(a) high throughput for a given size (as measured by the width of the belt);

(b) low power consumption;

(c) high reliability and trouble-free operation;

(d) low levels of dust emissions; and

(e) ease of transfer of material to and from the belt.

In view of the extreme importance of limiting spillage to a low, admissible level, it was decided at the outset to design the conveyability on the basis of a criterion of acceptable spillage. Then, consideration was given to high throughputs [feature (a) above] by studying the dependence of throughput on belt speed.

Item (b) above, the power consumption, was measured at the various operating points, with no attempt being made to modify the design of the belt being tested for lower power consumption.

[It should be kept in mind, however, that high power consumption might be one of the essential deciding factors when choosing between an open, skirted or covered conveyor belt system (1).]

High reliability and trouble-free operation, item (c) can only be ascertained after much longer periods of time than would be possible in this test program. Still, whenever possible and justified, incidents of operation, jamming of equipment or other conditions were noted and documented.

As will be detailed below, dust levels were recorded and evaluated in a relative, and to some extent, absolute manner. These levels were obtained at various "typical" locations (near transfer points, in the middle of a straight run, etc.), thus allowing to compare the dependence of dust levels on location as well as on the operating parameters and the kind of solid waste fraction being conveyed.

Finally, the ease of transfer of the material studied onto and from the belt will be highlighted in two principal ways. First, by observing and recording trajectories of the material at the discharge point from the conveyor belt, and comparing them to those predicted by methods conventionally used in applications for materials other than solid waste. Secondly, experimental observations, largely qualitative, and *ad hoc* improvements made during the course of the tests should serve as a guide for assessing the "proper" mode of feeding the belt with a variety of feedstocks. This is particularly true in the case of a steeply inclined belt, for which transfer and acceleration on the belt in the zone located directly under the chute or feeding stream are the mechanisms critically limiting throughput and/or producing surges.

Horizontal Belt: Choice of Test Variables and Parameters

As a help in the discussion, a schematic representation of the conveyor belt system is shown in Figure 5. The belt has length L_B, and can be either horizontal ($\alpha = 0$) or inclined at angle α on the horizontal. At the inlet point A, the input mass flow rate (having dimension mass/unit time, or (MT^{-1}}) is noted $\dot{m}_{in}$; the mass flow rate exiting the belt at Point B is noted $\dot{m}_{out}$.

Spillage Rate --

The spillage rate, $\dot{s}$, is a relative measure of the mass of conveyed material being spilled, per unit of mass flow rate conveyed and unit length of belt.

This would appear as a quite logical definition, but it should be kept in mind that it implicitly contains some assumptions or simplifications. Firstly, the input mass flow rate,

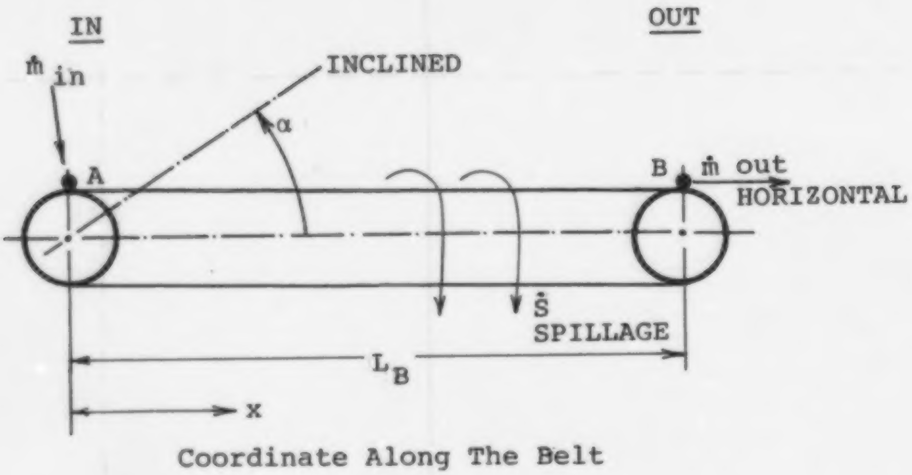
IN
OUT
ṁ in
INCLINED
α
A
B
ṁ out
HORIZONTAL
Ṡ
SPILLAGE
L_B
x
Coordinate Along The Belt

Figure 5. Schematic of belt conveyor system.

BEGIN LAST LINE OF TEXT
3/8"
BOTTOM OF IMAGE AREA: OUTSIDE DIMENSION FOR TABLES AND ILLUSTRATIONS

$\dot{m}_{in}$ defined above and in Figure 5, is assumed to be known and constant. In actuality, the mass flow rate $\dot{m}_{in}$ is steadily decreasing with time, due to spillage and the fact that the mass spilled is not replaced on the belt. For small spillage rates (1% or less over the length considered), this effect is of second order provided the duration of the test is not too long. This is quantified in Appendix B. Secondly, the rate of spillage is construed to be proportional to belt length, and for long, straight runs, this might be the case only after the "discrete" spillage at transfer points A and B in Figure 5 has been subtracted from the total spillage. More will be said about these limitations further in the text, when discussing the experimental procedure and test results.

Let $\dot{m}_s$ be the mass flow rate of material spilled per unit length of belt. The formal definition of the spillage rate, as a fraction (p.u.), or percentage, will be (with the above qualifications):

$$s = \frac{d\dot{m}_s/dx}{\dot{m}_{in}} = \frac{\dot{m}_{in} - \dot{m}_{out}}{\dot{m}_{in} \times L_B} \qquad \text{(per unit)}$$

or

$$\dot{s}_{\%} = 100\ \dot{s} \qquad \text{(percent)}$$

Note that $\dot{s}$ and $\dot{s}_{\%}$ have dimensions mass/unit time and length $\{ML^{-1}T^{-1}\}$.

For example, spillage rate of 10^{-5} or 0.001% per 0.30 m (1 ft) of belt, on a belt 30.5 m (100 ft) long fed at the rate of 1.8 Mg/h (2 ton/h), would amount to a total amount of mass spilled, over 1 hour, equal to

$$10^{-5} \times 10^{2} \times 1.8 \text{ Mg} = 1.8 \text{ kg (4 lb)}$$

This would represent 28 dm^3 (1 ft^3) of a material having a bulk density of 64 kg/m^3 (4 lb/ft^3).

The concept of admissible (or maximum) spillage rate, $\dot{s}_{max}$, can now be introduced at that upper bound on the spillage rate which, over the time periods and lengths of belt considered, is deemed to be tolerable under the conditions of use. As sketched in Figure 6, the designer might be able to choose, for a given material and system geometry, an operating point "P" leading to a lower spillage, $\dot{s}$, than the maximum tolerable one, $\dot{s}_{max}$.

Obviously, the absolute level of such spillage rate is partly a matter of judgment, partly specific to the material conveyed and the operating conditions at the site. By the same token, in designing a test procedure for the present investigation, the admissible (or maximum) spillage rate was selected on the basis of engineering judgment; not so small that it could

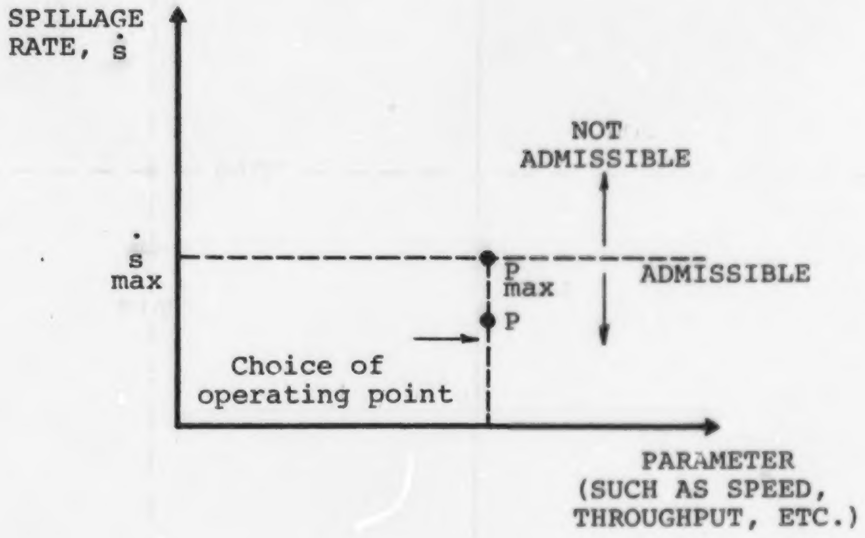
SPILLAGE RATE, $\dot{s}$
NOT ADMISSIBLE
$\dot{s}_{max}$
P_{max}
ADMISSIBLE
P
Choice of operating point
PARAMETER (SUCH AS SPEED, THROUGHPUT, ETC.)

Figure 6. Choosing an operating point for lower spillage than maximum admissible.

BEGIN LAST LINE OF TEXT
BOTTOM OF IMAGE AREA, OUTSIDE DIMENSION FOR TABLES AND ILLUSTRATIONS
3/8"

not be measured with a good degree to accuracy, yet not so large that it would make the volumes physically intractable and the flow rates unsteady. Thus, to some extent the choice of threshhold "$\dot{s}_{max}$" is also influenced by the material conveyed, the characteristics of the experimental set-up and the attainable ranges of test parameters, such as capacity, belt speed, etc.

Materials Conveyed:

In the present discussion, the material being conveyed is assumed to be given, from among the fractions listed and described in Section 2. Its properties and characteristics, in the sense explained previously, have been measured and recorded.

System Geometry --

The size and geometric characteristics of the conveyer belt are assumed to be known. In the present case, this amounts to giving (Figure 7):

- the belt width, w. This width can be divided in the part of the belt resting on the horizontal rollers, w_1, and the part resting on the idlers w_2; $W = w_1 + w_2$;
- the idler angle, β
- the spacing between idlers, ℓ, along the direction of the motion (not represented in Figure 7)

Static Capacity --

Assume that along a length of belt sufficiently long to be able to ignore end effects, the material under study is piled up on the belt, at rest, so that the edge of the pile, on either side, touches the edge of the belt. If a unit length (L = 1) of

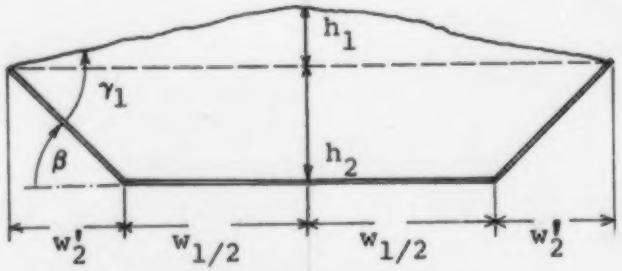

Figure 7. Cross-section of loaded belt (at rest).

BEGIN FIRST LINE OF TEXT HERE
CENTER OF PAGE
TOP OF IMAGE AREA
DROPPED HEAD. BEGIN SECTIONS HERE
6-1/2"
9-1/8"
BEGIN LAST LINE OF TEXT
3/8"
BOTTOM OF IMAGE AREA; OUTSIDE DIMENSION FOR TABLES AND ILLUSTRATIONS
PAGE NUMBER
EPA Form 2350-4 (4-80)
(PREVIOUSLY CIN. EPA FORM 287)
☆ U.S. GOVERNMENT PRINTING OFFICE 1980-660-639
TYPING GUIDE SHEET

belt is considered, it has a cross-section similar to that sketched in Figure 7. The static capacity, C_{ST}, will be defined by the area of this cross-section, computed as

$$C_{ST} = \frac{h_1}{2} (w_1 + 2w_2') + w_2 \tan \beta (w_2' + w_1) \qquad [1]$$

with $w_2' = \frac{1}{2} w_2 \cos \beta$ where β is the idler angle and h_1 is measured.

Note that C_{ST} has the dimension of an area $[L^2]$, and C_{ST} x 1 is the volume of material resting on a length L of belt.

Dynamic Capacity --

If in the experiment outlined above we set the belt in motion, the material resting on the belt will tend to "crumble" along the sides of the (two-dimensional) pile, and the cross-sectional area occupied by the material will decrease below the value at rest, C_{ST}.

In other words, the belt volumetric carrying capacity will not be that which would be realized if the cross-sectional area C_{ST} could be maintained without spillage under dynamic conditions (belt at speed V_B); namely

$$Q = C_{ST} V_B \quad [L^3T^{-1}] \qquad [2]$$

To quantify this reduction, it is proposed that a prescribed degree of spillage (per unit time and unit length of belt) be specified in advance, $\dot{s}$, say. Under such conditions, a measured (or computed) area of "capacity" C_{DYN} is obtained experimentally. The reduction in capacity resulting from the motion is then assessed by a reduction coefficient:

$$k_{Red} = \frac{DYN}{C_{ST}} \qquad [3]$$

which itself is a function of the dynamic parameters, as described hereunder, and of the prescribed degree of spillage. Intuitively, it is obvious that the dynamic capacity would, all other factors being equal, be expressed by a larger number if the allowed rate of spillage is larger.

One way to look at relationship [3] is to consider k_{RED} as a measure of the "efficiency" with which the volume above the belt is occupied under dynamic conditions, compared to the maximum volume achievable at rest, for a prescribed degree of spillage.

Fundamental Test Variables --

After these preliminaries, it is possible to state what the independent and dependent variables should be in the "basic" test proposed.

The geometry, size of the system, and the conveyed material are given. Among other properties, its bulk density, in the "conical" mode, has been determined. It is assumed that the variations of this density with the speed and loading of the belt are small and neglected (a fact qualitatively confirmed by observation).

The fundamental variables:

- mass flow rate, $\dot{m}$
- area of cross-section of the belt occupied by the material, or dynamic capacity, C_{DYN}
- V, belt speed

are related to each other and the measured bulk density, ρ_b, by

$$m = \rho_b C_{DYN} V$$

We are at liberty to select V, the belt speed, as an independent variable. Increasing it might increase the conveyor carrying capacity, but this is not uniformly true since excessive speeds would increase spillage beyond tolerable limits due to blow-back and vibrations.

Similarly, we could select C_{DYN}, the cross-sectional area of the material on the belt, as an independent variable, and attempt to increase it (for fixed V) to increase the carrying capacity. Again, this might only be possible to a point, due to excessive "mass spillage" from the crumbling sides of the moving load.

Finally, the throughput $\dot{m}$ and belt speed V could be varied, but the dynamic capacity, calculated from equation [4], would still need to be related to the observed spillage rate.

Thus, in actuality, equation [4] should be used as an equation to compute C_{DYN}, given a spillage rate $\dot{s}$ related to the throughput and belt speed by

$$\dot{m} = F(\dot{s}, V) \qquad [5]$$

or solving for $\dot{s}$:

$$\dot{s} = (\dot{m}, V) \qquad [6]$$

In this preferred form, the choice of independent and dependent test variables is apparent:

- for a series of experiments, the mass flow rate $\dot{m}$ will be set at a fixed value, $\dot{m} = \dot{m}$ (independent variable: $\dot{m}$)

- in that series of experiments, the velocity of the belt, V, will be varied over an operating range, i.e., $V = V_1$ such that $V_{min} \leq V_1 \leq V_{max}$ (independent variable: V)

For every pair $(\dot{m}_1, V_1)$, the spillage rate $\dot{s}$ will be measured as the dependent variable. As explained before, if $\dot{s} = s_*$ (some chosen value) for some pair $(\dot{m}_*, V^*)$ obtained from experimental or graphed results, C_{DYN}, the dynamic capacity for spillage rate s_*, is computed as

$$C^*_{DYN} = \frac{m_*}{\rho_b \; V^*} \qquad [7]$$

Dividing this expression by C_{ST}, previously defined, the dynamic coefficient of reduction in capacity, k^*_{RED} (corresponding to spillage rate s_*) is

$$k^*_{RED} = \frac{C^*_{DYN}}{C_{ST}} = \frac{m_*}{\rho_b \; C_{ST} \; V^*} \qquad [8]$$

In summary, it appears logical to select the throughput $\dot{m}$ and belt velocity V as independent variables, and to measure the spillage rate $\dot{s}$ as a dependent variable. Other subsidiary quantities, such as the dynamic capacity or coefficient or reduction in dynamic capacity or coefficient of reduction in static capacity, can tehn be computed from the previous ones.

On physical grounds, the expected dependence of the spillage rate on belt speed and mass flow rate can be obtained.

(a) Fixed Spillage Rate: Indeed, consider for given spillage rate, $\dot{s} = s^{\cdot}$, the dynamic reduction coefficient, k^*_{RED}. At very low speeds, this quantity is expected to be smaller than, but on the order of, 1. At very large speeds, on the other hand, the whole mass being conveyed will be spilled, due to aerodynamic effects, vibrations and shocks on the idlers. Ideally, $k^*_{RED} \to 0$ when $V^* \to V^*_1$, as shown in Figure 8. Thus, k^*_{RED} is conjectured to have the shape of a monotonously decreasing function, over the range of interest for V*. But, since the mass flow rate $\dot{m}_*$ corresponding to velocity V* and spillage rate $\dot{s}_*$ is $\dot{m}^* = \rho_b \; C_{ST} \; k^*_{RED} \; V^*_2$, it follows that $\dot{m}^*$ should have a maximum, shown as point Z in Figure 8. Thus: At

BEGIN FIRST LINE OF TEXT HERE
CENTER OF PAGE
TOP OF IMAGE AREA
DROPPED HEAD; BEGIN SECTIONS HERE
6-1/2"
9-1/8"
BEGIN LAST LINE OF TEXT
BOTTOM OF IMAGE AREA; OUTSIDE DIMENSION FOR TABLES AND ILLUSTRATIONS
3/8"
PAGE NUMBER
EPA Form 2350-4 (4-80)
(PREVIOUSLY CIN. EPA FORM 287)
☆ U.S. GOVERNMENT PRINTING OFFICE: 1980-660-639
TYPING GUIDE SHEET

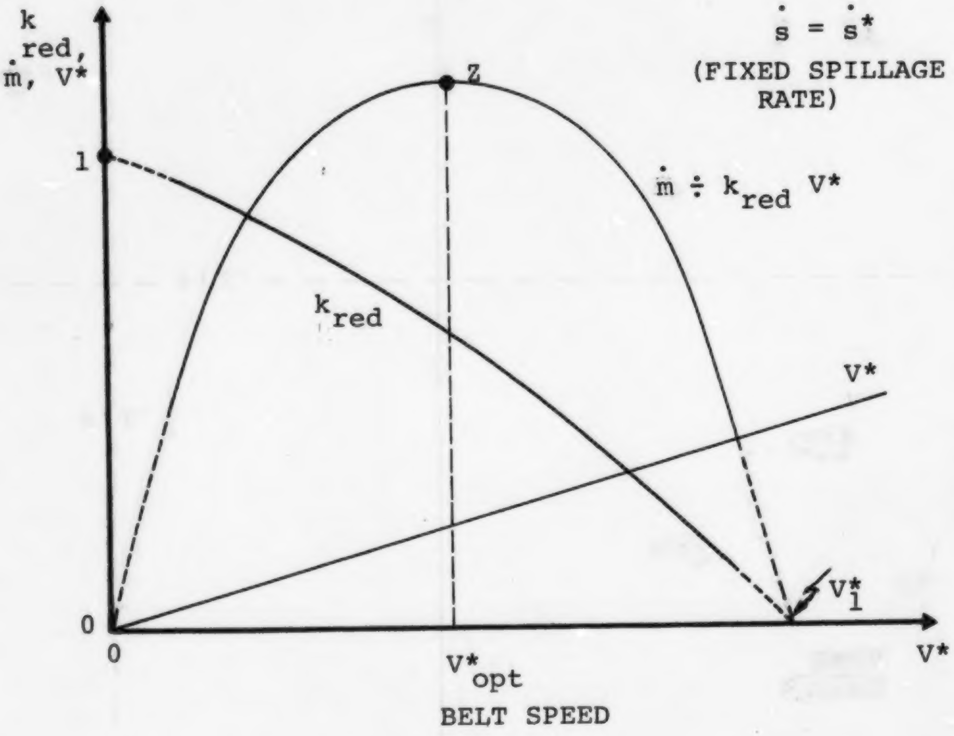

Figure 8. Shape of curves of dynamic reduction coefficient vs. speed, and mass flow rate vs. speed (fixed spillage).

BEGIN LAST LINE OF TEXT
BOTTOM OF IMAGE AREA, OUTSIDE DIMENSION FOR TABLES AND ILLUSTRATIONS
3/8"

given spillage rate, there should exist an optimal velocity, for which throughput is maximized.

(b) Fixed Mass Flow Rate. Using Figure 8, in a plane of coordinates mass flow rate, velocity of $(\dot{m}, V)$, it is thus possible to locate two points, of abscissa V_C, V_D, respectively and ordinate $\dot{m}$, which are on a locus $\dot{m} = (\dot{s}_*, V)$, i.e., a curve of constant spillage rate, $\dot{s}_*$ (Figure 9).

If a number of plots such as Figure 8 were drawn, a family of curves having the shape sketched in Figure 9 and corresponding to various mass flow rates could be obtained. From these, in turn, curves, giving the spillage rate vs. V, for given mass flow rate $\dot{m}$, are derived and given by equation $\dot{s} = (\dot{m}, V)$. For convenience, these curves will be labeled the "$\mathcal{S}$" curves (Figure 10).

(c) Use of the $\mathcal{S}$ Curves in System Design. In Figure 9, possible uses of the network of curves are illustrated, such as:

- checking that a selected operating point, say P of coordinates $(V_P, \dot{m}_P)$ on Figure 10 corresponding to a combination of belt speed and throughput, has a spillage rate $\dot{s}_P$ which is considered acceptable
- determining the maximum throughput, $\dot{m}_Q$, and corresponding velocity V_Q, achievable at the prescribed maximum spillage $\dot{s}_{max}$ (Figure 10)
- choosing a preferred operating point between the two points (P and R on Figure 10) corresponding to a rate of spillage $\dot{s}_P < \dot{s}_{max}$. If, for example, the range $(\dot{m}_P, \dot{m}_T)$ has to be covered in operation, then R would be preferable to P, since the rate of spillage corresponding to $(V_P, \dot{m}_T)$ exceeds the maximum admissible $\dot{s}_{max}$. Such is not the case for point R, for which $\dot{s}_U$, corresponding to the higher speed V_R and a mass flow rate $\dot{m}_T$, is lower than the maximum admissible.

Inclined Belt: Analysis of Test Procedure and Variables

Preliminary Comments --

The geometry of the inclined conveyor belt is sketched in Figure 11. In the present case, the inclination, α, is not zero.

If α is progressively increased until it reaches a threshold, α_{TH}, or angle of maximum inclination, the material will roll

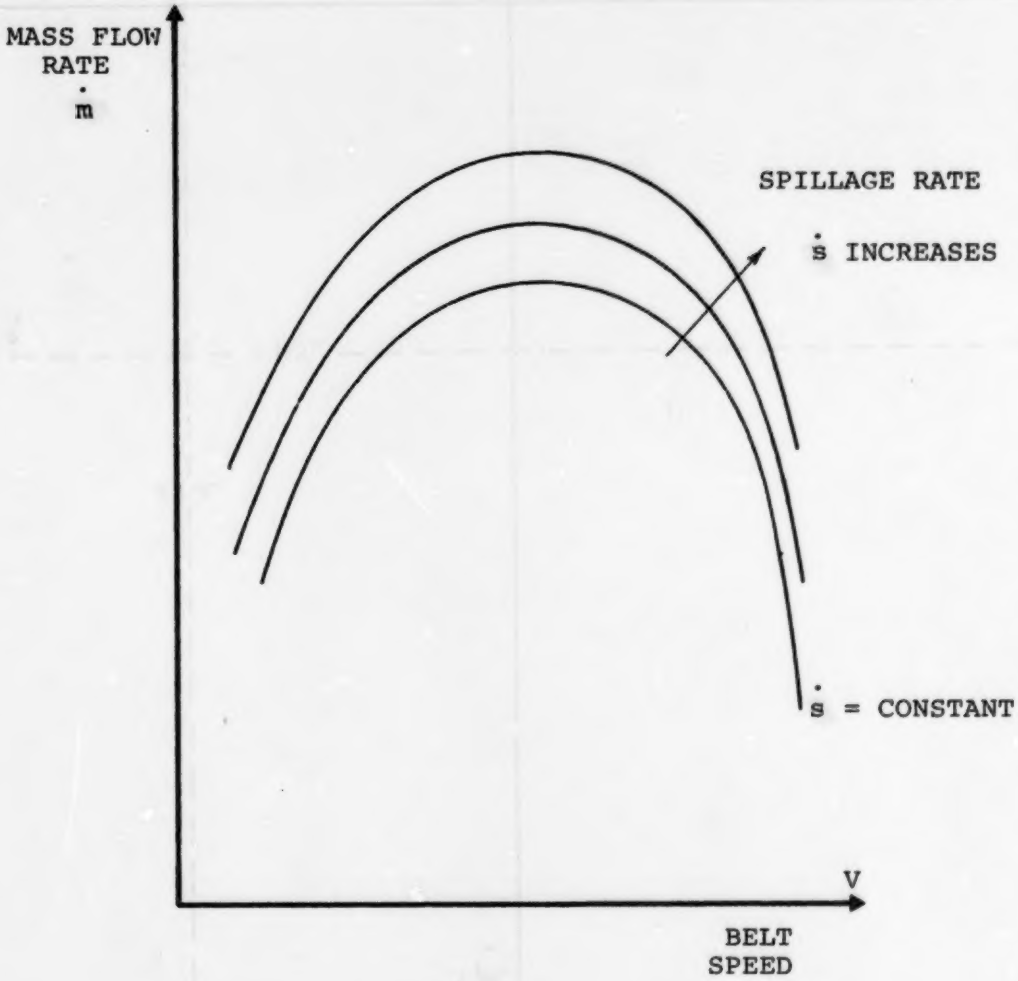

Figure 9. Curve of mass flow rates vs. belt speed for various spillage rates

BEGIN LAST LINE OF TEXT
3/8"
BOTTOM OF IMAGE AREA; OUTSIDE DIMENSION FOR TABLES AND ILLUSTRATIONS

PAGE NUMBER
EPA Form 2350-4 (4-80)
(PREVIOUSLY CIN. EPA FORM 287)
U.S. GOVERNMENT PRINTING OFFICE 1981 [illegible]
TYPING GUIDE SHEET

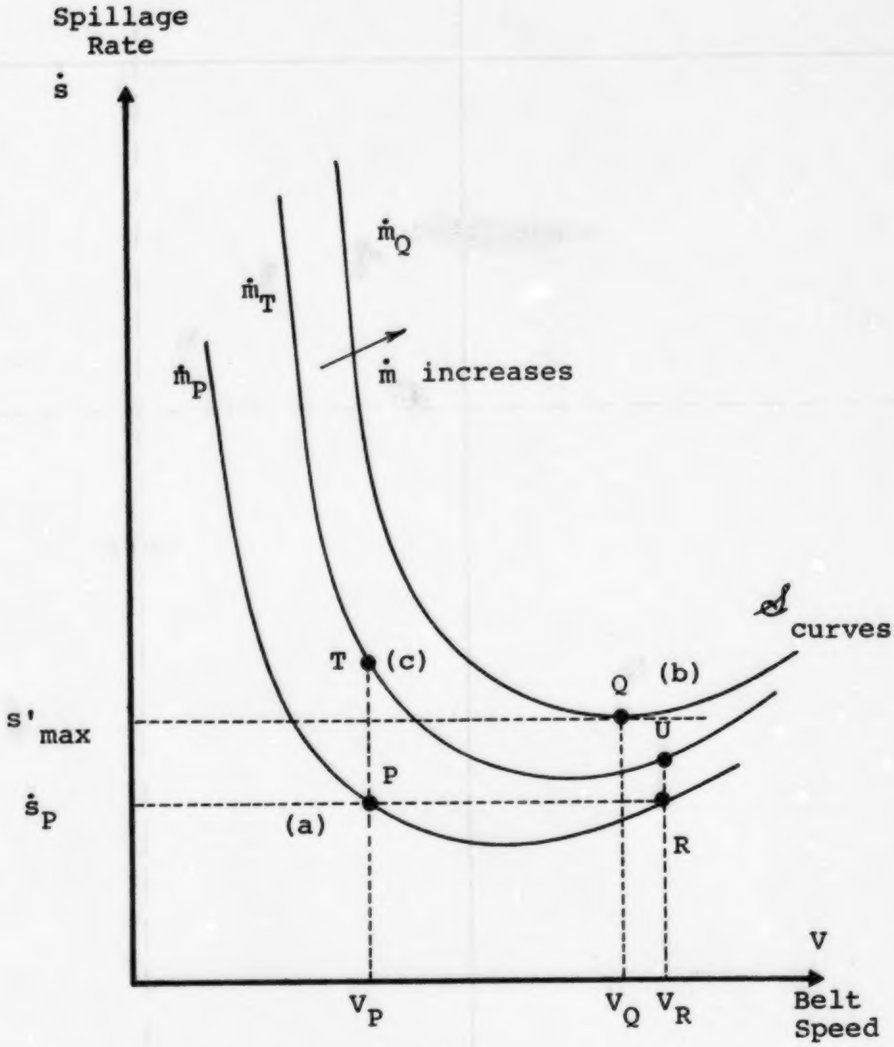

Figure 10. Examples of use of $\mathscr{S}$ curves.

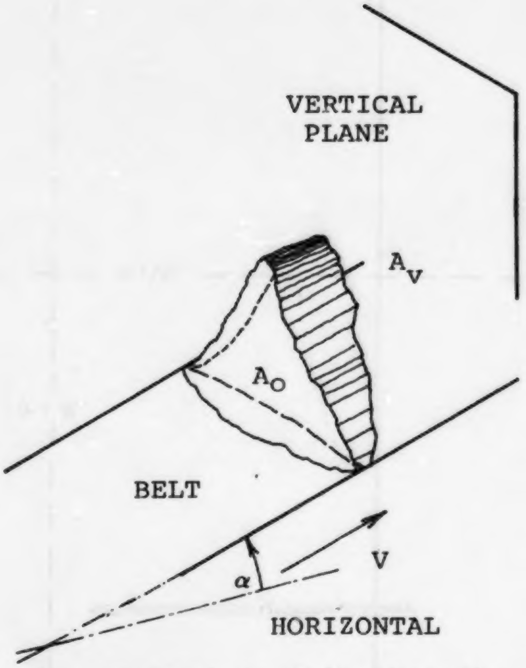
VERTICAL PLANE
A_V
A_O
BELT
V
α
HORIZONTAL

A_O: normal to belt through and belt speed

A_V: vertical - $A_V = \dfrac{A_O}{\cos \alpha} > A_O$

Figure 11. Increase in vertical cross section with inclination.

BEGIN LAST LINE OF TEXT
3/8"
BOTTOM OF IMAGE AREA; OUTSIDE DIMENSION FOR TABLES AND ILLUSTRATIONS

back on the belt. The forward motion of the material on the supporting inclined belt becomes impossible.

From the results in Table 3, Section 2, it is observed that threshold α_{TH} is significantly lower than the angle of slide on the conveyor belting material. At angles equal to or larger than α_{TH}, backsliding becomes so pronounced that adequate, steady feeding cannot be maintained at the transfer point between the apron-feed/chute and the tail pulley of the belt. Accordingly, the experiments were limited to an upper limit for the inclination angle, α, relatively close to but lower than α_{TH}. For example, as described in detail in the test results below, for MSW:

Angle of maximum inclination of the belt: $\alpha_{TH} = 19°$

Angles selected for inclined tests: 18° (max.), 14°.

Choice of Variables --

As explained above in the case of the horizontal belt, it appears logical to select as independent variables, for a given inclination angle α of the belt on the horizontal (refer to Figure 10):

- the belt speed V
- the mass flow rate, or carrying capacity, $\dot{m}$.

The dependent variable will again be: $\dot{s}$: spillage rate per unit mass of throughput and unit length of belt (as previously defined).

In a gross, qualitative sense, the arguments given in the preceding pages to justify the dependence of the spillage rate on the belt speed, at given mass flow rate $\dot{m}$, and of the spillage rate on the mass flow rate, at given belt speed, are expected to remain valid for the inclined belt, provided the angle of inclination is not too close to that leading to generalized slip and rollback.

Hence the curves mass flow rate vs. belt speed, given V belt speed, should have the general shape shown in Figure 9. Those giving spillage rate vs. V, belt speed, given the capacity $\dot{m}$, would then look like the "α" curves of Figure 10. The "steepness" of the sides, value of the optimum speed leading to minimum spillage and generally, position of the curve in the plane of representation are expected, obviously, to depart from those corresponding to the horizontal case.

BEGIN FIRST LINE OF TEXT HERE
CENTER OF PAGE
TOP OF IMAGE AREA
DROPPED HEAD: BEGIN SECTIONS HERE
6-1/2"
9-1/8"
BEGIN LAST LINE OF TEXT
BOTTOM OF IMAGE AREA; OUTSIDE DIMENSION FOR TABLES AND ILLUSTRATIONS
3/8"
PAGE NUMBER
EPA Form 2350-4 (4-80)
(PREVIOUSLY CIN. EPA FORM 287)
☆ U.S. GOVERNMENT PRINTING OFFICE 1980-660-639
TYPING GUIDE SHEET

Increasing the Inclination at Given Mass Flow Rate and Belt Speed --

Qualitatively speaking, an argument could be put forth that increasing the inclination, from zero, leads to cross-section A_V (instead of A_0, for $\alpha = 0$) larger and with steeper slopes (Figure 11). In the horizontal case, at relatively "low" V, the increase in carrying cross-section (or dynamic section) necessary to carry the same mass flow rate $\dot{m}$ at lower speed is accompanied by an increase in spillage rate. A similar effect can be presumed to exist if the belt is inclined: moderate for moderate inclinations, but extremely pronounced as α approaches the belt maximum inclination α_{TH}. As a function of V, the effect should be less important at high speeds than at low speeds, since less of the belt width is utilized and the height of burden can be kept smaller for the same capacity (Figure 11).

An increase in mass flow rate, when conveying a given material on a belt of given inclination α running at a given speed V, entails an increase in area of the cross-section on the belt occupied by material. This should cause an increase in spillage rate, as schematized in Figure 12.

Assuming the "$\mathcal{S}$" curves giving: $\dot{s} = \alpha(m, V)$ for inclination α have the shape shown in Figure 13, then there exists a minimum spillage $\dot{s} = \dot{s}_*$, at given mass flow rate $\dot{m} = \dot{m}_*$, corresponding to an optimum operating belt speed equal to V_*.

Operating Point --

At inclination α and mass flow rate $\dot{m}_P$, two operating points, P and Q, might exist corresponding to a spillage rate $\dot{s}$ not exceeding the admissible one, $\dot{s}_{max}$ is reached.

Operating Range --

The experimental results described below show that, in most instances, the sensitivity of the spillage rate to an increase in flow rate and/or inclination is, for the same level of spillage, much smaller in the upper range of belt speeds (i.e., to the right of the point). In such cases, it would be recommended to operate in this range, for lower spillages under deliberate or accidental variations of belt speed and mass flow rates about the nominal design conditions. Figuratively speaking, at any practical inclination, the belt should be operated "fast and lean" rather than "slow and loaded."

Other Comments --

At high speed, the increase in spillage rate is due to aerodynamic "blow-back" and vibrations and shocks on the rollers

BEGIN LAST LINE OF TEXT
3/8"
PAGE NUMBER
BOTTOM OF IMAGE AREA: OUTSIDE DIMENSION FOR TABLES AND ILLUSTRATIONS
EPA Form 2350-4 (4-80)
(PREVIOUSLY CIN. EPA FORM 287)
TYPING GUIDE SHEET

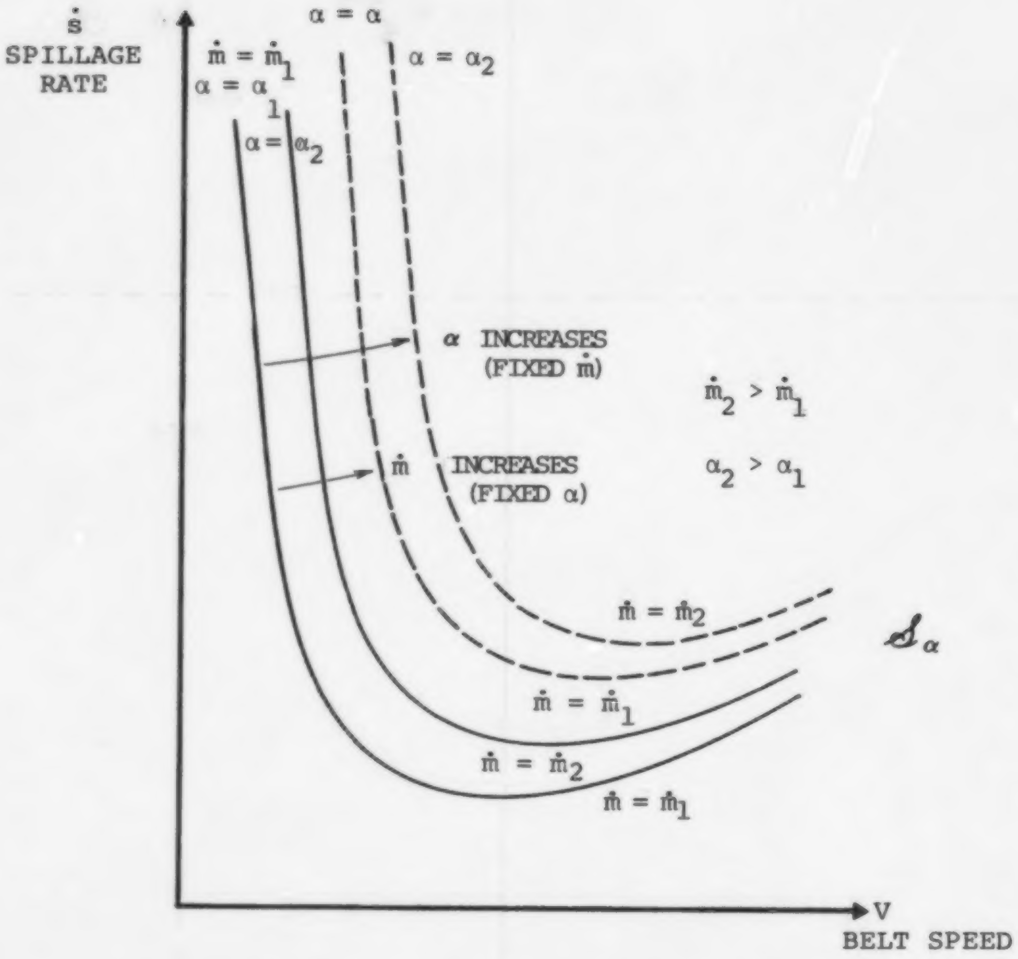

Figure 12. Family of curves "$\mathcal{S}_\alpha$."

BEGIN LAST LINE OF TEXT
3/8"
BOTTOM OF IMAGE AREA; OUTSIDE DIMENSION FOR TABLES AND ILLUSTRATIONS

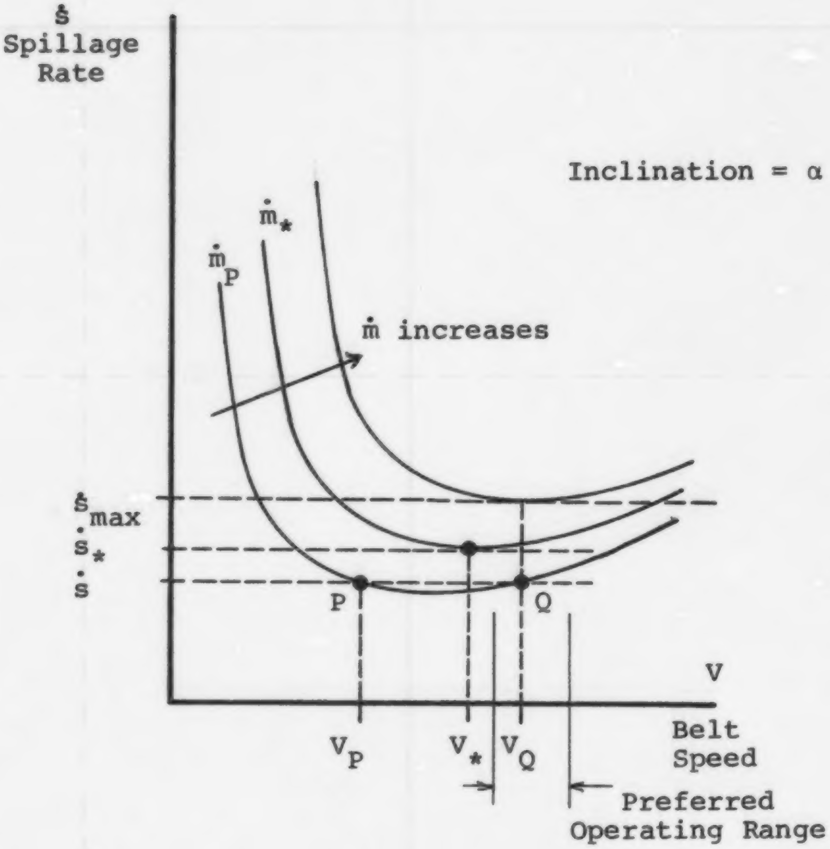

Figure 13. Optimum speed V_* and preferred operating range, at inclination α.

BEGIN LAST LINE OF TEXT
3/8"
BOTTOM OF IMAGE AREA; OUTSIDE DIMENSION FOR TABLES AND ILLUSTRATIONS

and idlers. Physically, aerodynamic "detachment" and "vibrations" should not depend to any degree on inclination, at small angles to the horizontal. Thus, the level of spillage, all other factors being equal, should not vary much with the inclination α if the material is flat and self-compacting, as is the case with RDF. However, waste or fractions thereof containing a fair percentage of spherical or cylindrical fractions thereof containing a fair percentage of spherical or cylindrical pieces likely to roll down the inclined belt, should show a rapid increase of spillage with speed in the upper range of speeds.

BELT CONVEYORS: SUMMARY OF RESULTS

Test Belt Conveyor and Test Procedures

The 7.63 m (25 ft) long and 0.457 m (18 in.) wide test belt conveyor was mounted in the closed loop rig shown in Figure 1. A variable speed drive provided a belt speed range of 0.20 m/s (40 fpm) to 2.55 m/s (480 fpm). Three-roller idlers of 20 and 35° and spaced at 0.91 m (3 ft) were used for the tests. A feed chute and 1.1 m (3.5 ft) of skirting were installed (following CEMA installation criteria) at the tail (feed) end of the conveyor in order to guide the material onto and across the conveyor belt. No other skirting was used during the tests.

By fixing the test conveyor speed (with all other belt speeds fixed) and placing a certain fixed mass of material on the test rig, a quasi-constant mass flow rate was provided. The material was recirculated for a period of 30 minutes and then all spillage from the test belt, including its frame, pulleys and from the floor was accumulated and weighed. The sides of the test conveyor were isolated plastic sheets to avoid including spillage from the return and feed conveyors (Figure 2).

Horizontal Mode Test Results

Dependency of Spillage on Speed and Mass Flow Rate --

Results are given in Figures 14 to 22 for:

- shredded MSW, RDF and heavy fraction for three mass flow rates and two idler angles (20 and 35°) (Figure 14-19); and
- the ferrous fraction, d-RDF and d-RDF/coal blends for three mass flow rates and 35° idlers (Figures 20-22).

Note that the spillage is presented as a spillage rate reported as a percent of mass flow rate over the 7.63 m (25 ft) length test belt.

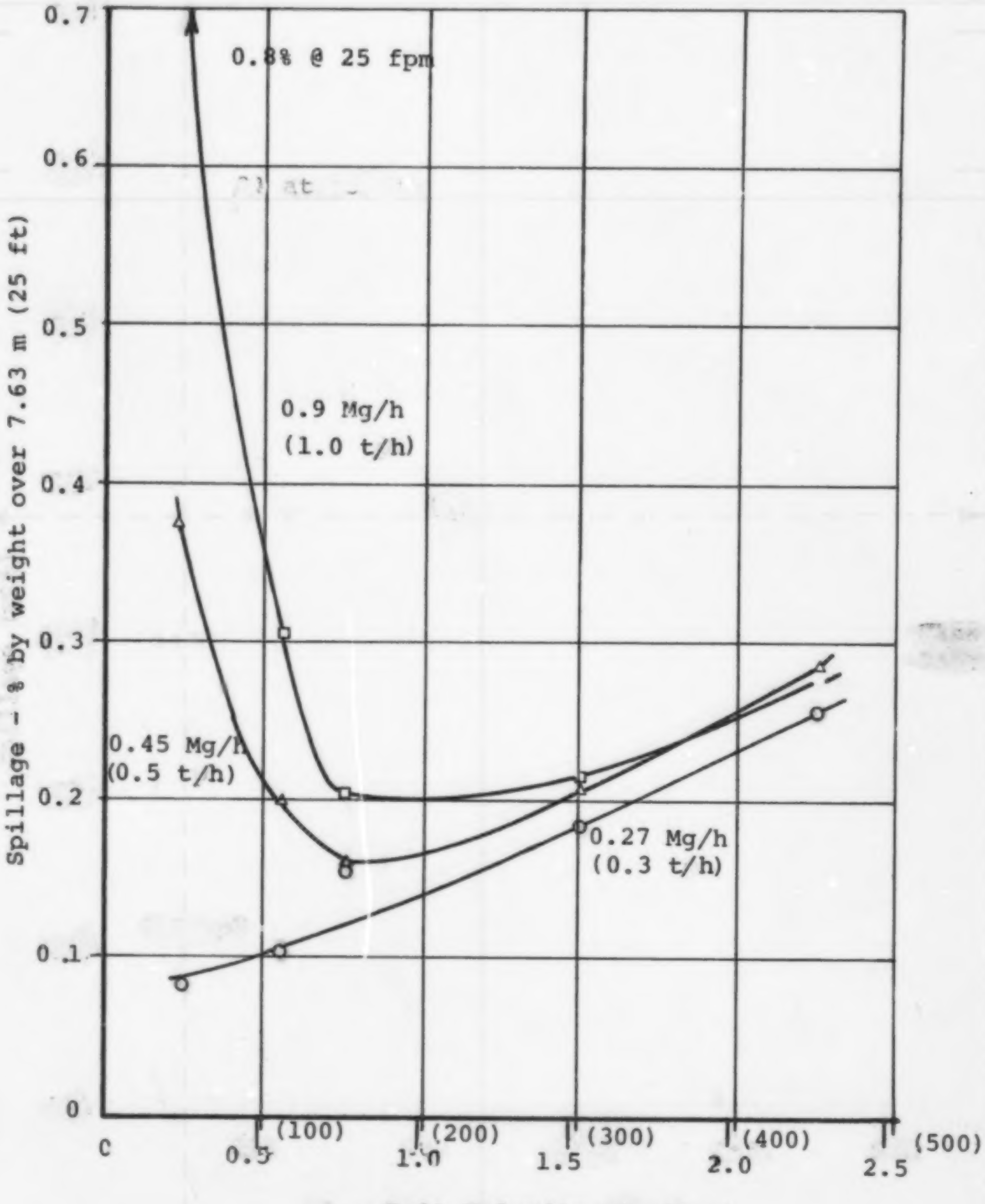

Figure 14. MSW sample spillage vs. belt velocity and mass flow rate with horizontal belt and 20° idlers.

LAST LINE OF TEXT
3/8"
OUTSIDE DIMENSION FOR TABLES AND ILLUSTRATIONS
PAGE NUMBER
EPA Form 2350-4 (4-80)
(PREVIOUSLY CIN. EPA FORM 257)
TYPING GUIDE SHEET

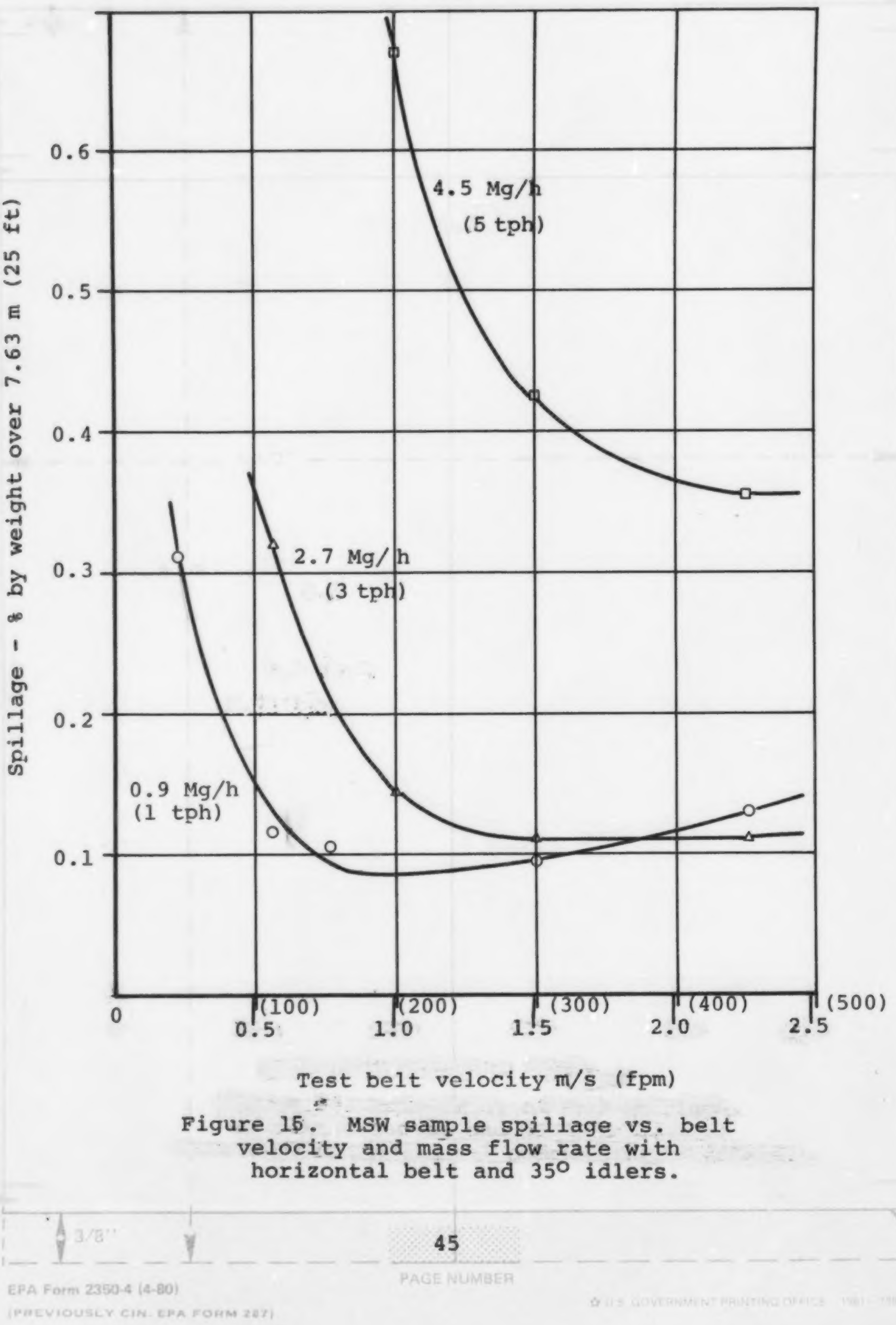

Figure 15. MSW sample spillage vs. belt velocity and mass flow rate with horizontal belt and 35° idlers.

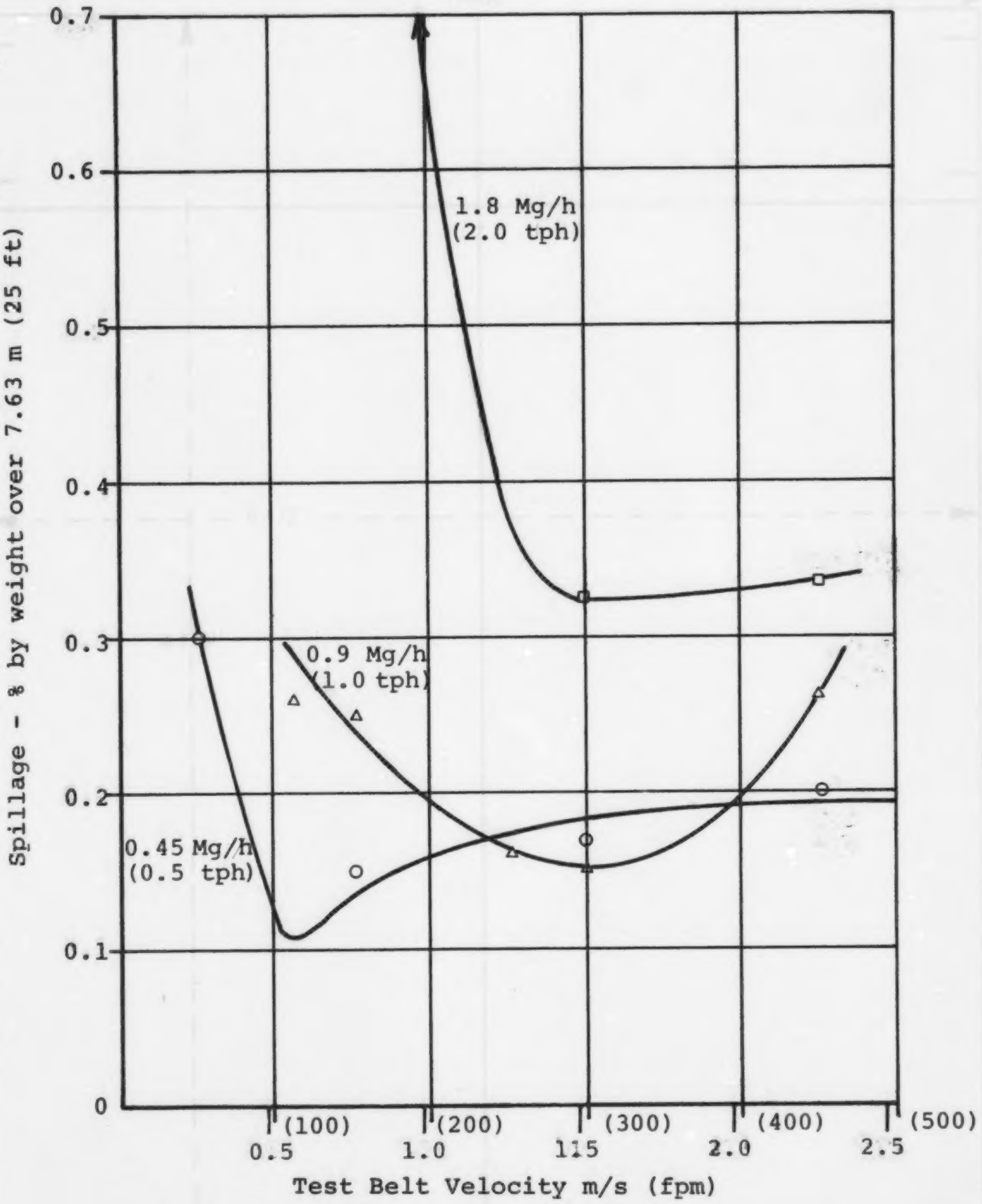

Figure 16. RDF sample spillage vs. belt velocity and mass flow rate with horizontal belt and 20° idlers.

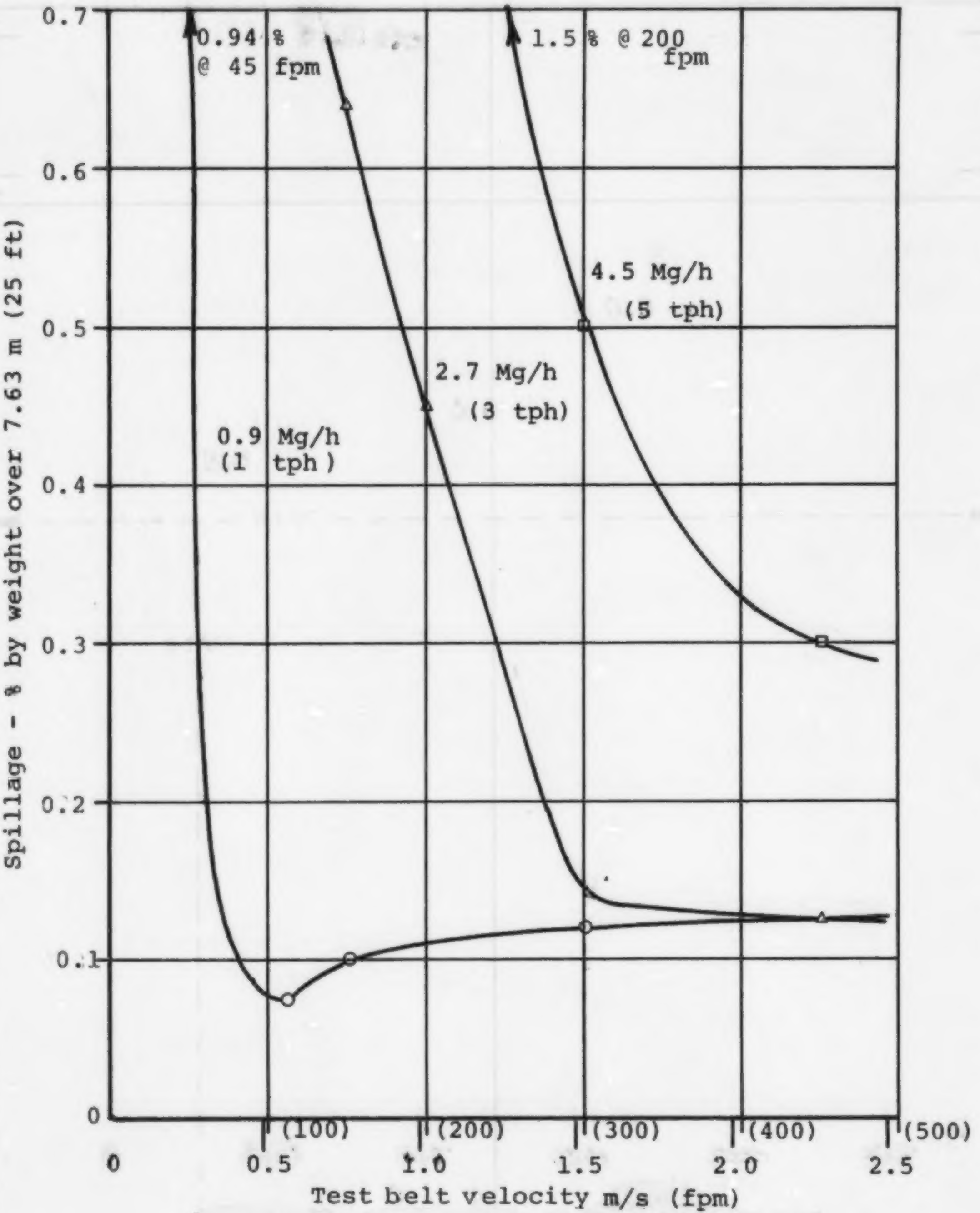

Figure 17. RDF sample spillage vs. belt velocity and mass flow rate with horizontal belt and 35° idlers.

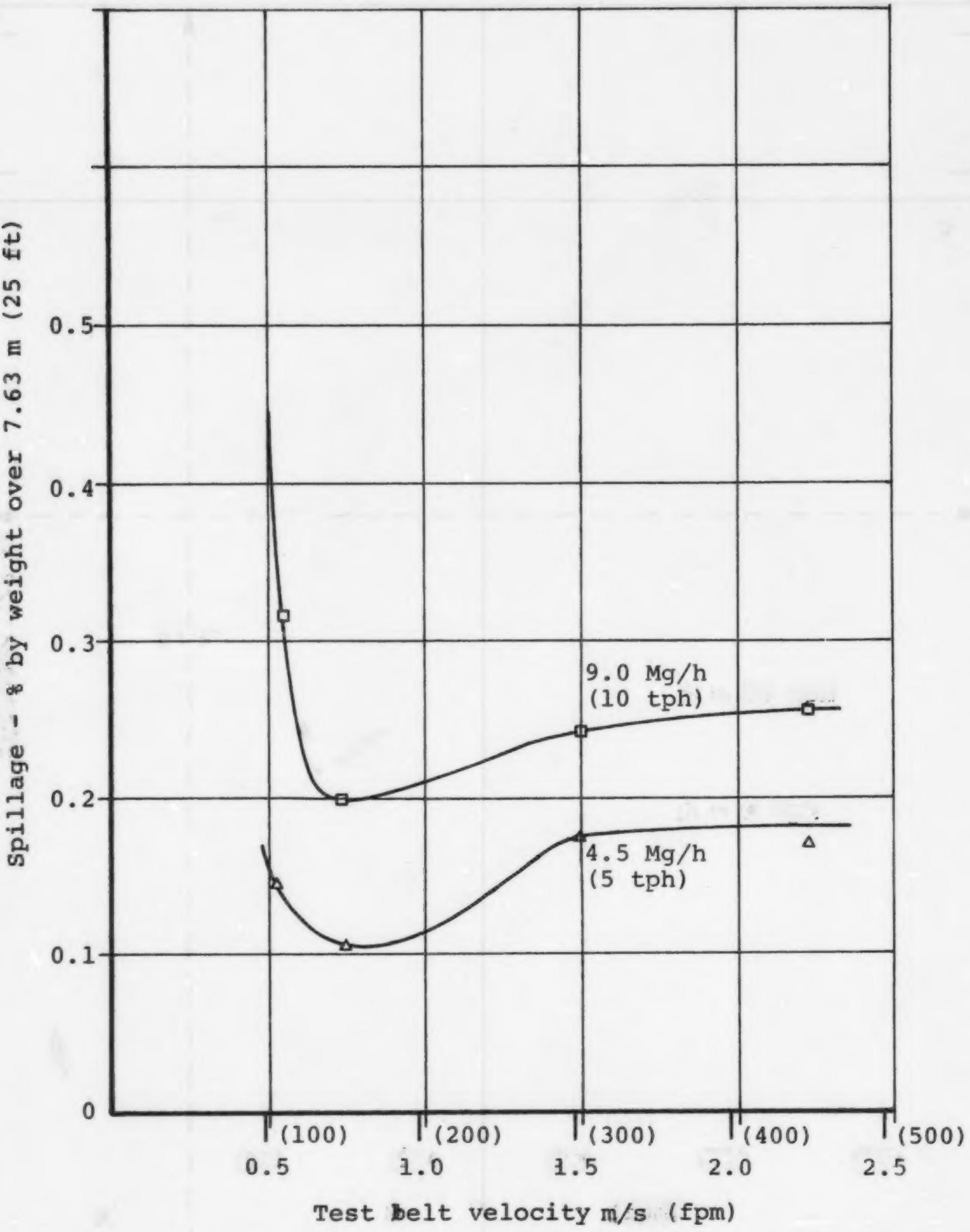

Figure 18. Heavy fraction sample spillage vs. belt velocity and mass flow rate with horizontal belt and 20° idlers.

BEGIN FIRST LINE OF TEXT HERE

DROPPED HEAD: BEGIN SECTION HERE

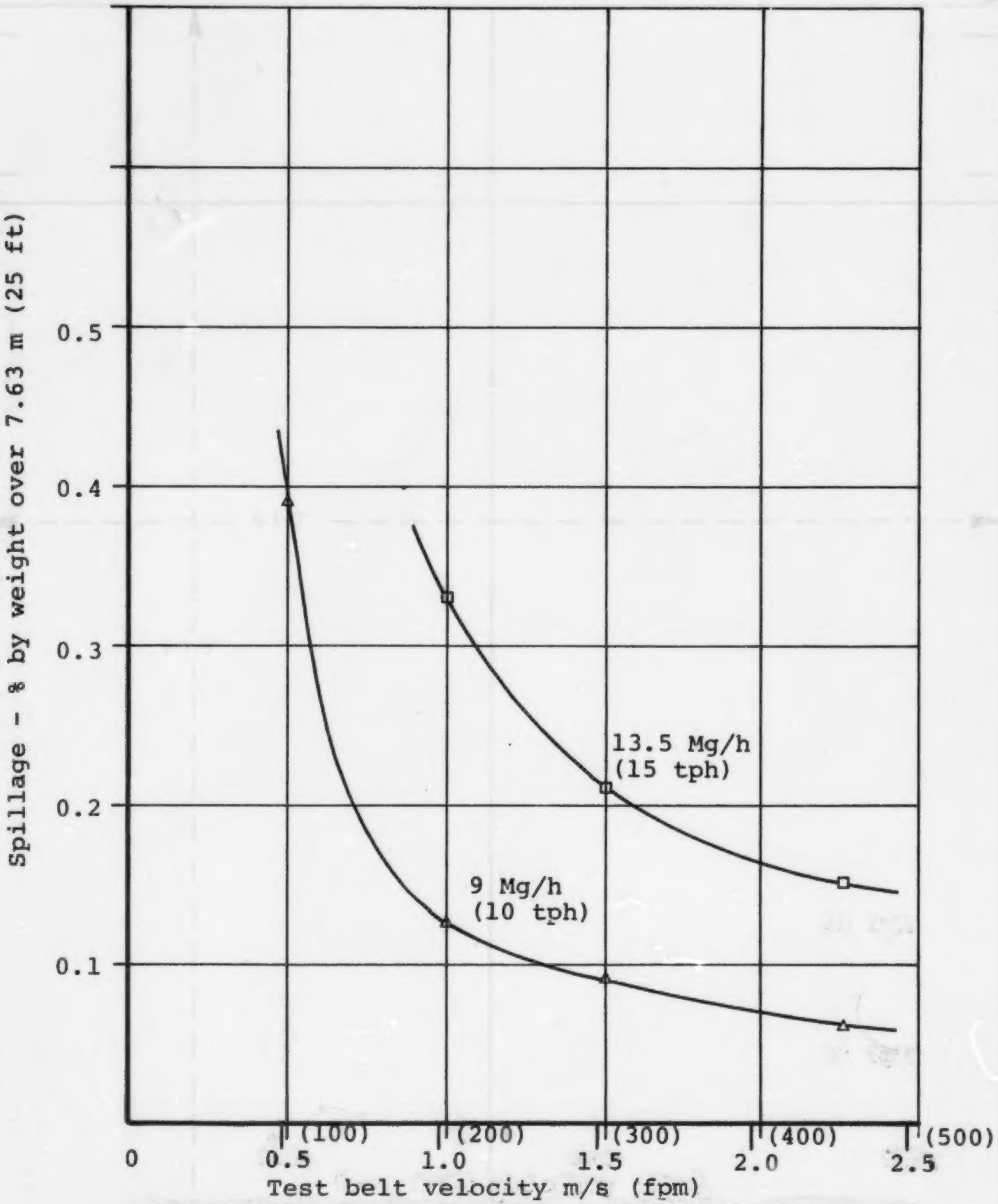

Figure 19. Heavy fraction sample spillage vs. belt velocity and mass flow rate with horizontal belt and 35° idlers.

BEGIN LAST LINE OF TEXT

BOTTOM OF IMAGE AREA OUTSIDE DIMENSION FOR TABLES AND ILLUSTRATIONS

3/8"

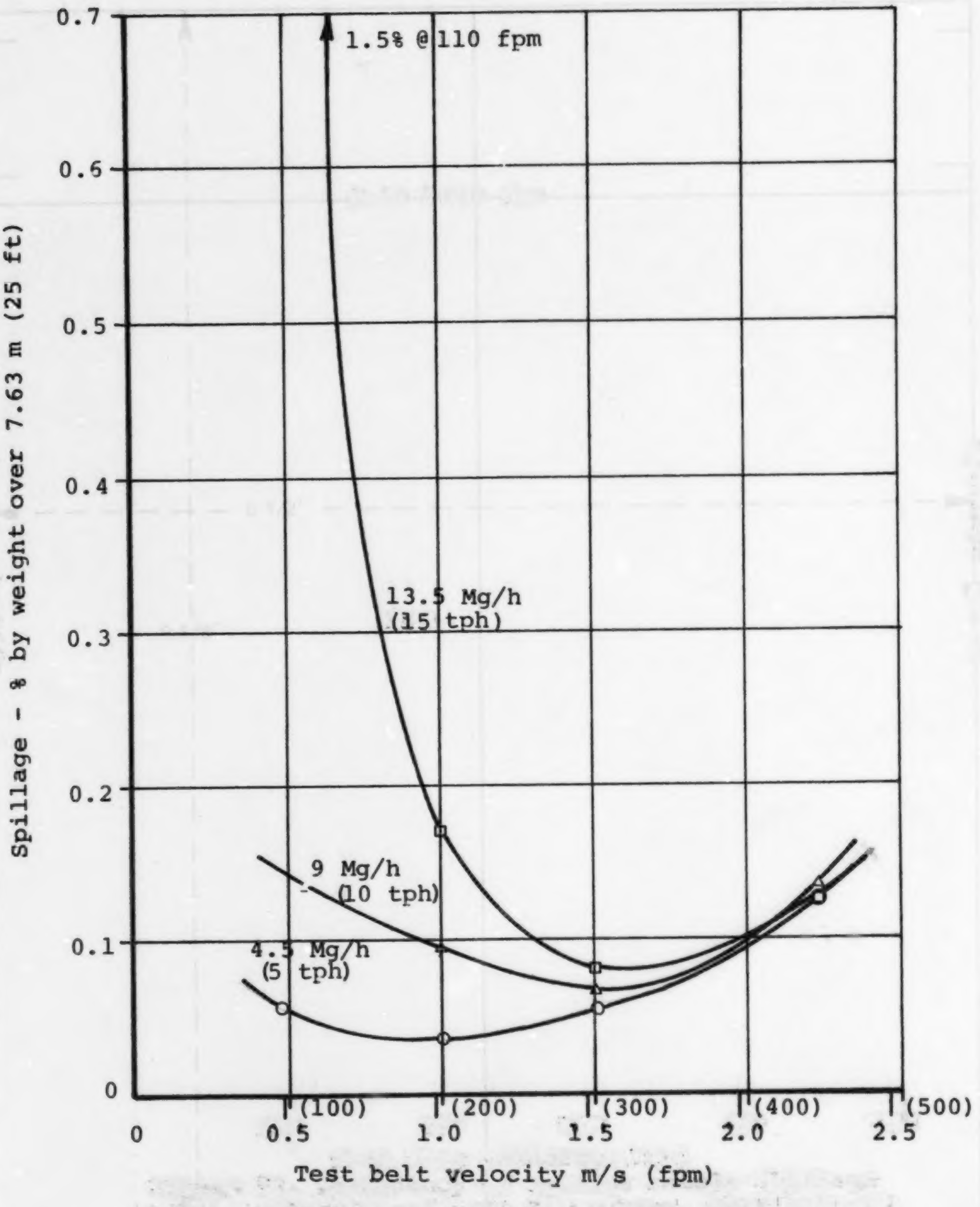

Figure 20. Ferrous metal sample spillage vs. belt velocity and mass flow rate with horizontal belt and 35° idlers.

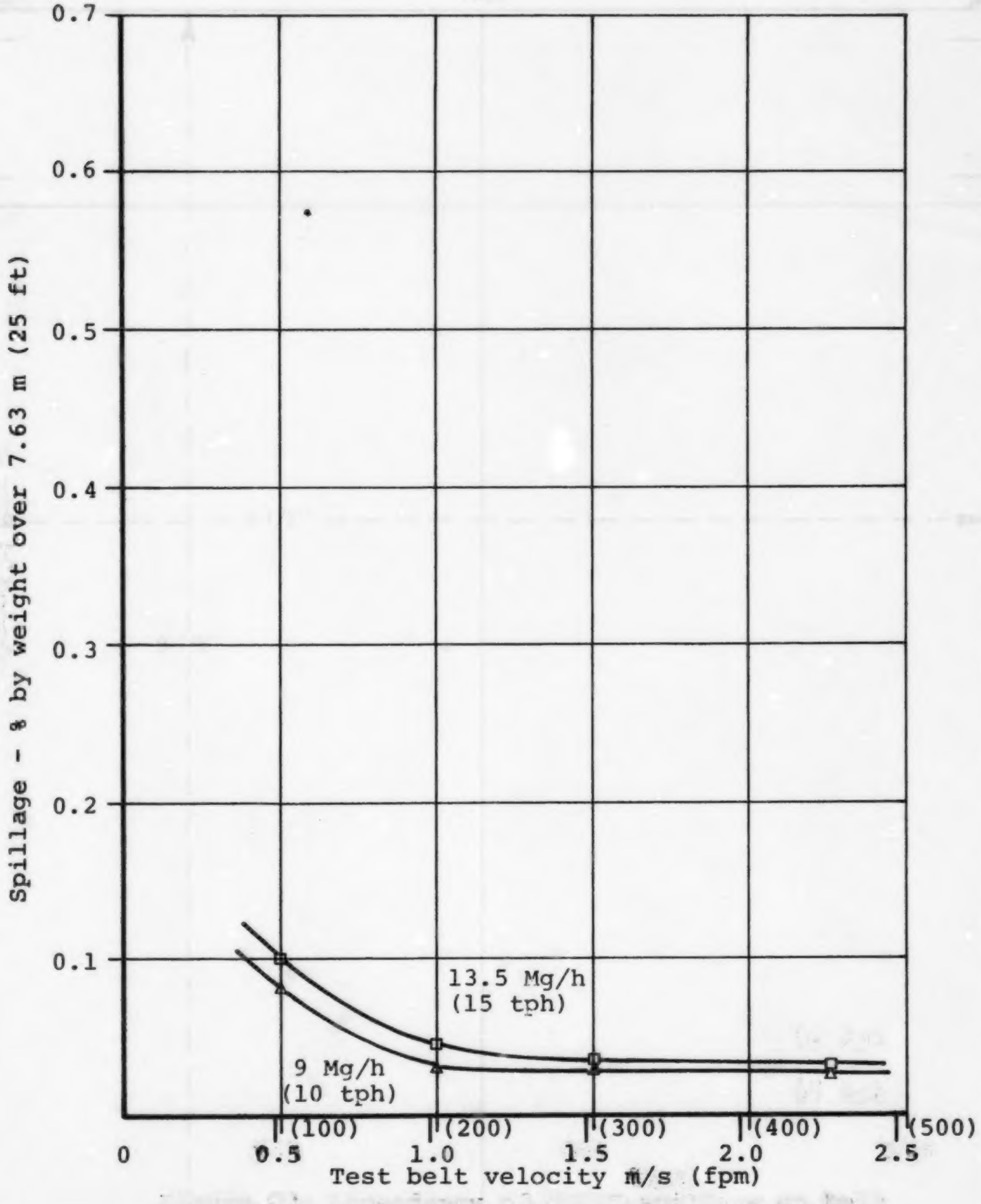

Figure 21. d-RDF sample spillage vs. belt velocity and mass flow rate with horizontal belt and 35° idlers.

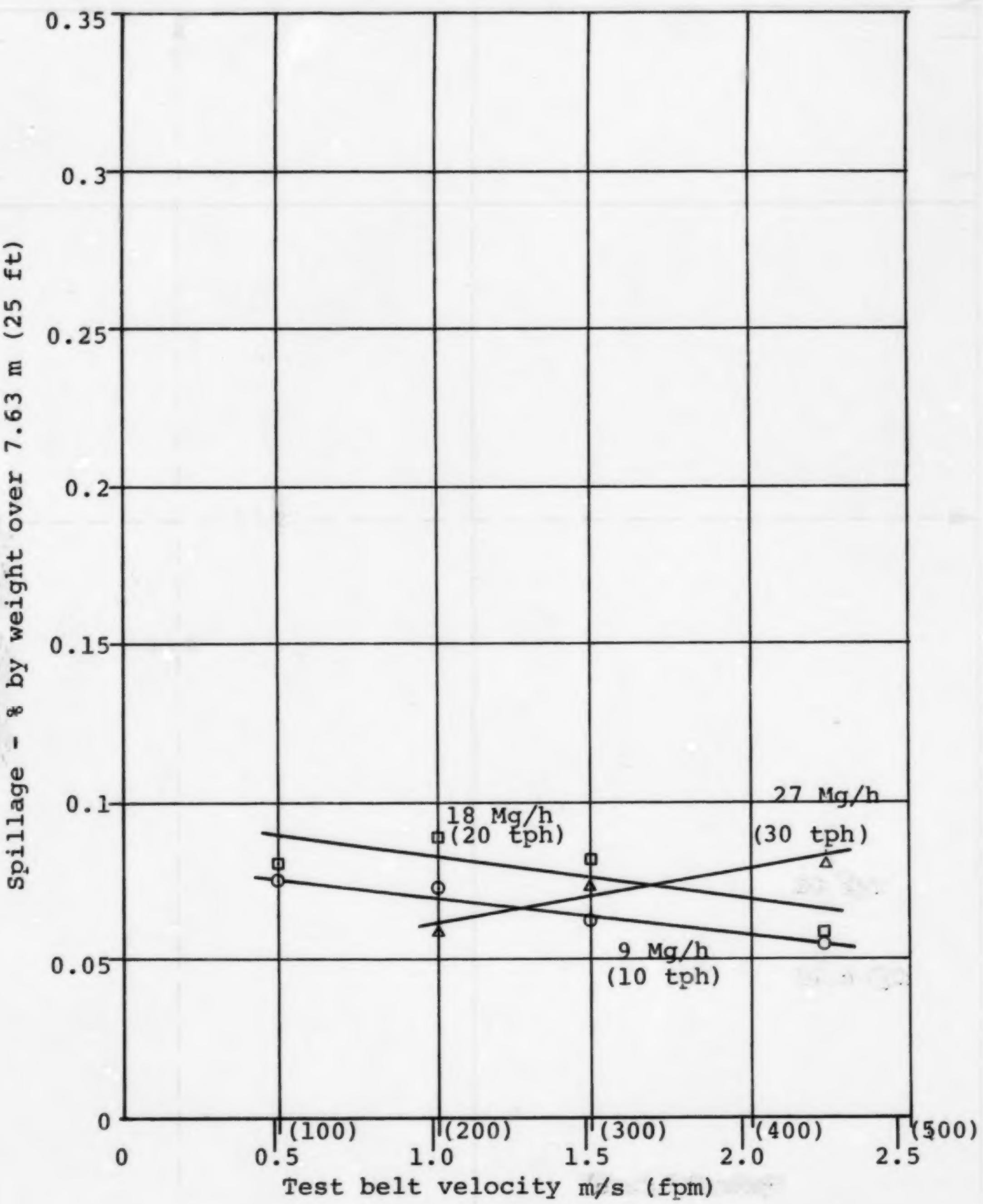

Figure 22. Coal/d-RDF blend sample spillage vs. belt velocity and mass flow rate with horizontal belt and 35° idlers.

These results confirm the analysis outlined in the previous section. High spillage rates are observed at lower belt speeds, then as belt speed increases, the rate of spillage (for a constant mass flow rate) is reduced to a minimum. Gradually, spillage rates increase again with increased velocity. Higher mass flow rates, for a given test material and belt speed, lead to higher spillages, and the location of the minimum spillage points move toward the higher belt speeds. A discussion of the distribution and causes of the spillage are discussed in the next section.

Although all the solid waste fractions show similar patterns of behavior (Figures 14 to 22), the specific spillage rates for each individual fractions are dependent on its properties and characteristics. For example, d-RDF, a relatively homogeneous and uniform material, shows a much lower spillage rate than other, more heteorogeneous and coarse fractions (Figure 21).

It is interesting to note from the data that operation of a conveyor belt to transport solid waste fractions, unless for very low throughputs, always generates spillage. Also, the results clearly indicate that utilization of 35° troughing idlers help in obtaining higher conveying throughput rates for the same velocity and amount of material spilled over a given time. For example, in Figure 14, if the admissible spillage rate is arbitrarily established at 0.2%, a belt conveyor with 20° idlers operated at 1.02 m/s (200 fpm) has a maximum carrying capacity of 0.9 Mg/h (1.0 tph) of MSW. However, maintaining the velocity at 1.02 m/s (200 fpm) utilizing 35° idlers (Figure 15), the maximum capacity, applying the same spillage criteria, is approximately 2.9 Mg/h (3.25 tph) of MSW. Similar increases in carrying capacity were observed with all of the other test fractions.

Spillage Distribution Along the Test Belt Conveyor --

The test data reported in Figures 14 to 22 indicate the total weight of material spilled from the full length of conveyor length during the test period. On selected tests, data were also collected to establish the proportion of spillage from one of four conveyor sections. The results provide some insight to specific problem areas, and suggest the zones where conveyor modifications (skirting, hoods, etc.) could most effectively reduce spillage.

For this test, the belt conveyor, as in Figure 23, was divided into four sections (labeled 1 to 4, measured from the tail to the head pulley) of length 1.1 m (3.5 ft), 1.7 m (5.5 ft), 3.7 m (12 ft) and 1.2 m (4 ft) respectively (see Figure 23). Spillage was separately collected and weighed for each of these sections.

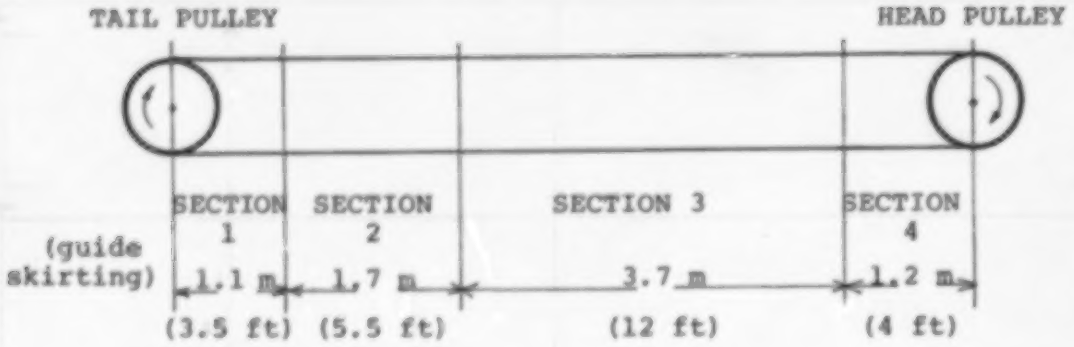

Figure 23. Sub-division of the test belt conveyor for sectional spillage measurements.

Care was taken in isolating the spillage from one area and preventing carryover of material from one section to another. Sheeting was used to prevent material falling on the return idlers frame or on the return side of the belt and being carried back towards the tail pulley.

Table 12 presents the results of sectional spillage measurements on four fractions at a single mass flow rate and three velocities. The observations made on the nature and mechanisms of spillage from each belt section are instructive. The results for RDF are used as an example. At a lower speed of 0.76 m/s (150 fpm), most of the RDF spillage occurs in the first two sections. The spillage in Section 1 (37.5%) was a result of fines, mainly inert, inorganic particles, wedging between the belt and its skirting, and being squeezed and blown out by material falling on the belt. The spillage in Section 2 (43.0%) is the result of crumbling and sluffing of the RDF, particularly from surges, over the sides of the conveyor. The proportion of material spilled in Sections 3 and 4 is relatively low at this lower conveyor speed.

The spillage of RDF measured for the same loading but higher speeds of 1.53 m/s (350 fpm) and 2.28 m/s (450 fpm) is observed to shift proportionally from Sections 1 and 2 to Section 4. As the material is transported faster and in a thinner strip, it has less tendency to crumble and spill under the skirting and over the sides. The greater spillage in Section 4 may be the result of several factors. Air currents (blow-back) created at higher speeds are observed to sweep paper and lighter materials off the belt. The reaction of the belt as it passes over the idlers is also amplified at higher speeds and results in a rhythmic bounce which will increase spillage of more dense com-

TABLE 12. SECTION CONVEYOR SPILLAGE AS A PERCENT OF TOTAL SPILLAGE

Product	Belt Section	Percent of Total Spillage Test Conveyor Velocity, m/s (FPM) 46 (150)	 92 (300)	 137 (450)
RDF at 2.7 Mg/h (3.0 tph)	1	37.5%	23.5%	24.2%
	2	43.0%	9.5%	13.1%
	3	13.2%	14.6%	13.6%
	4	6.3%	52.4%	49.1%
MSW at 2.7 Mg/h (3.0 tph)	1	41.7%	30.2%	29.7%
	2	39.7%	16.4%	14.9%
	3	11.6%	10.9%	13.9%
	4	7.0%	42.6%	42.5%
Heavy Fraction at 9.1 Mg/h (10.0 tph)	1	38.5%	33.3%	50.0%
	2	46.2%	44.4%	25.0%
	3	6.4%	5.6%	8.3%
	4	9.0%	16.7%	16.7%
Ferrous Fraction at 9.1 Mg/h (10.0 tph)	1	25.0%	15.0%	6.7%
	2	50.5%	18.1%	56.3%
	3	17.9%	59.1%	31.9%
	4	6.7%	7.6%	5.1%

Table 12. (cont'd)

Product	Belt Section	Percent of Total Spillage Test Conveyor Velocity, m/s (FPM) 46 (150)	 92 (300)	 137 (450)
d-RDF/coal blend at 9.1 Mg/h (10.0 tph)	1	89.1%	72.8%	67.0%
	2	2.9%	2.5%	4.8%
	3	3.0%	6.8%	11.7%
	4	4.9%	17.8%	16.4%
d-RDF at 13.6 Mg/h (15.0 tph)	1	15.0%	20.0%	66.7%
	2	2.5%	10.0%	11.1%
	3	47.5%	10.0%	11.1%
	4	35.0%	60.0%	11.1%

ponents of RDF (glass, wood) or higher density fractions (heavy fraction or ferrous metals). Higher speeds also result in more turbulence and associated dusting and spillage at the discharge. The MSW fraction exhibited similar patterns of spillage as the RDF.

These results with RDF contrast with the ferrous fraction where the highest spillages were in Sections 2 and 3 at all speeds. This was observed to be mainly influenced by the bounce and roll of materials continuing after the loading section. The absence of wind-induced spillage or dusting at the discharge is also evident in the low Section 4 spillage.

The results in Table 12 for the heavy fraction and d-RDF/coal blend are somewhat similar with higher spillage rates in the first two sections. As described earlier, pieces of glass, lumps of coal, etc., tend to wedge between the belt and skirting causing small particles to spill out.

It should be noted that the majority of the spillage, measured in Sections 2, 3 and 4 for the d-RDF/coal blend, were in the form of fine coal dust which settled on the floor. It was not possible to distinguish between the rapidly settling coal dust from the particles of coal or d-RDF directly spilled from a conveyor.

The spillage distribution results for the d-RDF do not indicate a clear trend. The total spillage rates for the d-RDF are relatively small overall (reference Figure 21) and the variation may only reflect the random spillage characteristics for the material.

Belt Conveyor Discharge Trajectories --

The trajectories or discharge paths of material over the end pulley of a conveyor are important to the proper design and function of discharge chutes, wear plates or splitters. A method for calculating discharge trajectories is available from CEMA (1) and was applied to the MSW, RDF, heavy and ferrous fractions using the properties of these materials and conveyor dimensions and operational parameters from the test program.

Corresponding experimental measurements were made of the discharge trajectories for the four fractions at a fixed mass flow and for varying belt velocities. The material was observed to discharge in the form of a band, and the horizontal and vertical coordinates were measured directly using the mid-points of the stream. The theoretical and experimental discharge trajectories are plotted in Figures 24 to 27. It can be seen the values correspond reasonably well suggesting the calculations could be successfully used to predict trajectories of these waste fractions accurately.

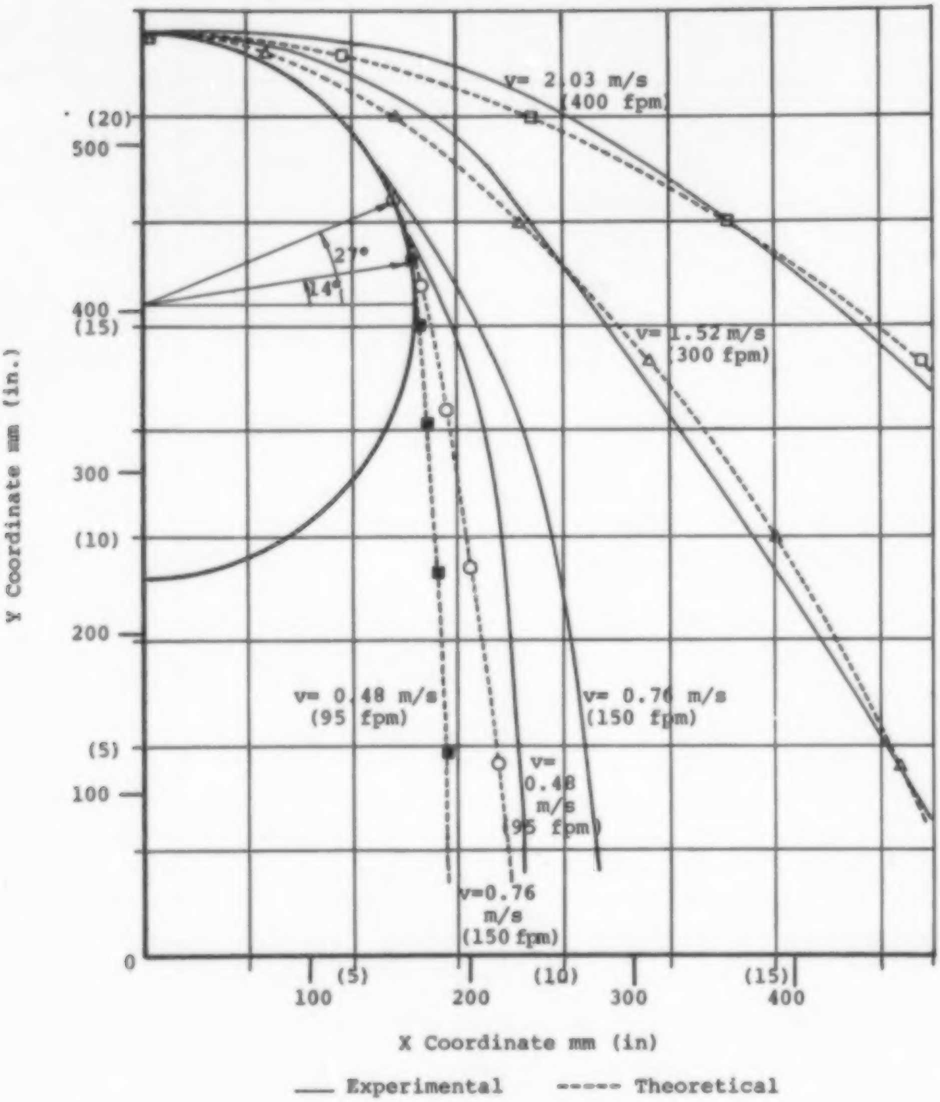

Figure 24. Trajectories for heavy fraction at 4.5 Mg/h (5 tph) and 20° idlers.

BEGIN LAST LINE OF TEXT
3/8"
BOTTOM OF IMAGE AREA OUTSIDE DIMENSION FOR TABLES AND ILLUSTRATIONS

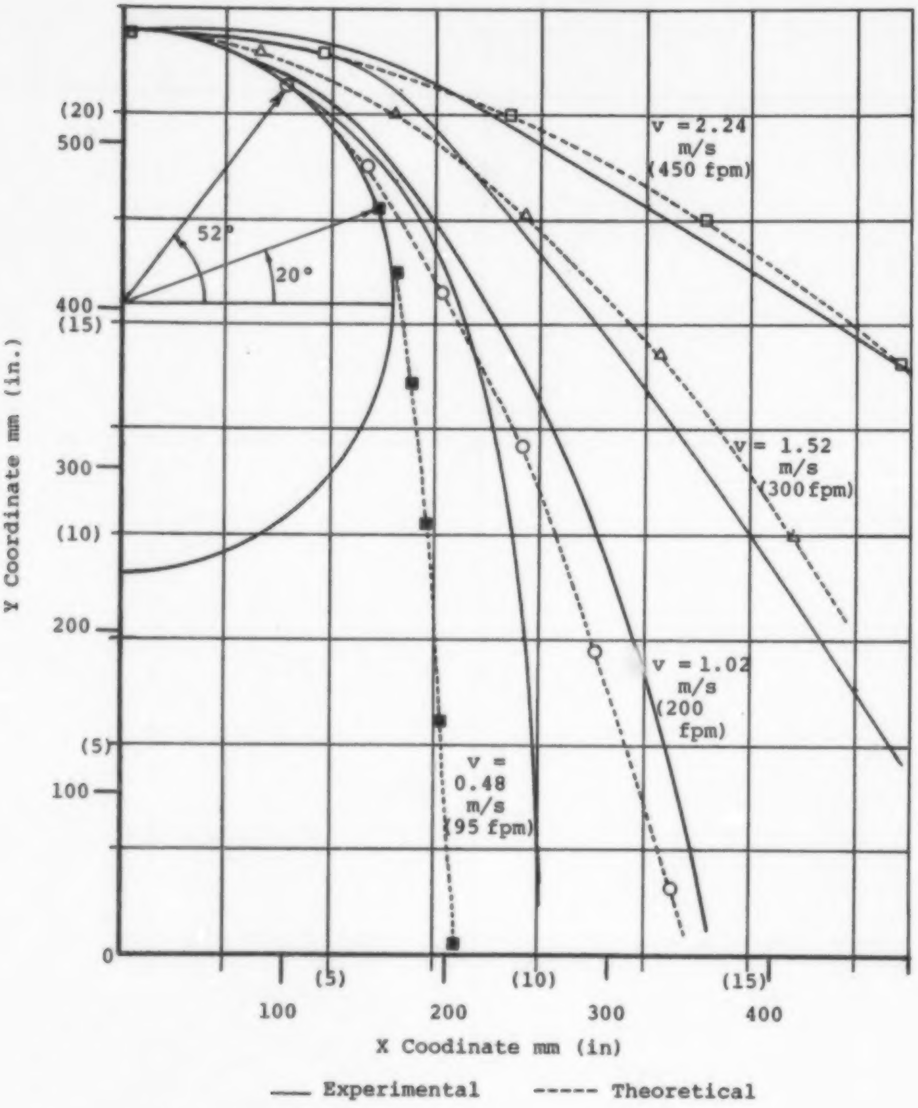

Figure 25. Trajectories for ferrous metals fraction at 4.5 Mg/h (5 tph) and 20° idlers.

BEGIN LAST LINE OF TEXT
3/8"
BOTTOM OF IMAGE AREA; OUTSIDE DIMENSION FOR TABLES AND ILLUSTRATIONS

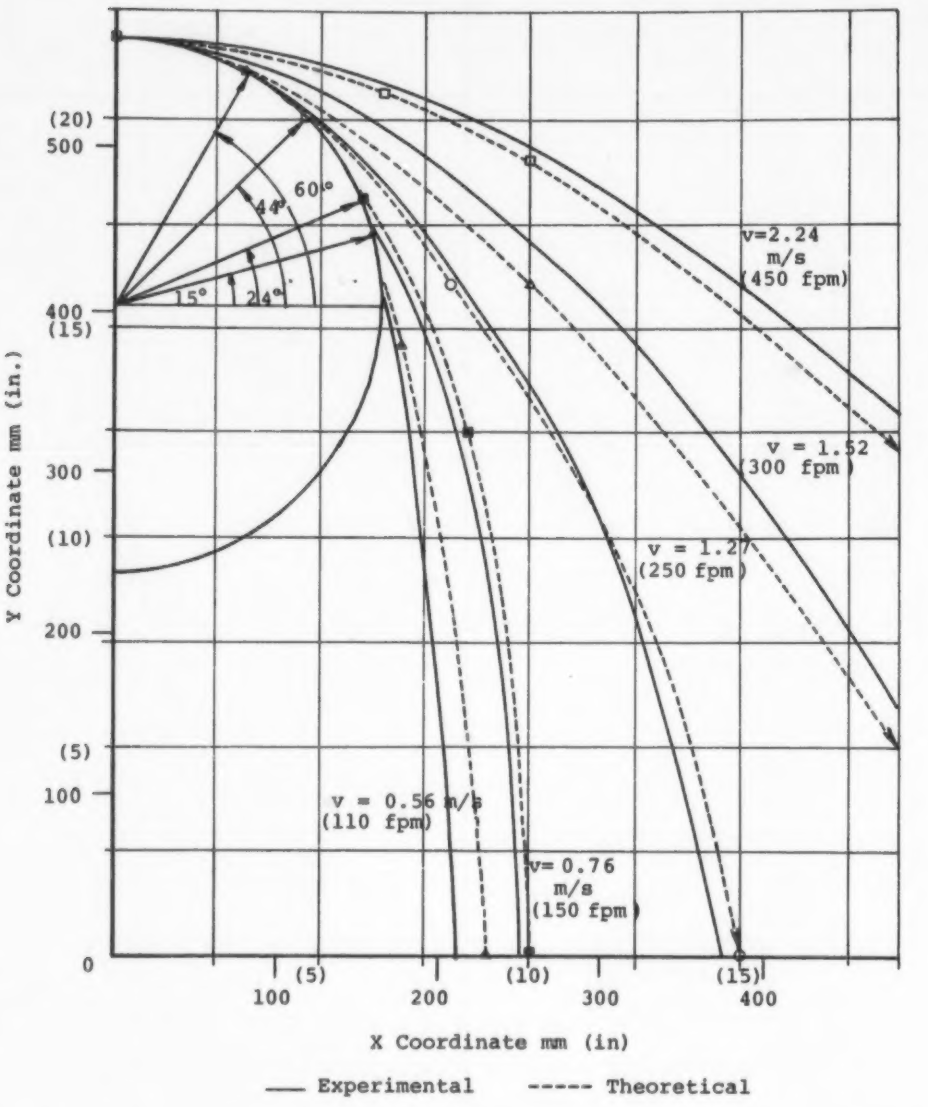

Figure 26. Trajectories for RDF fraction at 0.9 Mg/h (1 tph) and 20° idlers.

BEGIN LAST LINE OF TEXT
3/8"
BOTTOM OF IMAGE AREA OUTSIDE DIMENSION FOR TABLES AND ILLUSTRATIONS

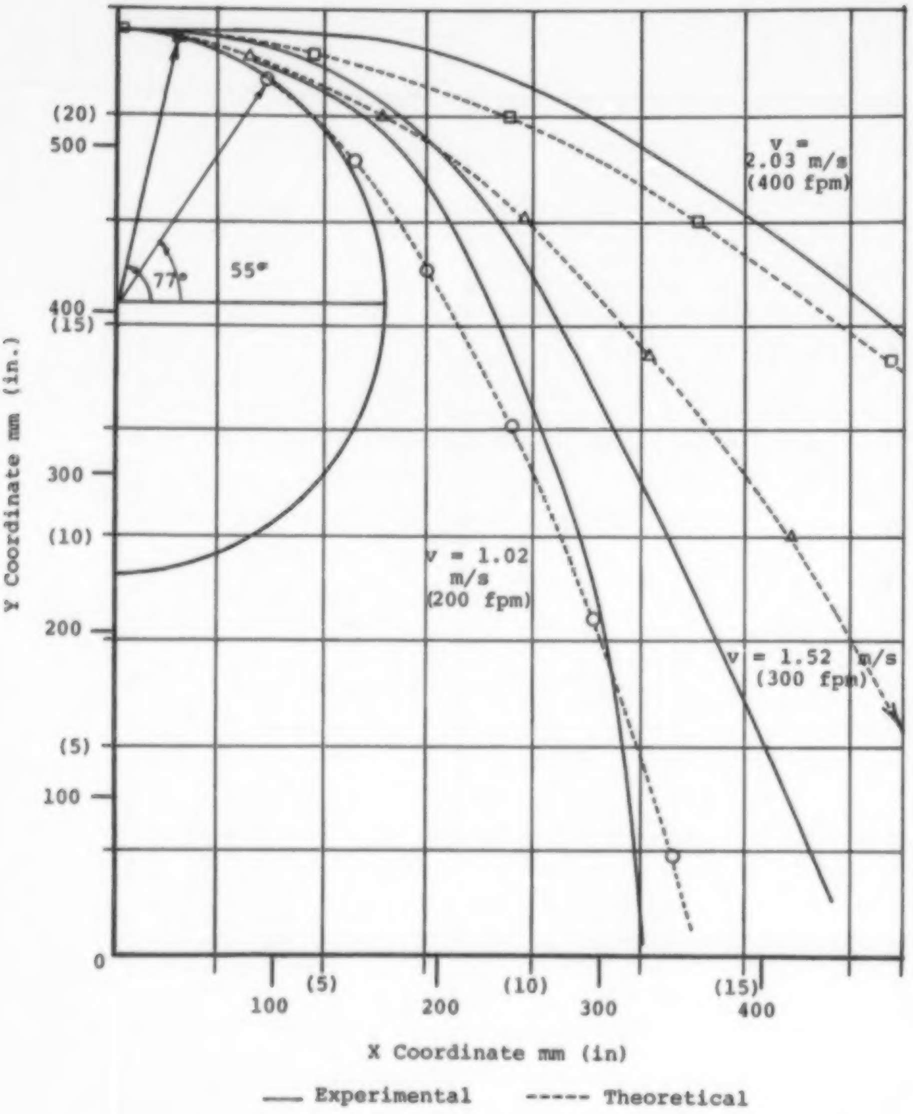

Figure 27. Trajectories for MSW fraction at 2.7 Mg/h (3 tph) and 20° idlers.

Conveyor Power Consumption --

The test belt conveyor drive includes a motor connected by variable pitch pulleys to a shaft-mounted reducer. Initial tests were conducted to establish relationships between mass flow rate and velocity and the power consumption using an ammeter to measure motor current as an indicator of power consumption.

Contrary to what was expected, results showed negligible measurable change in the motor current for a wide range of velocities or flow rates. This negligible change in power consumption - despite extreme variations in conveying conditions - such as speed, incline and load - is probably attributable to use of a motor larger than that required for these applications.

A consideration related to sizing of conveyor drive systems (motor, reducers, shafts, etc.) is the use of skirt-boards. While continuous rubber skirting or flashing would help alleviate spillage of some materials, the increase in frictional resistance and, therefore, the horsepower requirements can be substantial. Specific information and procedures for detailed calculation of conveyor power requirements is available in Reference 1.

Inclined Mode Test Results

Dependency of Spillage on Speed and Mass Flow Rates --

Tests were conducted to study the measured spillage vs. mass flow rate and speed for a given quantity of material and test belt inclination. Inclinations of 14 and 18° were tested. The results are reported in Figures 28 to 33, which overall corroborate the analysis that higher spillages are encountered on increasing the conveyor inclination and that, as before, a preferred speed or range of speeds exists for a given mass flow rate and inclination.

Figure 33 illustrates increases in spillage rate of MSW with increasing the conveyor inclination. The data from the horizontal tests are included for reference. It was observed that spillage on the incline was often precipitated by slippage or roll back of material on the belt. For relatively homogeneous material such as d-RDF and d-RDF/coal blends, the increase in spillage on increasing the conveyor inclination is not as severe. (Compare Figures 21 to 22 and Figures 31 to 32.) Apparently, the higher density and relative uniformity makes such materials less prone to slipping or rolling back on the inclined conveyor.

Dust Generation

High volume air samplers (Sierra Model 305-2050H) were used to determine the magnitude of dust generated during transport of the solid waste fractions on the inclined test belt conveyor.

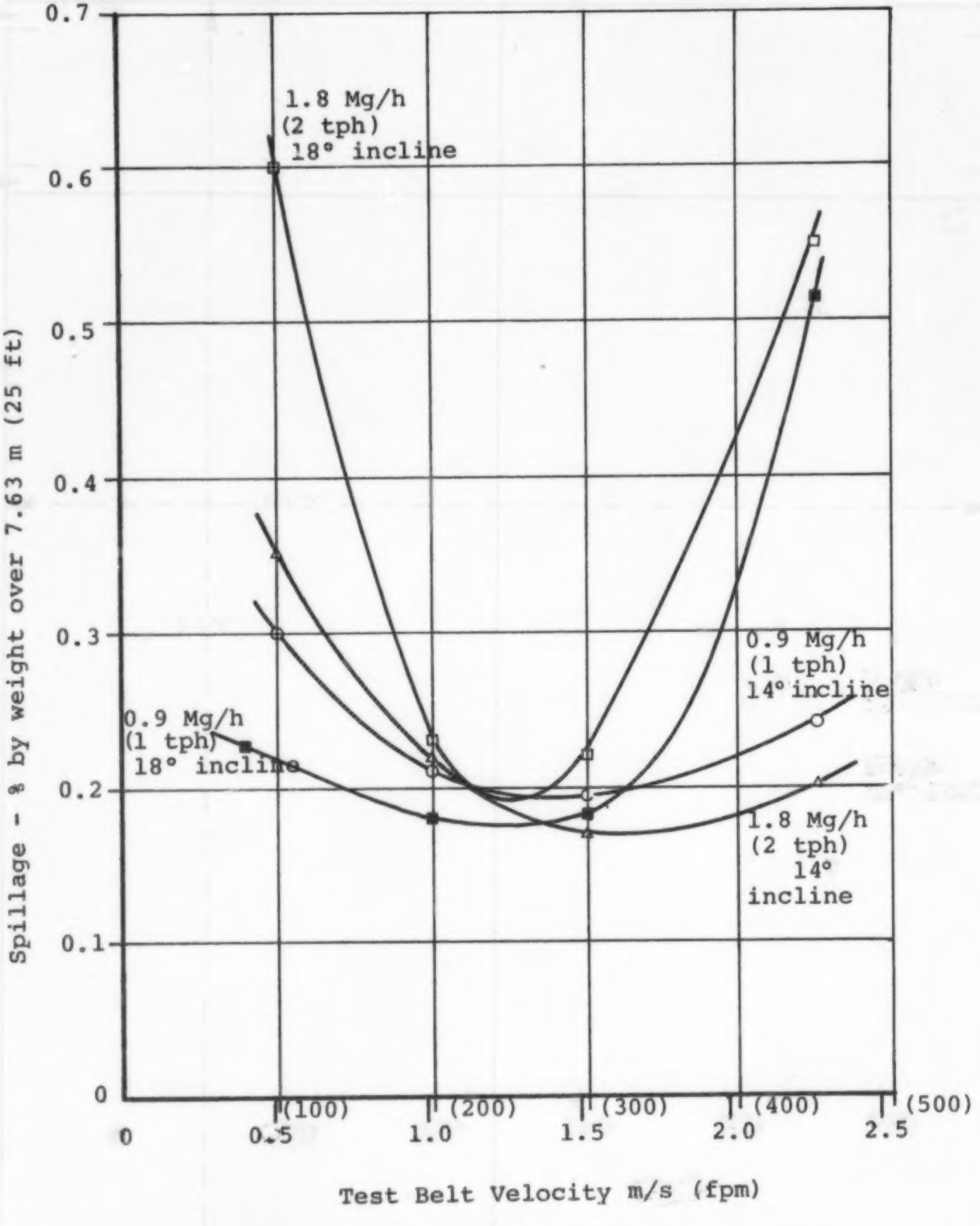

Figure 28. MSW sample spillage vs. belt velocity and mass flow rate with inclined belt and 35° idlers.

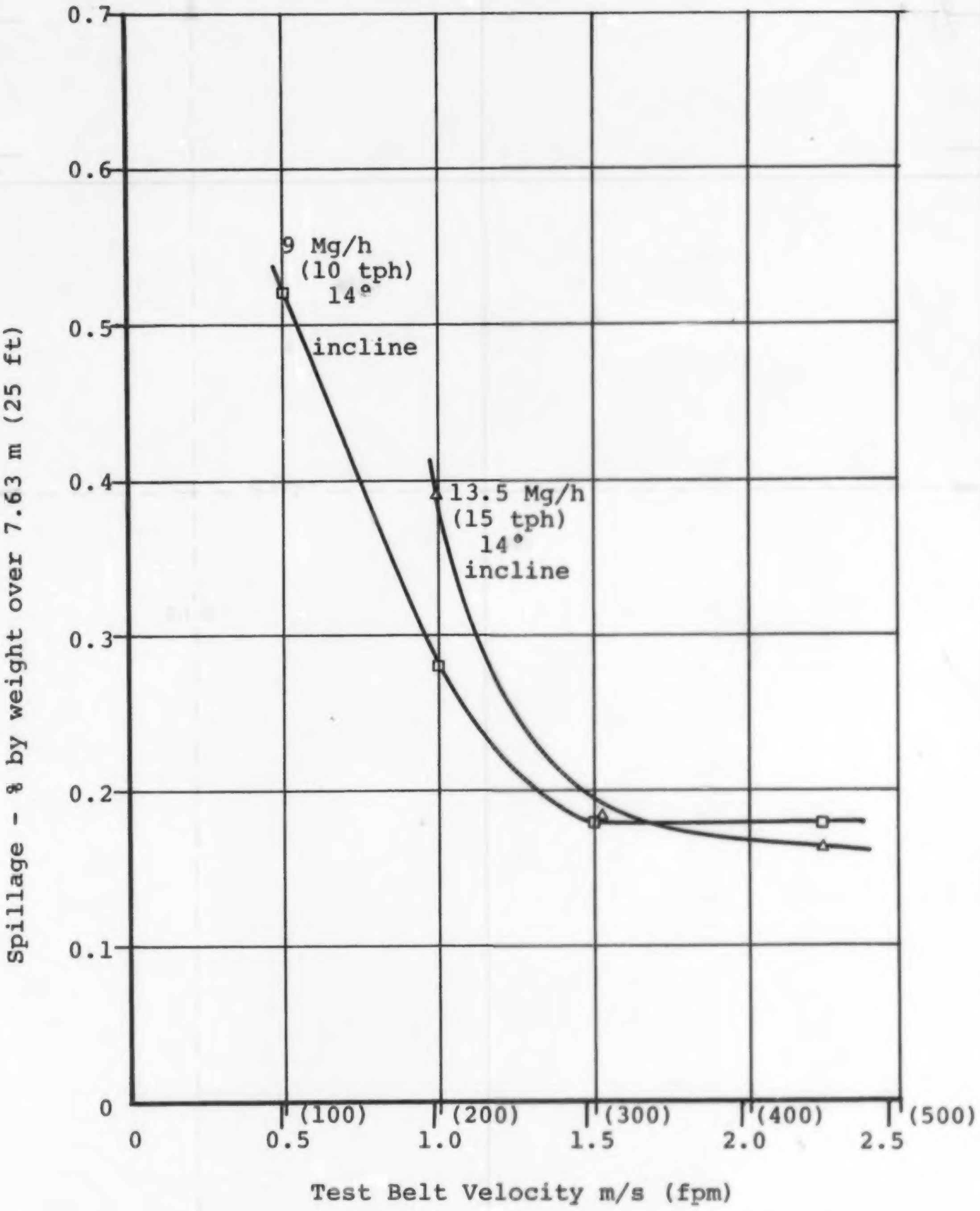

Figure 29. Heavy fraction sample spillage vs. belt velocity with inclined belt and 35° idlers.

BEGIN FIRST LINE OF TEXT HERE
DROPPED HEAD. BEGIN SECTION HERE
BEGIN LAST LINE OF TEXT
3/8"
PAGE NUMBER
EPA Form 2350-4 (4-80)
(PREVIOUSLY CIN. EPA FORM 287)
TYPING GUIDE SHEET

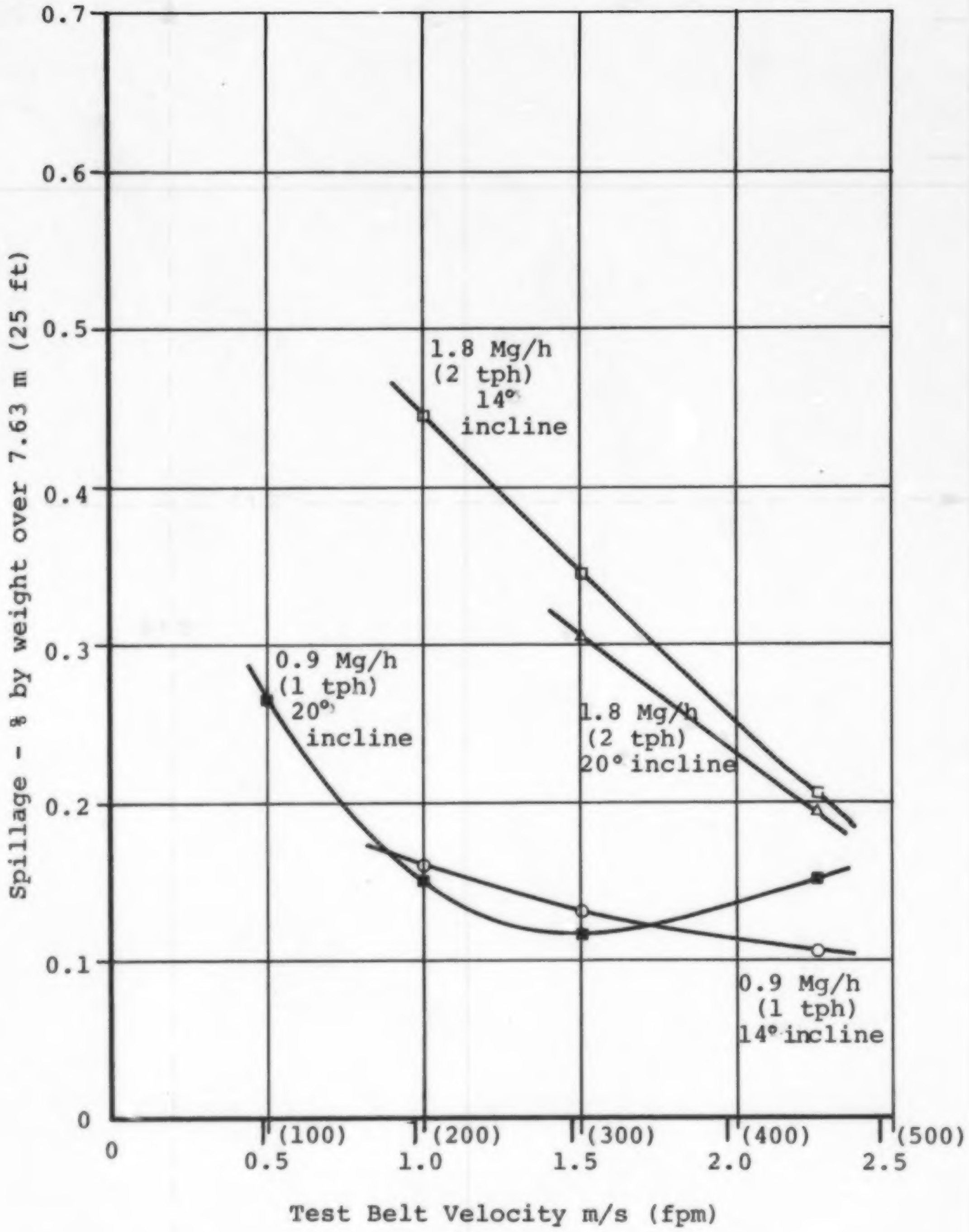

Figure 30. RDF sample spillage vs. belt velocity with inclined belt and 35° idlers.

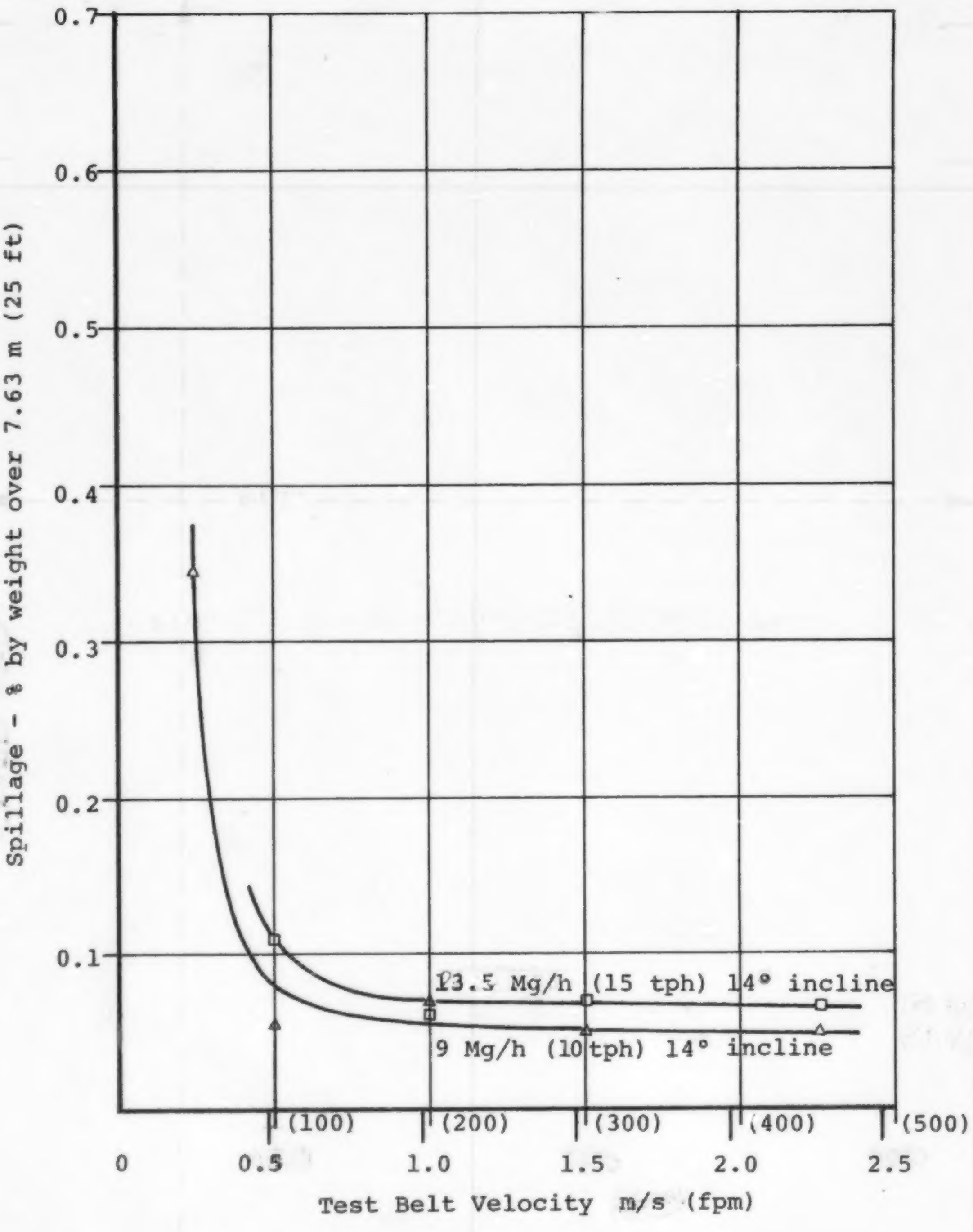

Figure 31. d-RDF sample spillage vs. belt velocity with inclined belt and 35° idlers.

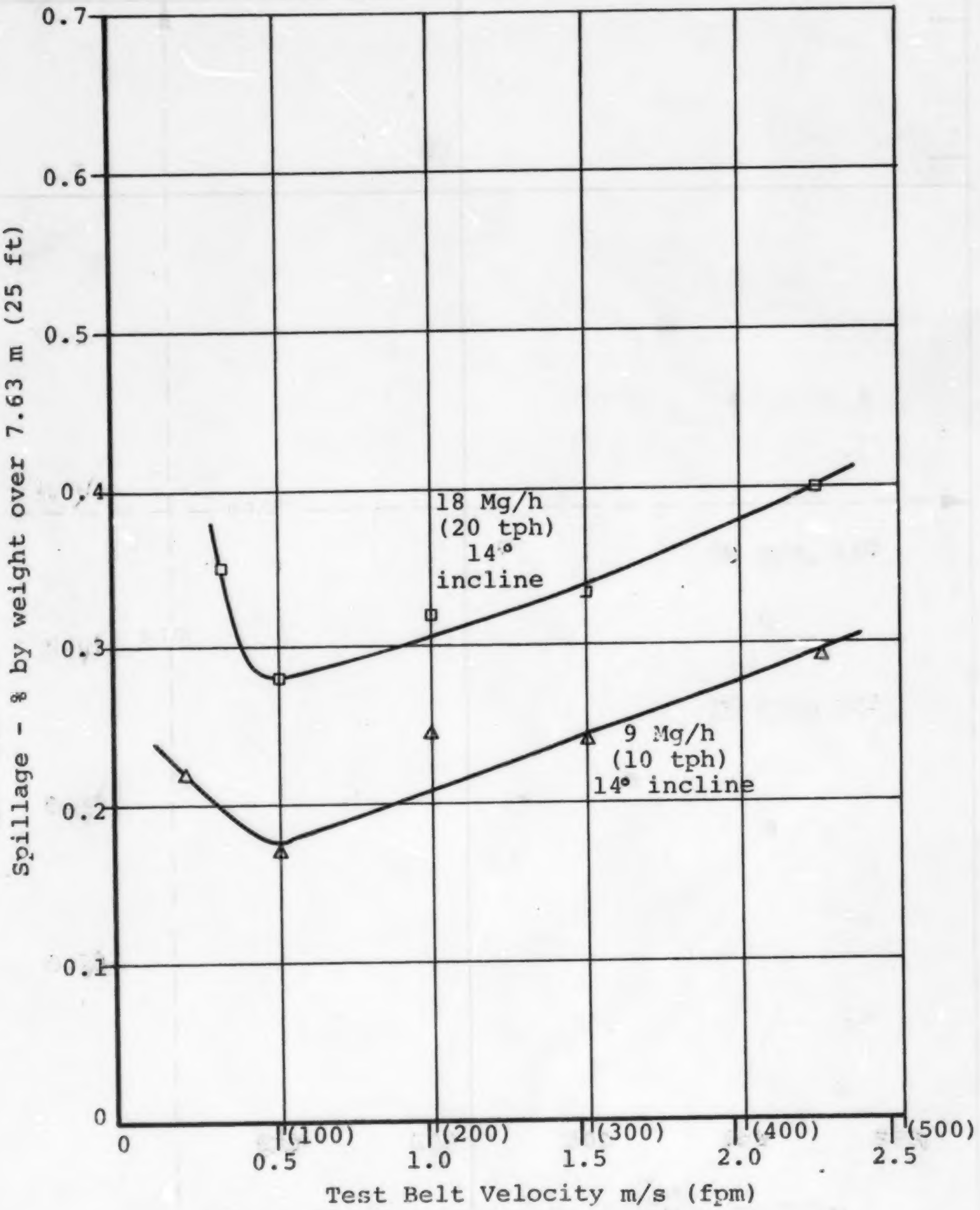

Figure 32. Coal/d-RDF blend sample spillage vs. belt velocity with inclined belt and 35° idlers.

BEGIN LAST LINE OF TEXT

3/8"

BOTTOM OF IMAGE AREA, OUTSIDE DIMENSION FOR TABLES AND ILLUSTRATIONS

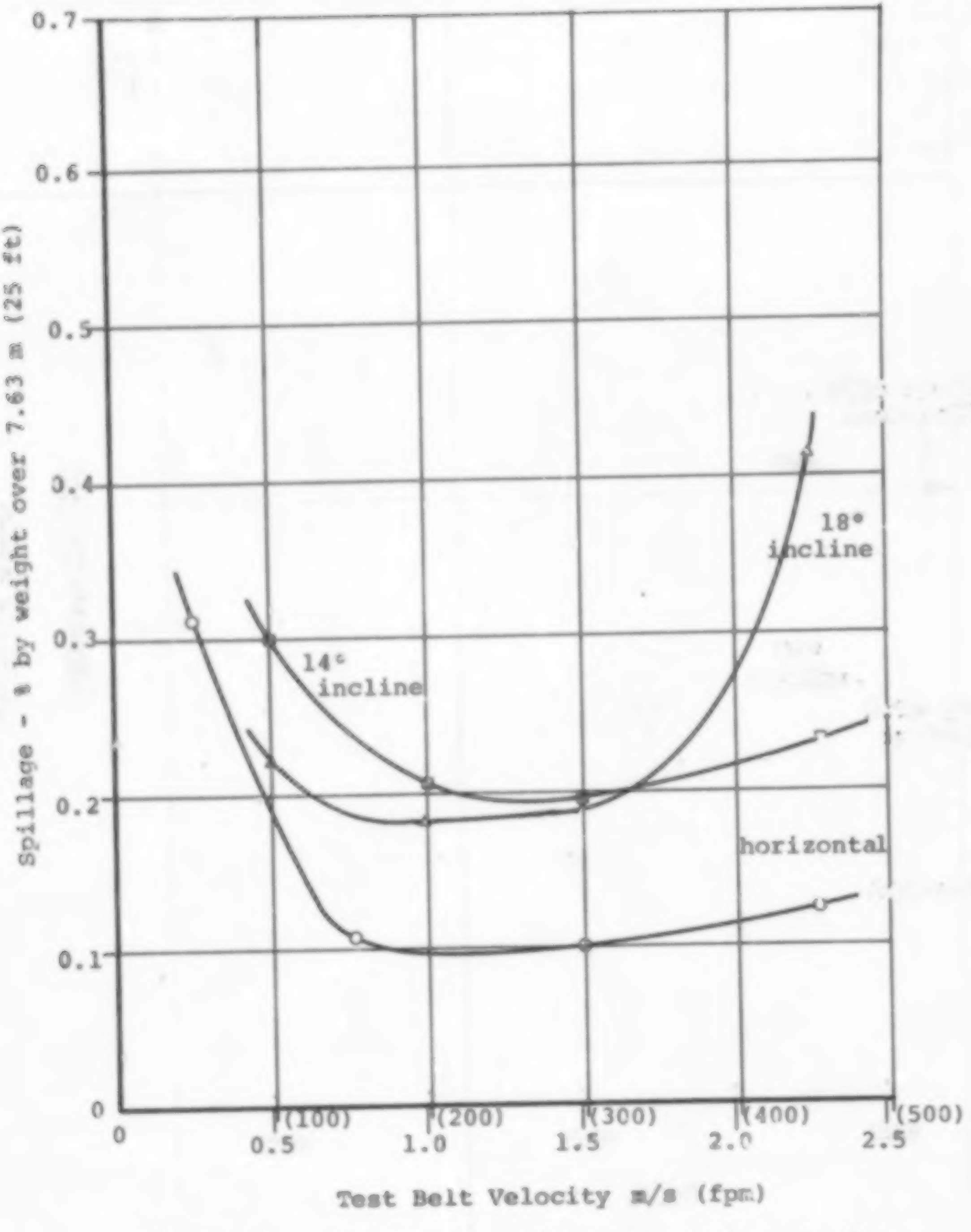

Figure 33. MSW sample spillage vs. belt velocity for a fixed 0.9 Mg/h (1 tph) mass flow rate and 35° idlers.

The objective was to determine if any relationship between the extent of dust generated for parameters such as the feed type, mass flow rate or the test belt velocity or angle of inclination. One dust sampler was placed approximately 1.6 m (5 ft) from the tail end to measure the quantity of dust generated around the infeed end of the belt conveyor. A second dust sampler was located approximately 6.1 m (20 ft) perpendicularly off the center of the conveyor system. The results of the second sampler were found to be inconsistent and unreliable. This may be due to reflection of dust from the walls or air currents in the testing area. Therefore, only the dust loadings measured by the sampler located at the conveyor feed end are reported.

The test results provide the total suspended dust. Particle size distribution or any further characterization of the dust was not attempted. The test method and calculations are given in Appendix A.9. For complete details on dust sampling methods and procedures, also refer to ASTM Standards D 2009 and D 1356.

The test results are reported in Figures 34 to 38. While there are inconsistencies in several cases and no trends common to all tests, Figures 34 and 35 indicate that for higher mass flow rates and belt conveyor inclinations, there is a tendency towards greater dust generation.

The relatively high dust loadings in the vicinity of the test conveyor for RDF, d-RDF and d-RDF/coal blends (Figures 36 and 37) suggest the necessity of utilizing a dust collection system at the conveyors feed end. OSHA's safety and health standards have established a threshold limit for employee dust exposure (5). OSHA requires that employee exposure to total dust in any 8-hour work shift of a 40-hour work week shall not exceed the time weighted average of 15 mg/m^3.

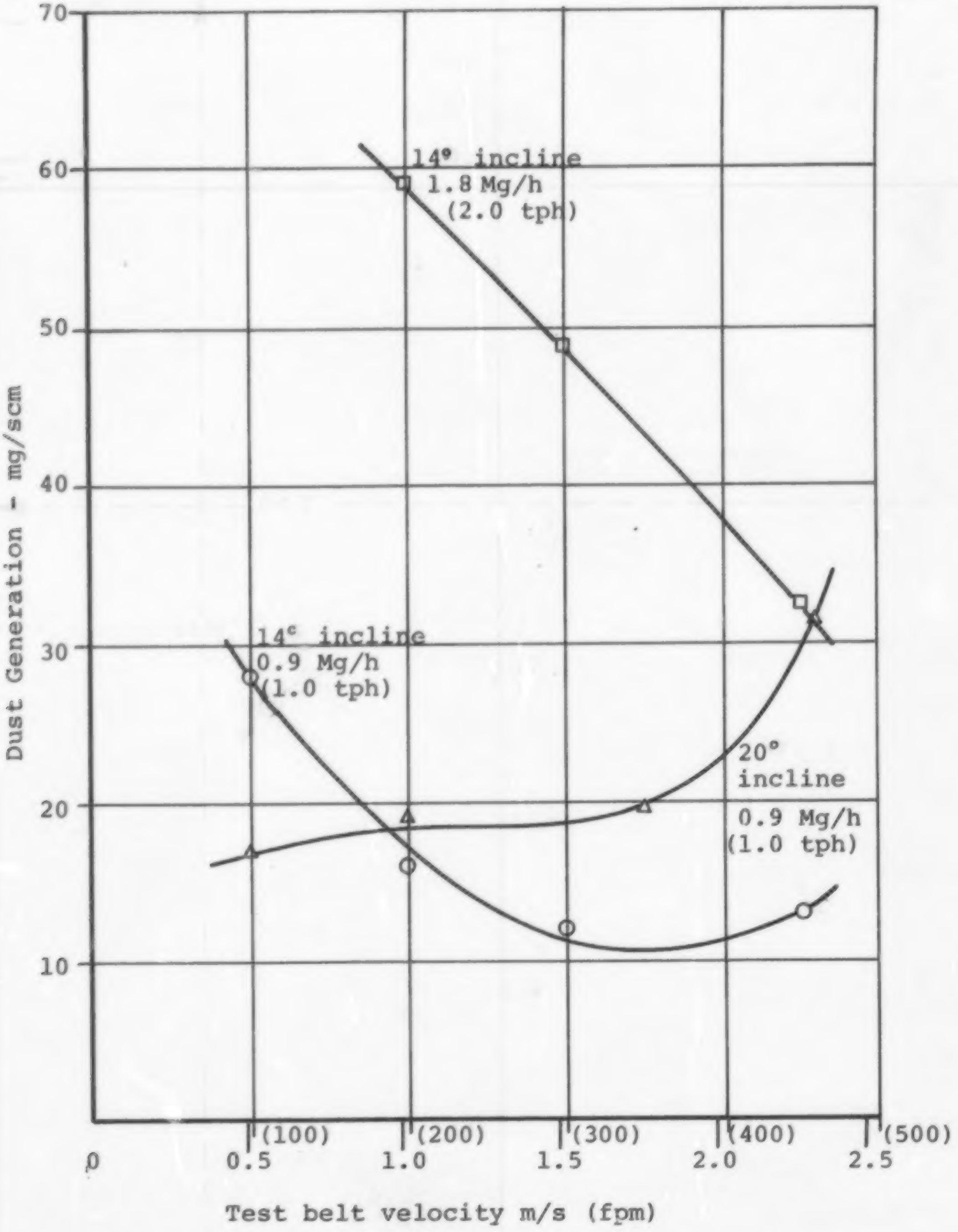

Figure 34. Magnitude of dust generated conveying RDF on test belt inclined at 14° and 20°.

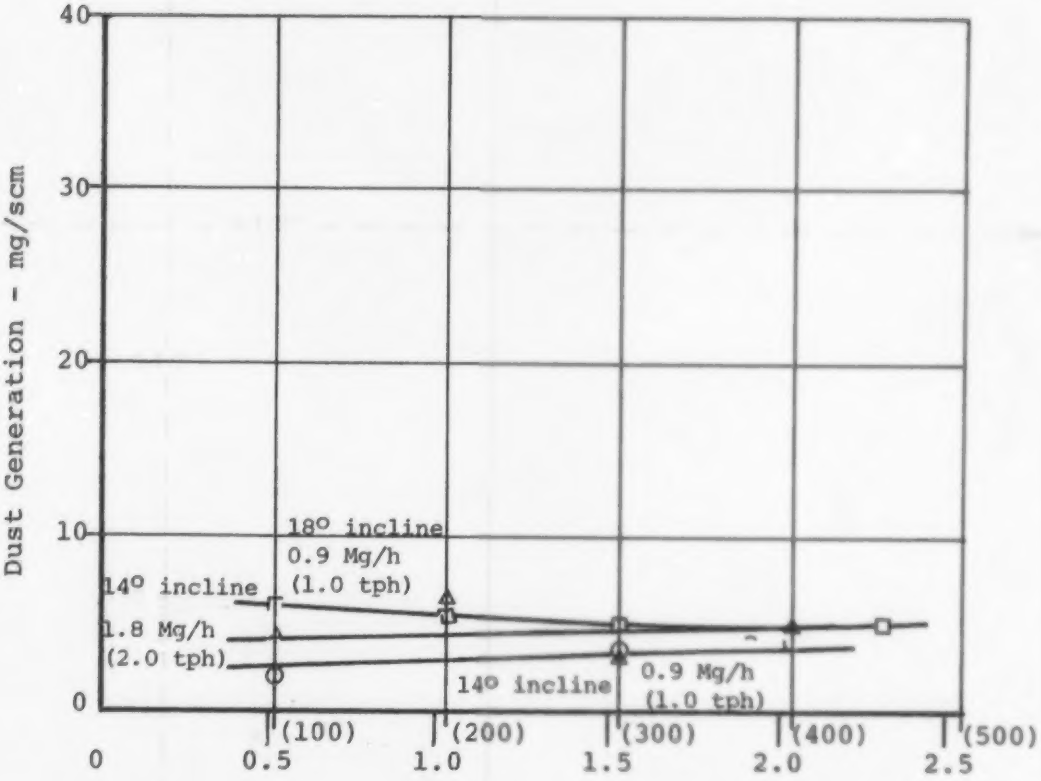

Figure 35. Magnitude of dust generated conveying MSW on test belt inclined at 14° and 20°.

BEGIN LAST LINE OF TEXT
BOTTOM OF IMAGE AREA OUTSIDE DIMENSION FOR TABLES AND ILLUSTRATIONS
3/8"

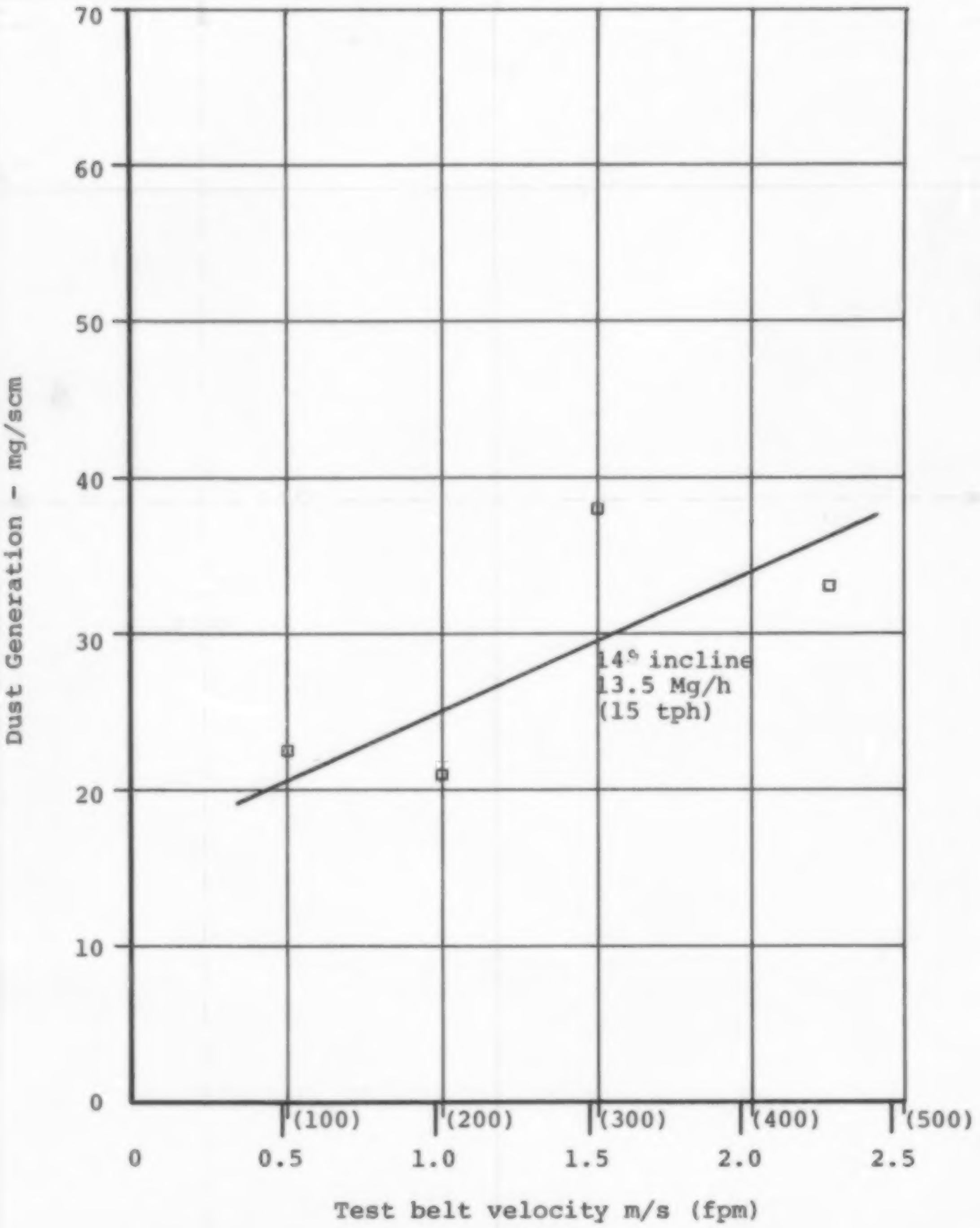

Figure 36. Magnitude of dust generated conveying d-RDF on test belt inclined at 14°.

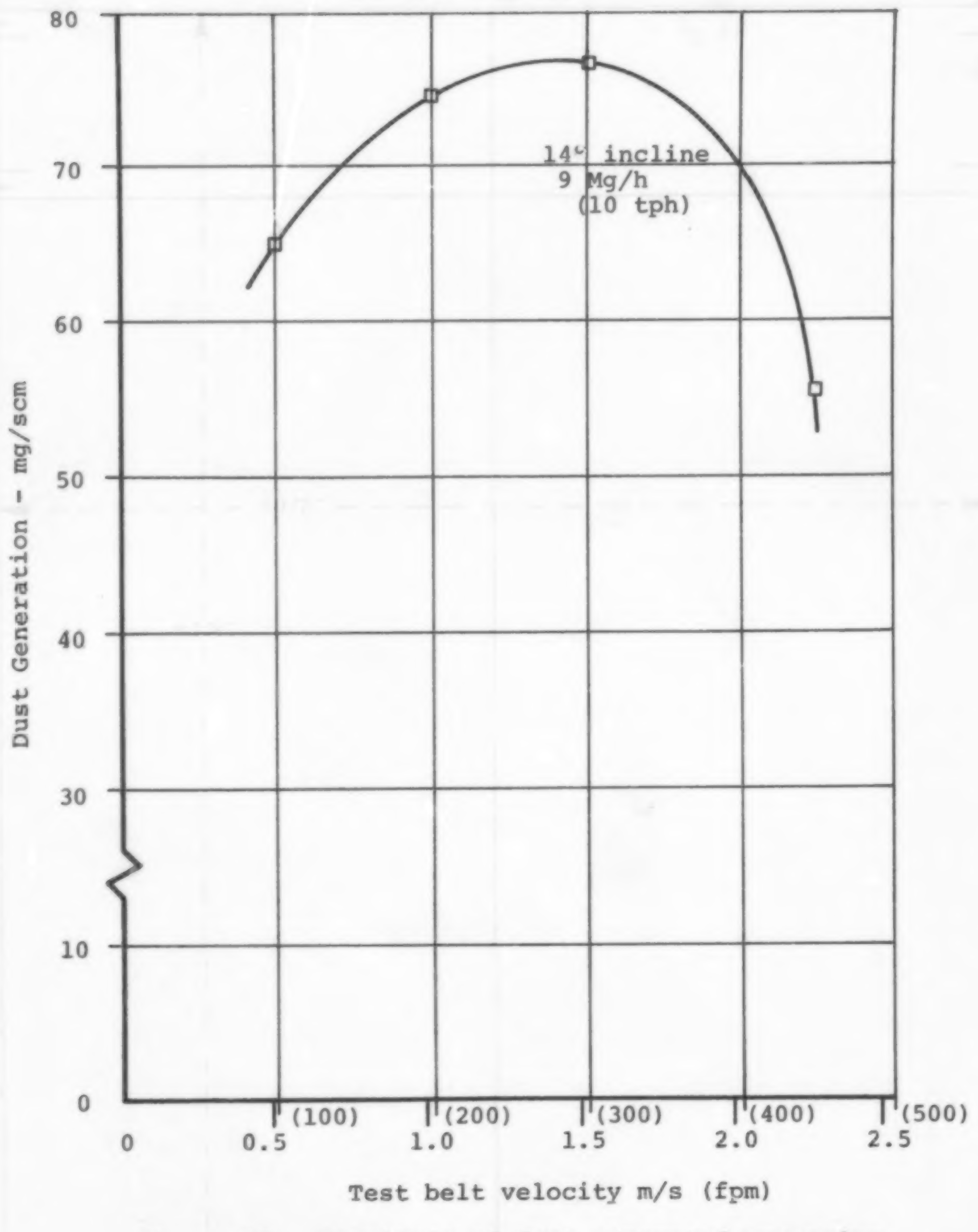

Figure 37. Magnitude of dust generated conveying d-RDF/coal blend on test belt inclined at 14°.

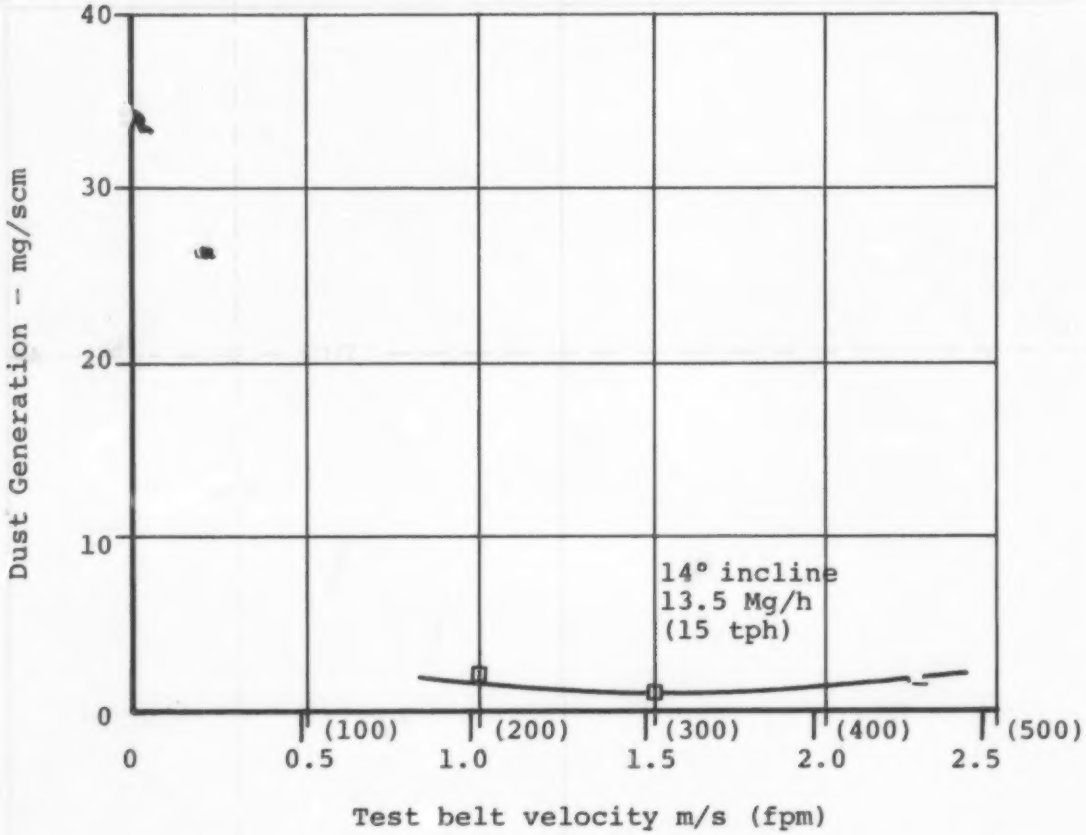

Figure 38. Magnitude of dust generated conveying heavy fraction on test belt inclined at 14°.

BEGIN LAST LINE OF TEXT
BOTTOM OF IMAGE AREA; OUTSIDE DIMENSION FOR TABLES AND ILLUSTRATIONS
3/8"

SECTION 4

VIBRATING CONVEYORS

INTRODUCTION

Vibrating conveyors have been utilized to transport bulk materials in the mining and other industries for many years. This type of conveyor has relatively few moving parts and is designed to operate with minimum maintenance. Typical applications of vibrating conveyors in a resource recovery plant have been in the feed or discharge from unit processing equipment such as shredders and air classifiers. In comparison to a belt conveyor, vibrating conveyors can level and distribute the feed and will not be damaged by impact of hot or abrasive material discharging from a shredder.

The principle of operation of vibrating conveyors is illustrated in Figure 39. The drive provides an acceleration to the pan with both vertical and horizontal components. A particle resting on the pan is lifted up and forward and is thrown in an arc that returns it to the pan during the next vibration period (one-cycle jump). Referring to the figure, the particle "a" leaves the pan at the time "t_s" (when the acceleration of the pan equals that due to gravity), strikes it again at "t_a" and leaves it at "$t_a + 1/f$" where f is the frequency of vibration (cycles/sec). In this example, the take-off and landing times are within one pan vibration period, referred to as a one-cycle jump. It is also possible to accelerate the material (by a higher stroke) to a two or more cycle jump but that mode would require a much higher energy input.

TEST VIBRATING CONVEYOR AND TEST PLAN

The test vibrating conveyor was 4.6 m(15 ft) long by 0.6 m (2 ft) wide with a pan height of 205 mm (8 in.). Manufactured by Carman Industries, the conveyor was driven by an eccentric rotating cam linked mechanically to the pan at 30 degrees. Major components of the conveyor are depicted in Figure 40 and pictured in the test rig installation in Figure 41.

Utilizing a variable speed drive and two interchangeable eccentric cams, the frequency could be varied between 400 and 570 cycles/min and the stroke set at either 12.7 m (0.5 in.) or 22.2

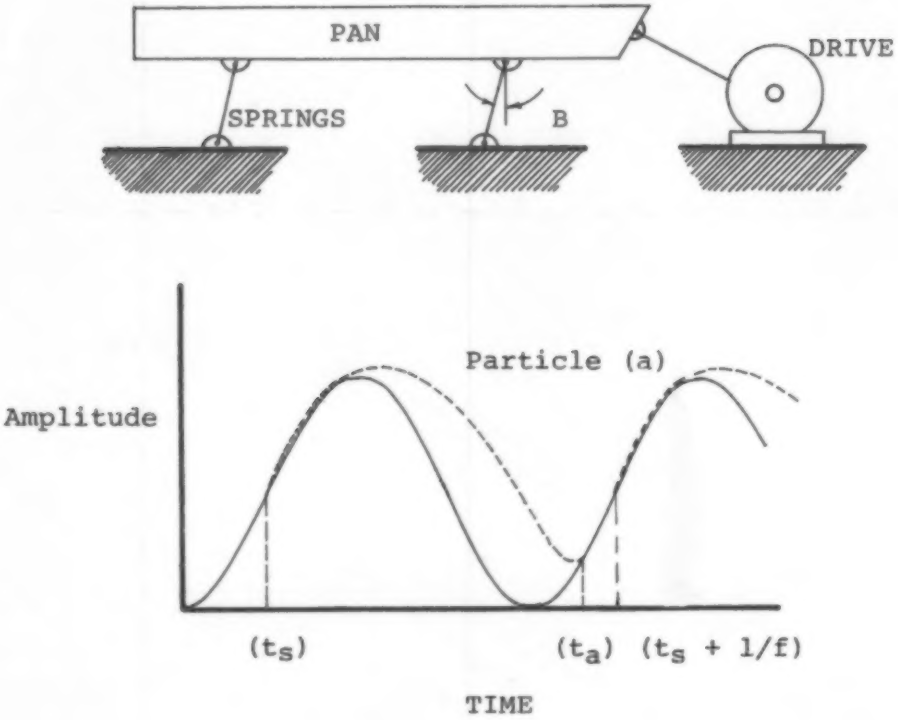
PAN
DRIVE
SPRINGS
B
Particle (a)
Amplitude
(t_s)
(t_a)
$(t_s + 1/f)$
TIME

Figure 39. Vibrating conveyor principle of operation.

BEGIN LAST LINE OF TEXT
BOTTOM OF IMAGE AREA OUTSIDE DIMENSION FOR TABLES AND ILLUSTRATIONS
3/8"

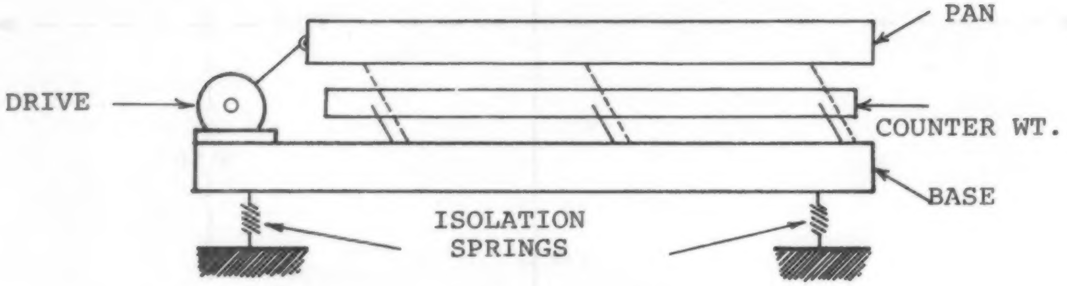
PAN
DRIVE
COUNTER WT.
BASE
ISOLATION SPRINGS

Figure 40. Schematic of vibrating conveyor.

BEGIN LAST LINE OF TEXT
BOTTOM OF IMAGE AREA. OUTSIDE DIMENSION FOR TABLES AND ILLUSTRATIONS
3/8"

PAGE NUMBER
EPA Form 2350-4 (4-80)
(PREVIOUSLY C/N. EPA FORM 287)
TYPING GUIDE SHEET

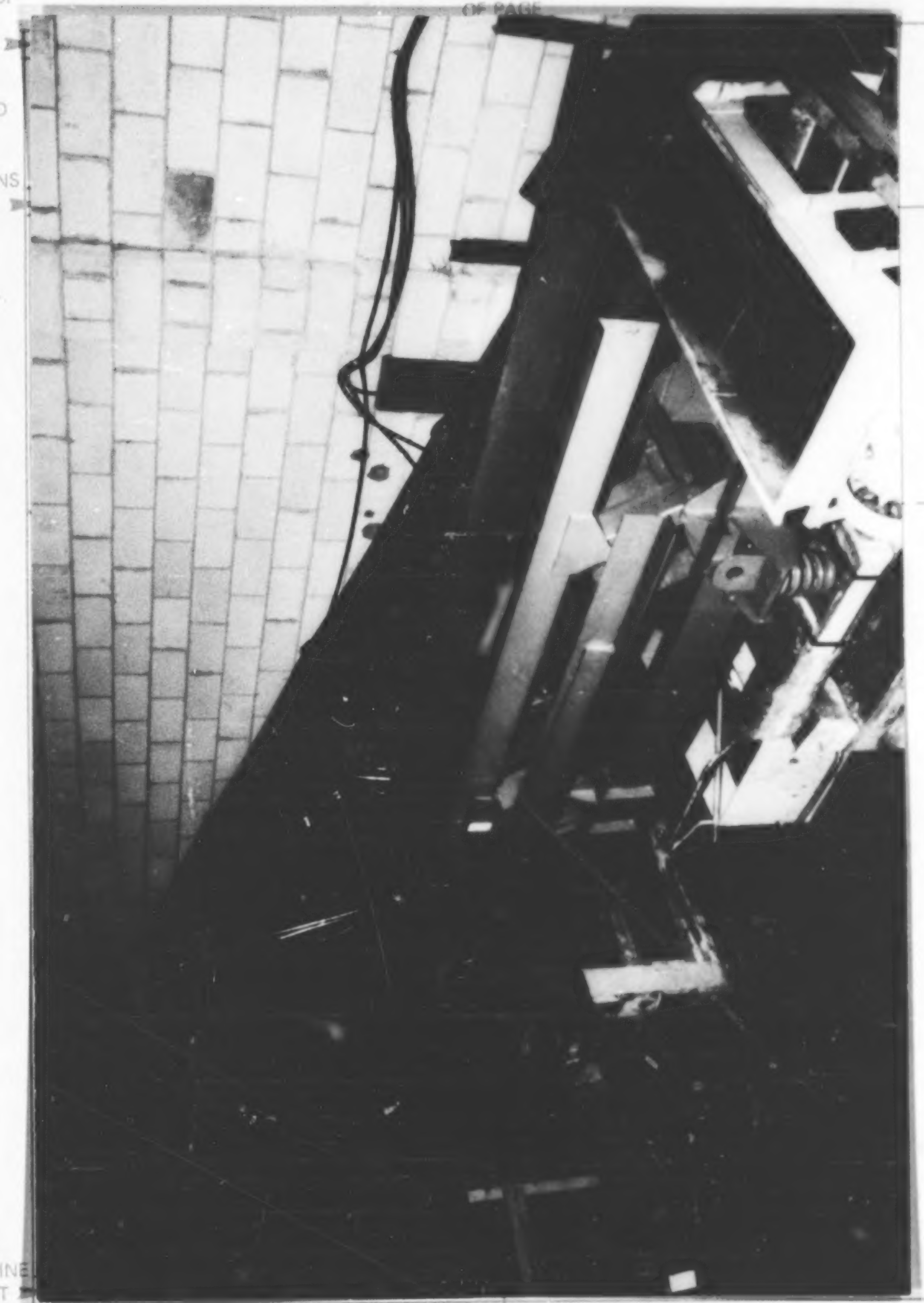

Figure 41. Vibrating conveyor installation.

BEGIN LAST LINE OF TEXT
BOTTOM OF IMAGE AREA; OUTSIDE DIMENSION FOR TABLES AND ILLUSTRATIONS
3/8"

PAGE NUMBER
EPA-287 (Cin.)
(4-76)

mm (0.875 in.).

To maintain a fixed stroke and frequency, it was necessary to dynamically balance the conveyor through removal or addition of leaf springs or counter weights. These efforts were not completely successful as can be seen in Table 13. This table shows the variation of the length of stroke in the conveyor sub-components with respect to frequency.

The conveyor is designed to operate so that the pan and counter weight should operate at similar and offsetting stroke lengths, and the base would thus remain steady. The results in Table 13 indicate that such was not the case, and there remained an imbalance in the system as well as limit on the range of operating frequencies. Unfortunately, the scope of this program did not allow resolution of this particular problem or, more generally, the investigation design of a variable stroke and frequency conveyor system.

The operating range thus had to be selected on an empirical basis with an imposed criteria that the vibration of the base not exceed 3.2 mm (1/8 in.). The variations in actual pan stroke have been accounted for in the presentation of the data in the following manner: all points corresponding to a pan vibration of 12.7 ± 3.2 mm (1/2 ± 1/8 in.) were considered "12.7 mm" stroke tests, and all points for which the amplitude was 22.2 ± 3.2 mm (7/8 ± 1/8 in.) were considered "22.2 mm" (7/8 in.) stroke tests. These conditions limited the range of operating frequency to 430 to 545 cpm at 22.2 mm stroke and 390 to 550 cpm for 12.7 mm stroke.

The objective of the tests were to determine, for the two values of stroke specified, the following:

- vibration frequency and stroke vs. maximum carrying capacity
- vibration frequency and stroke vs. conveying speed for a given mass flow rate
- energy consumption vs. material burden depth for a given frequency
- compaction of material along length of pan
- segregation of material
- dust generation

TABLE 13. TEST VIBRATING CONVEYORS OPERATING RANGE

Frequency (rpm)	7/8-in. Cam Stroke			1/2-in. Cam Stroke		
	Pan	Counter Wt.	Base	Pan	Counter Wt.	Base
390	5/8"	3/8"	3/16"	3/8"	3/16"	1/16"
410	5/8"	3/8"	1/8"	3/8"	3/16"	1/16"
430	11/16"	3/8"	1/8"	3/8"	1/4"	1/16"
450	11/16"	3/8"	1/8"	3/8"	1/4"	1/16"
470	3/4"	1/2"	1/16"	3/8"	1/4"	0
490	3/4"	1/2"	1/16"	7/16"	1/4"	0
510	13/16"	5/8"	0	1/2"	7/16"	0
530	7/8"	3/4"	0	9/16"	7/16"	0
550	1 1/16"	1 1/8"	3/16"	13/16"	9/16"	1/16"
570	Excessive vibration				1 1/16"	1/4"
Springs on	Pan assembly 11					
Springs on	Counter weight assembly 14					

TEST RESULTS

Vibration Frequency and Stroke vs. Maximum Carrying Capacity

Maximum carrying capacity here is defined as the maximum mass flow rate the vibrating conveyor will transport with negligible spillage. After fixing the conveyor frequency, the pan was loaded to the top of the sides with the solid waste fraction. The conveyor was started and the discharge timed and weighed to give the maximum carrying capacity.

From Figures 42 and 43, it is evident that the maximum carrying capacity increases with both stroke and frequency. By increasing the amplitude from 12.7 mm (1/2 in.) to 22.2 m (7/8 in.), the increase ~~in~~ carrying capacity (at 540 rpm) for RDF was 240%, MSW 262%, heavy fraction 170%, d-RDF 241%, and d-RDF/coal blend 205%.

Vibration Stroke and Frequency vs. Conveying Speed for a Given Mass Flow Rate

At a given mass flow rate, the conveying speed was measured for variations in frequency and stroke.

From Figure 44, it is seen that in all cases the conveying speed increased with higher frequencies. Increased speed may be desirable in reducing potential for build-up, jamming and spillages. A similar effect, as observed with frequency, is seen with changes in stroke. At 12.7 mm (1/2 in.) stroke and 540 cycles/min velocities between 0.20 to 0.25 m/s (40 to 50 ft/min) were observed while at 22.2 mm (7/8 in.) stroke and 540 cycles/min, the material conveying speed increased to between 0.46 and 0.51 m/s (90 and 100 ft/min).

Energy Consumption vs. Vibrating Frequency for a Given Mass Flow Rate

During the testing, the vibrating conveyor motor current was measured with a hand-held ampmeter. The measurements indicated no significant difference in energy consumption with frequency or stroke length in the ranges studied. Nor was there any increase in consumption at a given frequency or stroke for transporting denser bulk solids (d-RDF/coal vs. RDF, for example). The reason that changes in energy consumption were not detectable is probably attributable to use of a larger-sized drive motor than required for the application.

Conveying Speed vs. Material Burden Depth for a Given Frequency

At a fixed frequency of 510 rpm, and at two stroke lengths, the vibrating conveyor was uniformly loaded with the solid waste fraction at three different burden depths between 25 and 152 mm

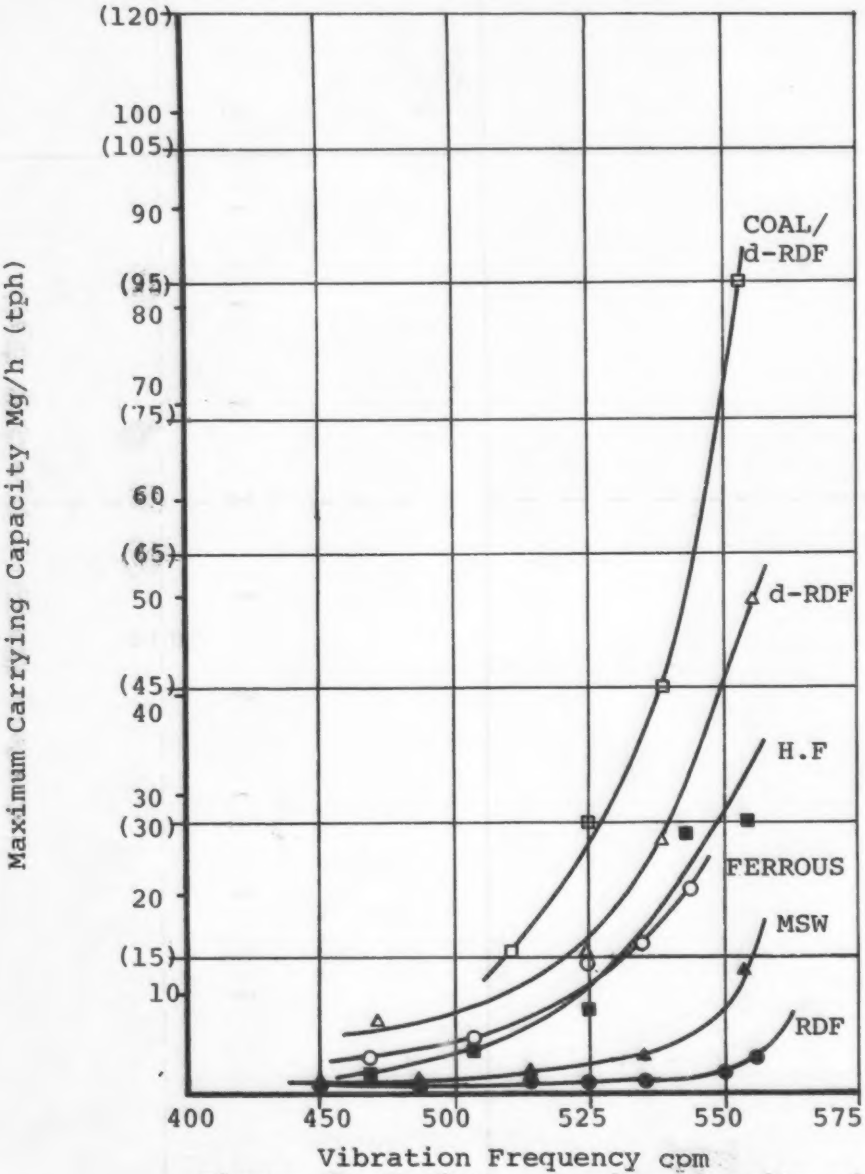

Figure 42. Maximum carrying capacity of test vibrating conveyor vs. vibration frequency for 12.7 mm (1/2") stroke.

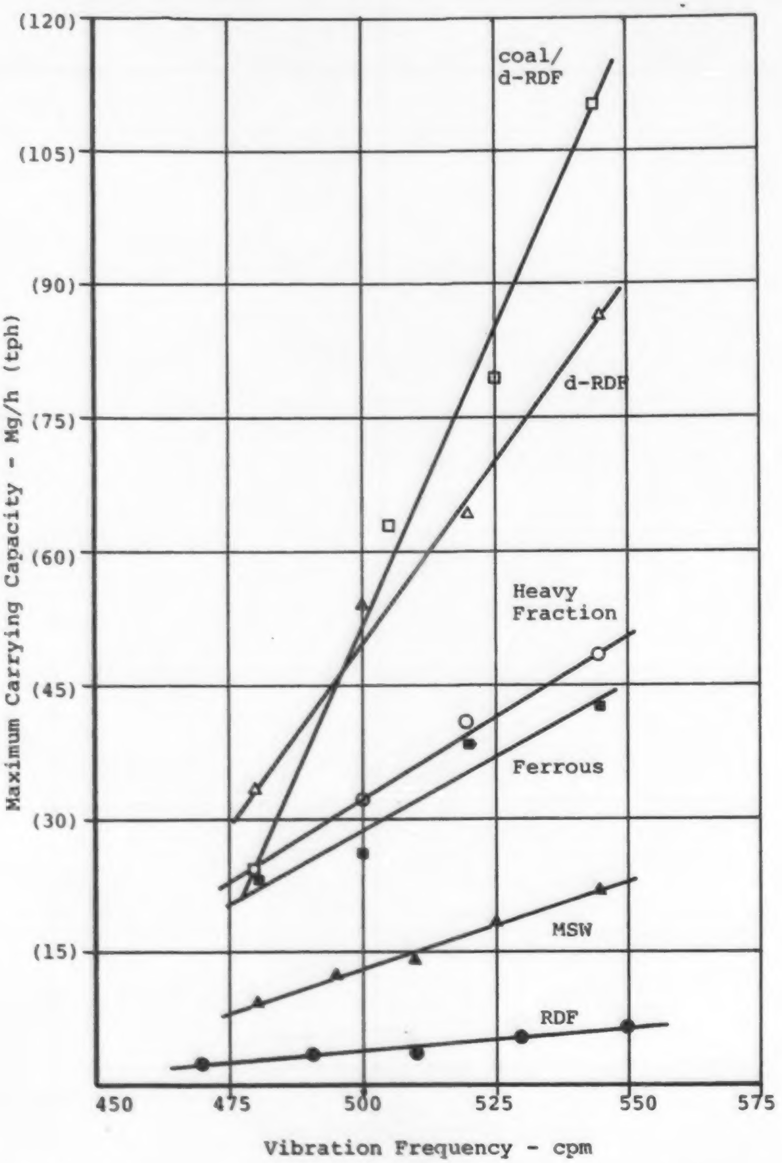

Figure 43. Maximum carrying capacity of test vibrating conveyor vs. vibration frequency for 22.2 mm (7/8") stroke.

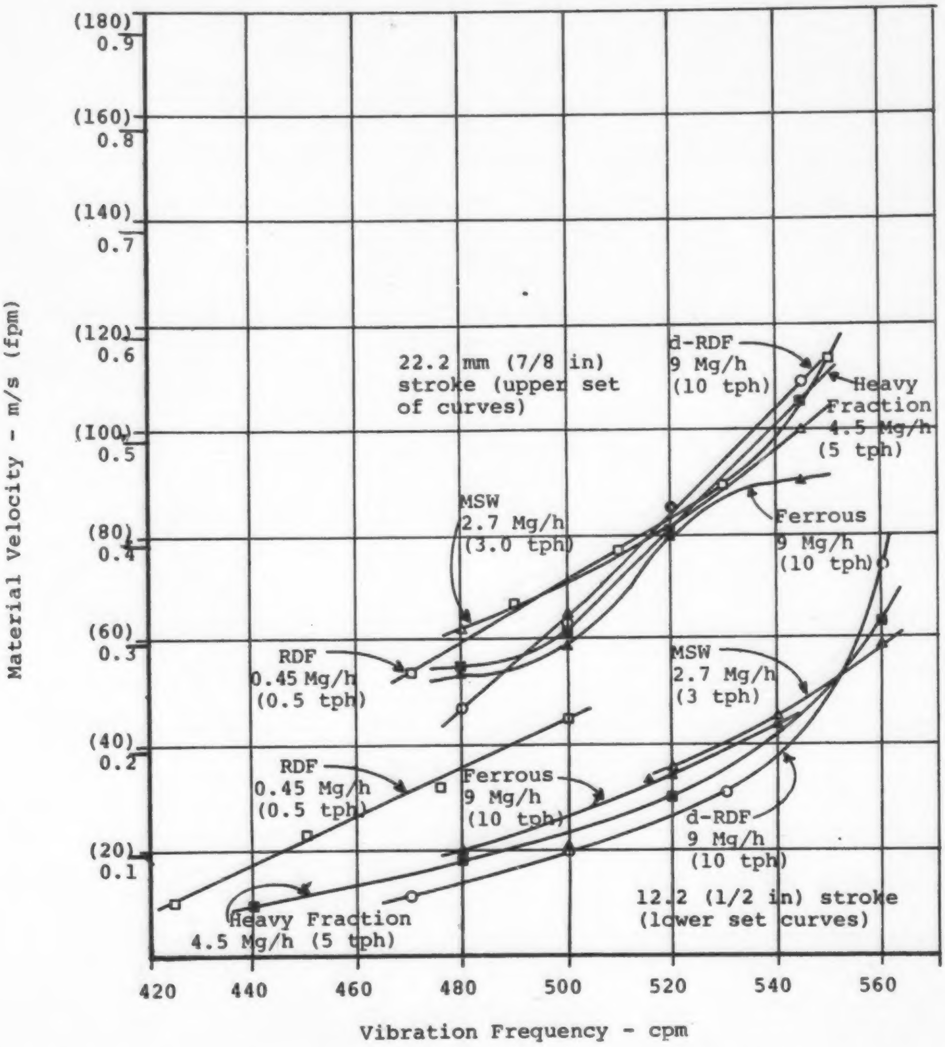

Figure 44. Material velocity versus vibration frequency on the test vibrating conveyor.

BEGIN LAST LINE OF TEXT
BOTTOM OF IMAGE AREA; OUTSIDE DIMENSION FOR TABLES AND ILLUSTRATIONS
3/8"

(1 and 6 in.). The conveying speed of the material was measured for each burden depth.

The results are given in Figure 45. For both the 12.7 and 22.2 mm strokes, a gradual decrease in conveying speed is observed for all material with increases in the material burden depth. Greater decreases in velocity were observed for the lighter materials (RDF and MSW) than more dense fractions (ferrous, heavy fraction). This suggests that lighter, lower density materials absorbed the energy imparted by the vibrating pan more than the denser materials.

Compaction of Material Along the Length of Pan

As the material vibrates on the conveyor, it has a tendency to gradually compact along the direction of travel. This test was conducted to determine the change in burden height and expected slope of material as it is being conveyed on the test vibrating conveyor, at a fixed capacity. Test results are presented in Table 14.

Table 14 indicates that there is a consistent tendency among the solid waste fractions to compact due to the vibration of the pan. The MSW and RDF fractions, relatively the most compressible, showed the highest degree of compaction.

Segregation of Material

Most processed waste fractions are composites of varying size and bulk density materials. For example, RDF which is predominately paper and plastics may have fines content (glass

TABLE 14. COMPARISON OF TENDENCY FOR COMPACTION

Solid Waste Fraction	Stroke (in.)	Frequency (rpm)	Slope	Percent lowering of burden height over 4.6 mm (15 ft) of conveyor length
RDF	7/8	520	-0.0049	39.1
d-RDF	7/8	520	-0.0028	31.0
MSW	7/8	520	-0.0052	44.1
HF	7/8	520	-0.0014	18.3

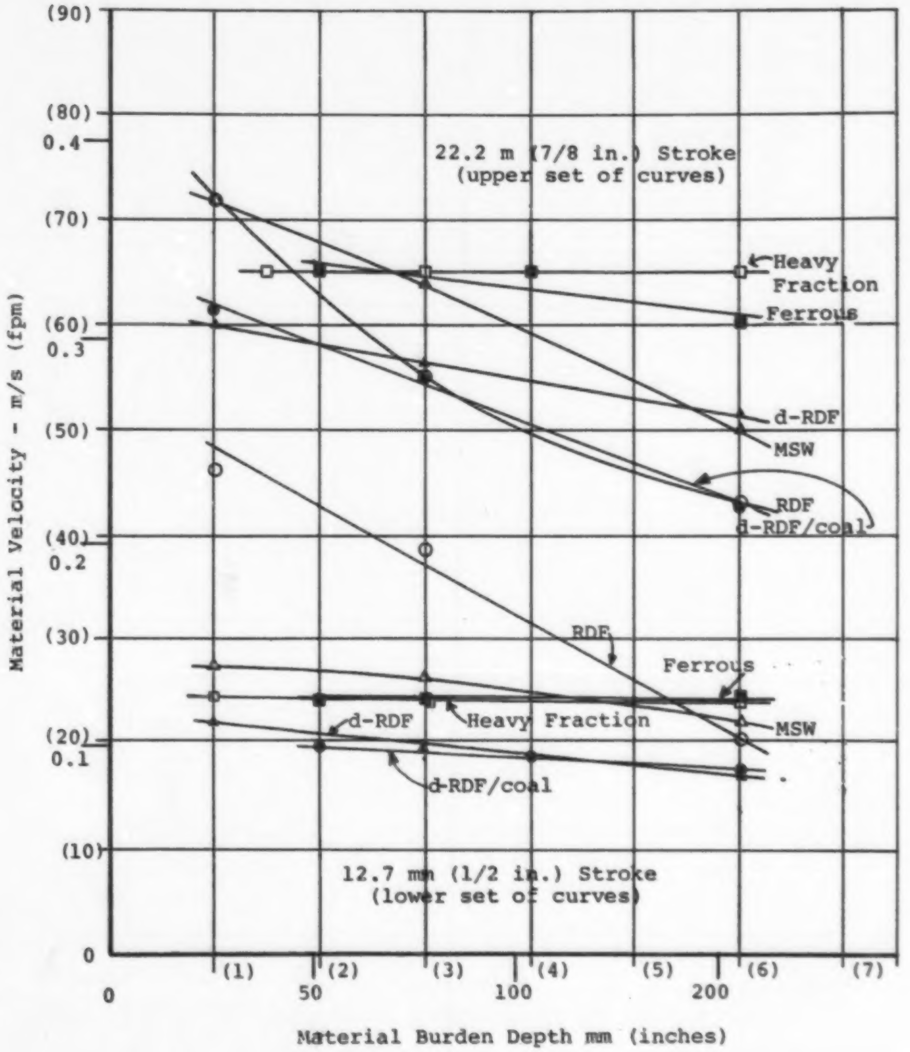

Figure 45. Material velocity versus material burden depth on the test vibrating conveyor.

BEGIN LAST LINE OF TEXT
3/8"
BOTTOM OF IMAGE AREA OUTSIDE DIMENSION FOR TABLES AND ILLUSTRATIONS

and sand) as high as 20%. A test was conducted to determine if various components of a solid waste fraction might segregate due to particle density or size differences.

While the material was being transported on the vibrating conveyor (510 cpm, 12.7 and 22.2 mm stroke), a technique was devised to split the stream at the discharge end into top and bottom layers of approximately equal depth. A particle size distribution was performed on the two layers in order to assess the extent of material segregation.

Particle size distribution results for the "top" and "bottom" layers of three materials are reported in Figures 46 and 47. It is interesting to note from the figures that the smaller particles in MSW and heavy fraction tend to concentrate in the bottom layer. These smaller particles were observed to be higher bulk density materials such as glass, stones and other inerts. On the other hand, the top and bottom layers of RDF are quite similar, the inerts and fines did not segregate to the same degree. This may be explained by the lower overall level of fines, the tendency of RDF to mat and interlock and for many of the fine particles stick or adhere on the paper flakes. For the MSW and heavy fraction, the segregation is slightly more accentuated at the higher (22.2 mm) stroke. The RDF shows little difference in segregation between the two strokes.

Dust Generation

As with the belt conveyor, high volume air samplers were used to measure the magnitude of dust generated for various equipment conditions and waste fractions. The test methods and calculations are given in Appendix A.9.

Fixing the frequency (at 510 cpm) and the material mass flow rate on the conveyor system, measurements were made of dust generation for different fractions and two stroke lengths. The dust sampler was placed approximately 1.6 m (5 ft) from the mid-point of the vibrating conveyor.

Table 15 provides the results and shows that the magnitude of dust generated at 22.2 mm (7/8 in.) stroke is higher for the RDF, MSW and coal/d-RDF blend than for the 13.7 mm (1/2 in.) stroke. The d-RDF/coal blend at 22.2 mm (7/8 in.) stroke exhibited exceptionally high dust levels relative to the other fractions most likely due to the presence of coal fines.

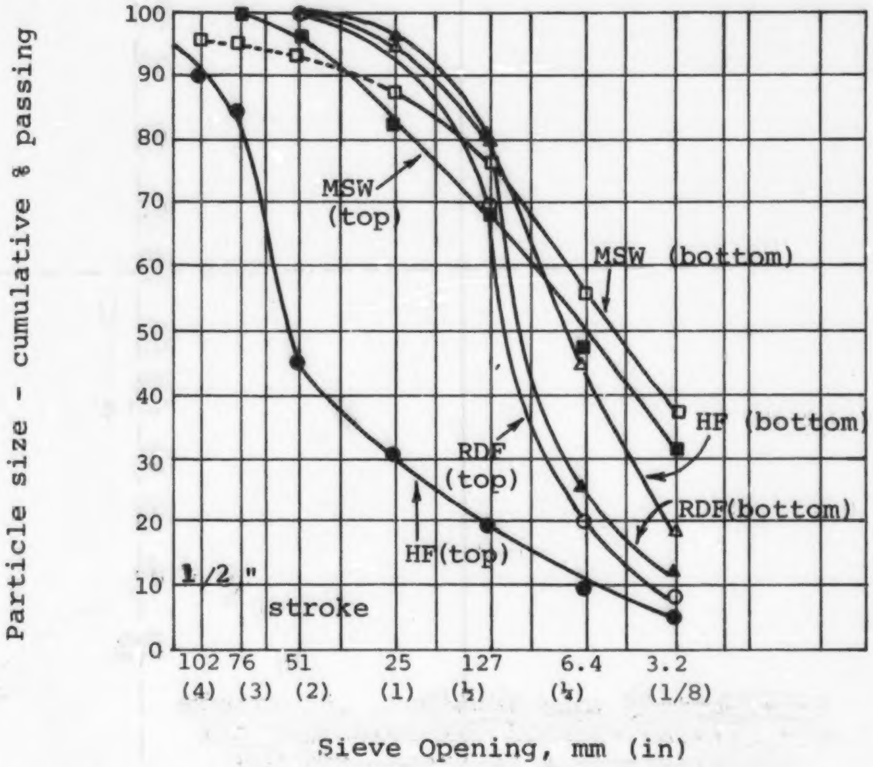

Figure 46. Particle size distribution and segregational effects between the conveyor - 13.7 mm (1/2") stroke.

BEGIN LAST LINE OF TEXT
BOTTOM OF IMAGE AREA; OUTSIDE DIMENSION FOR TABLES AND ILLUSTRATIONS
3/8"

EPA-287 (Cin.)
(4-76)

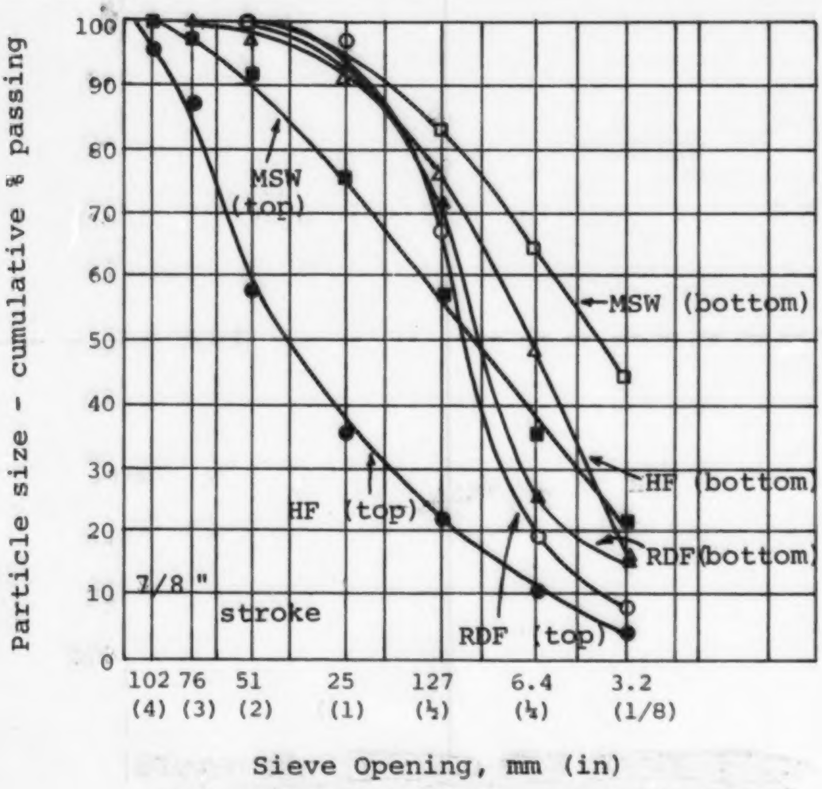

Figure 47. Particle size distribution and segregational effects between the conveyor - 22.2 mm (7/8") stroke.

BEGIN LAST LINE OF TEXT

BOTTOM OF IMAGE AREA; OUTSIDE DIMENSION FOR TABLES AND ILLUSTRATIONS

3/8"

PAGE NUMBER

EPA-287 (Cin.)
(4-76)

TABLE 15. RELATIONSHIP BETWEEN DUST GENERATION AND STROKE LENGTH

Solid Waste Fraction	Stroke Length mm (in)	Mass Flow Rate Mg/h (tph)	Dust Generated mg/scm of air
RDF	12.7 (1/2)	0.9 (1.0)	8.4
RDF	22.2 (7/8)	0.9 (1.0)	14.7
MSW	12.7 (1/2)	0.9 (1.0)	1.9
MSW	22.2 (7/8)	0.9 (1.0)	5.4
HF	12.7 (1/2)	4.5 (5.0)	0.9
HF	22.2 (7/8)	4.5 (5.0)	0.9
d-RDF	12.7 (1/2)	4.5 (5.0)	31.2
d-RDF	22.2 (7/8)	4.5 (5.0)	29.4
d-RDF/coal blend (1:1)*	12.7 (1/2)	8.2 (9.2)	18.1
d-RDF/coal blend (1:1)*	22.2 (7/8)	8.2 (9.2)	235.0

* Volumetric Basis

BEGIN FIRST LINE OF TEXT HERE
DROPPED HEAD; BEGIN SECTIONS HERE
CENTER OF PAGE
TOP OF IMAGE AREA
9-1/8"
6-1/2"
3/8"
BEGIN LAST LINE OF TEXT
BOTTOM OF IMAGE AREA; OUTSIDE DIMENSION FOR TABLES AND ILLUSTRATIONS
PAGE NUMBER
EPA Form 2350-4 (4-80)
[PREVIOUSLY CIN. EPA FORM 247]
☆ U.S. GOVERNMENT PRINTING OFFICE 1980-660-639
TYPING GUIDE SHEET

SECTION 5

APRON CONVEYORS

INTRODUCTION

Apron conveyors in resource recovery plants are most commonly used as receiving conveyors for unprocessed waste or at the discharge of size reduction equipment where loading or ballistic impact of material on the conveyor is of concern. An apron conveyor is made up of a series of hinged steel pans on a chain and roller assembly which ride on tracks underneath or outboard of the pans.

The equipment size and capacity required to model typical apron conveyor applications were considered beyond the scope of the original portion of this program and thus were not proposed. However testing of a small pan conveyor was initiated in a later phase of the project but only on a batch basis and only on feedstocks of d-RDF and a d-RDF/coal blend.

The apron conveyor utilized for the tests was a 0.76 m (30 in.) wide by 2.06 m (6.75 ft.) long apron conveyor with 152 mm (6 in.) wide pans, 102 mm (4 in.) sides and 51 mm (2 in.) cleats spaced every 406 mm (16 in.). The conveyor was equipped with an adjustable speed drive with a range of 0.05 - 0.23 m/s (10 - 45 fpm). The conveyor was configured to allow inclinations of 0° to 39°.

The apron conveyor evaluation involved measurement of the maximum angle of surcharge and tests to establish the maximum angle of inclination, maximum conveying capacity for various conveying speeds andinclinations.

TEST RESULTS

Maximum Angle of Surcharge

The maximum angle of surcharge (static) was obtained utilizing the same procedure used for the belt conveyors and outlined in Appendix A.4. The angle of surcharge is shown schematically in Figure 3. For the d-RDF the angle of surcharge was determined to be 40.5° and for the d-RDF/coal blend, the angle was 38.5°.

BEGIN FIRST LINE OF TEXT HERE
CENTER OF PAGE
TOP OF IMAGE AREA
DROPPED HEAD; BEGIN SECTIONS HERE
6-1/2"

As with the measurements on the belt conveyor, the angle of surcharge for the d-RDF is higher than for the d-RDF/coal blend, although in magnitude both materials have a lower angle than on the belt (Table 6).

Maximum Carrying Capacity vs. Conveyor Speed and Inclination

Maximum carrying capacity is the maximum mass flow rate that was obtained on the apron conveyor for a given speed and inclination. For the test, a 1 to 1.5 m (3 to 5 ft.) section of the conveyor was hand loaded to maximum static capacity. The conveyor was started and the discharge collected and weighed over a measured time period. Care was taken to avoid uneven material flows during starting and stopping. Multiple tests at single conditions showed good repeatability.

The results are presented in two formats for each material. Figures 48 and 50 show the results for the d-RDF and Figures 49 and 51 the results for the d-RDF/coal blend.

When carrying capacity is plotted vs. conveyor speed as in Figures 48 and 49, maximum carrying capacity is found to increase linearly with increasing velocity. This is to be expected since in the speed range evaluated (typical for apron conveyors carrying solid waste) the velocity is below the point at which the material would slip and bounce or be windblown off the belt. Also, since the conveying surface is rigid there is no bouncing effect as was seen as with the conveyor belt passing over idlers.

During the test it was observed that there was very little spillage off the sides. Most of the spillage that was observed occurred above 30° because of material falling back and off the low end of the conveyor.

When carrying capacity is plotted vs. inclination, (Figures 50 and 51) it can be seen that between 0° and 15°, inclination has little effect. (The reason for the anomaly at 0° for the top curve in Figure 51 and the middle curve in Figure 50 is not known.) However, from 15° to 39° carrying capacity drops sharply with increased inclination.

Maximum Angle of Inclination

The maximum angle of inclination for an apron conveyor was defined in this test as the maximum slope up which material can be conveyed for a given feed rate with the velocity fixed at 10 ft. per minute. For this test, the apron conveyor was fed by a vibrating feeder. Feed rates were 4 Mg/h (4.5 tph) for d-RDF and 5.9 Mg/h (6.5 tph) for the d-RDF/coal blend.

Although the cleats were removed, the hinge pin between each pan provided some resistance to back sliding. The criteria

BEGIN LAST LINE OF TEXT
BOTTOM OF IMAGE AREA OUTSIDE DIMENSION FOR TABLES AND ILLUSTRATIONS
3/8"

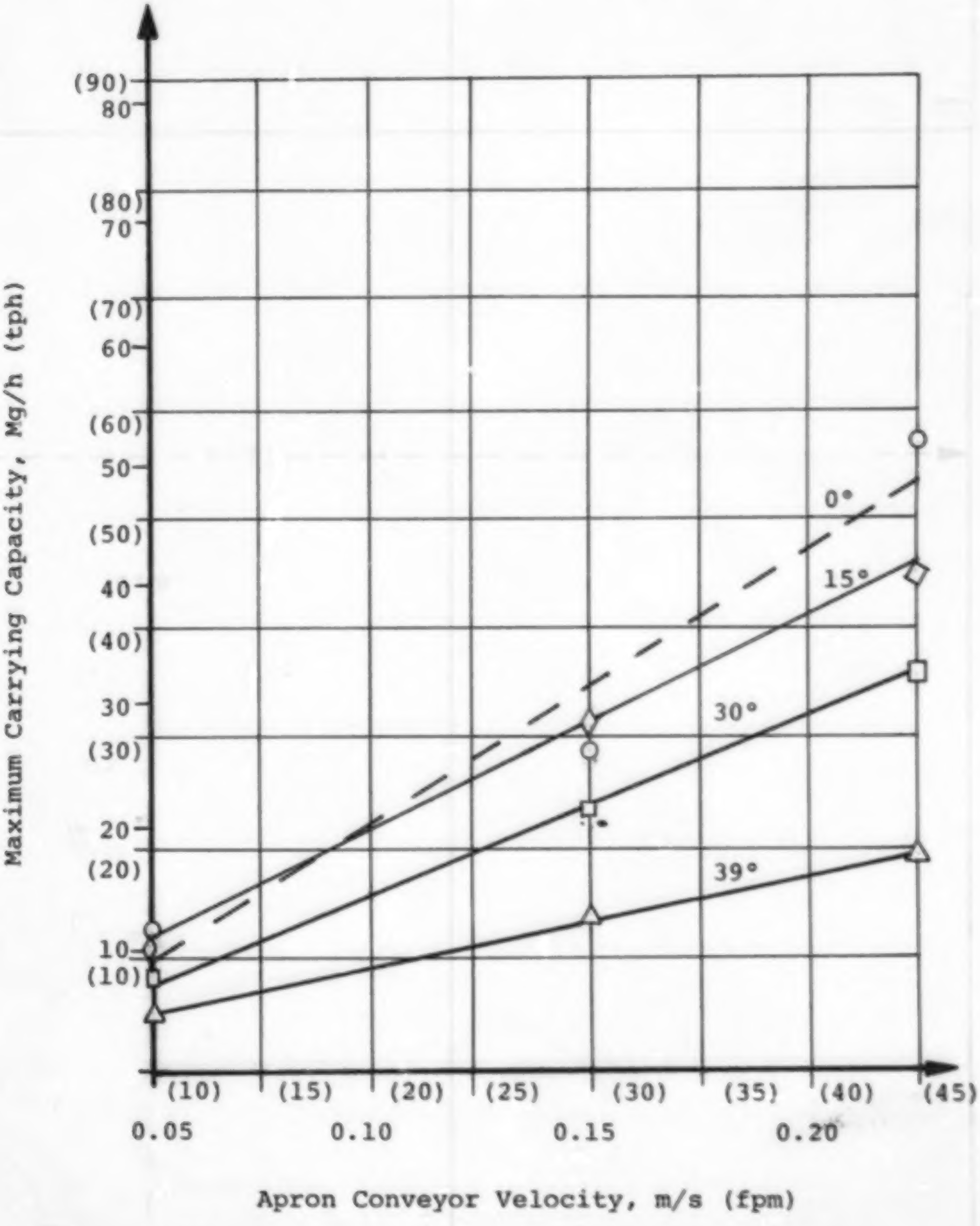

Figure 48. d-RDF maximum capacity vs. apron conveyor velocity.

BEGIN LAST LINE OF TEXT
BOTTOM OF IMAGE AREA OUTSIDE DIMENSION FOR TABLES AND ILLUSTRATIONS
3/8"
PAGE NUMBER

EPA-287 (Cin.)
(4-76)

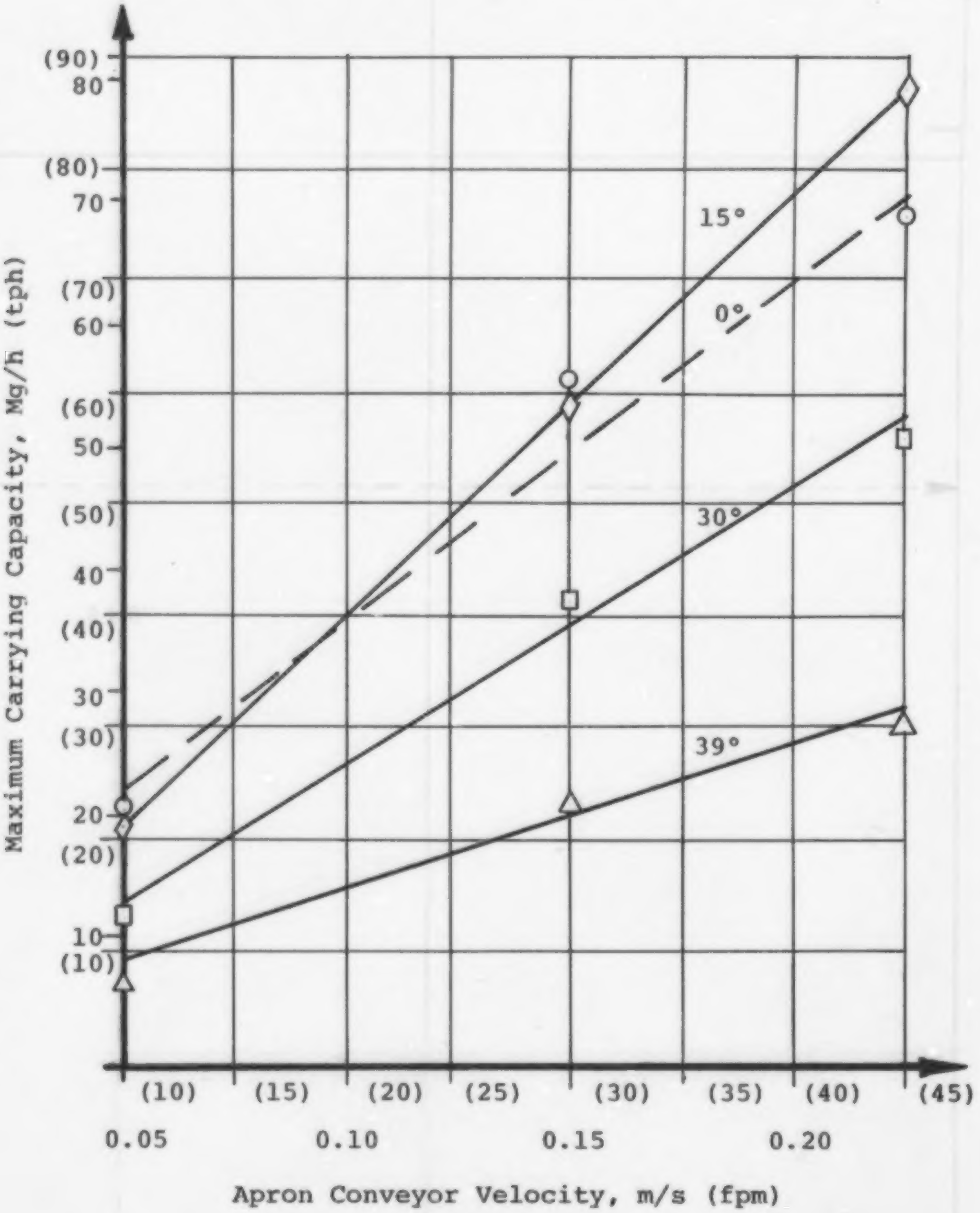

Figure 49. Coal/d-RDF maximum capacity vs. conveyor velocity.

BOTTOM OF IMAGE AREA; OUTSIDE DIMENSION FOR TABLES AND ILLUSTRATIONS
BEGIN LAST LINE OF TEXT
3/8"

PAGE NUMBER
EPA-287 (Cin.)
(4-76)

BEGIN FIRST LINE OF TEXT HERE
TYPING GUIDE SHEET
CENTER OF PAGE
TOP OF IMAGE AREA
DROPPED HEAD: BEGIN SECTION HERE

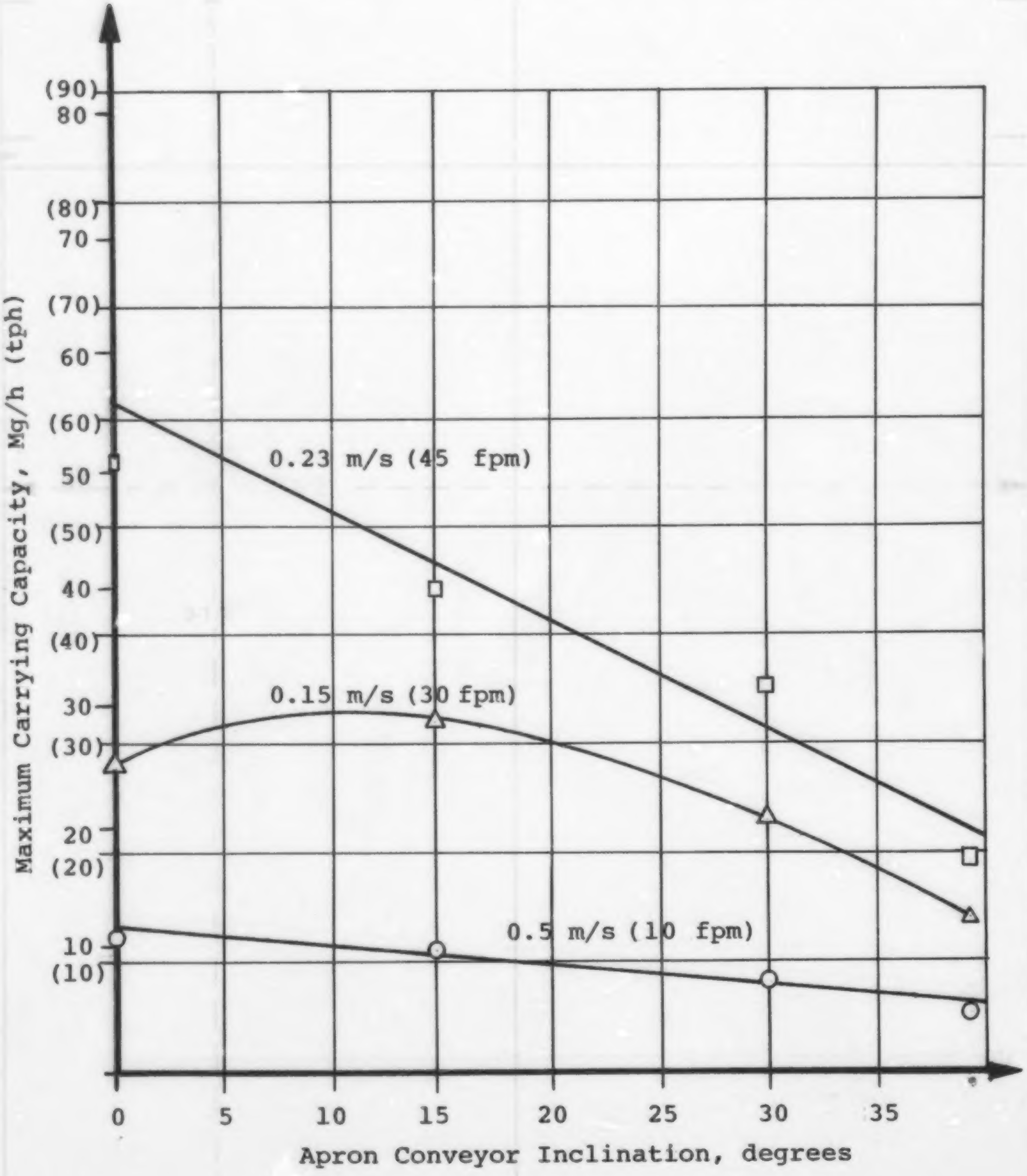

Figure 50. d-RDF maximum capacity vs. apron conveyor inclination.

BOTTOM OF IMAGE AREA; OUTSIDE DIMENSION FOR TABLES AND ILLUSTRATIONS
BEGIN LAST LINE OF TEXT
3/8"
PAGE NUMBER
EPA-287 (Cin.)
(4-76)

BEGIN FIRST LINE OF TEXT HERE
TYPING GUIDE SHEET
CENTER OF PAGE
TOP OF IMAGE AREA
DROPPED HEAD; BEGIN SECTION HERE

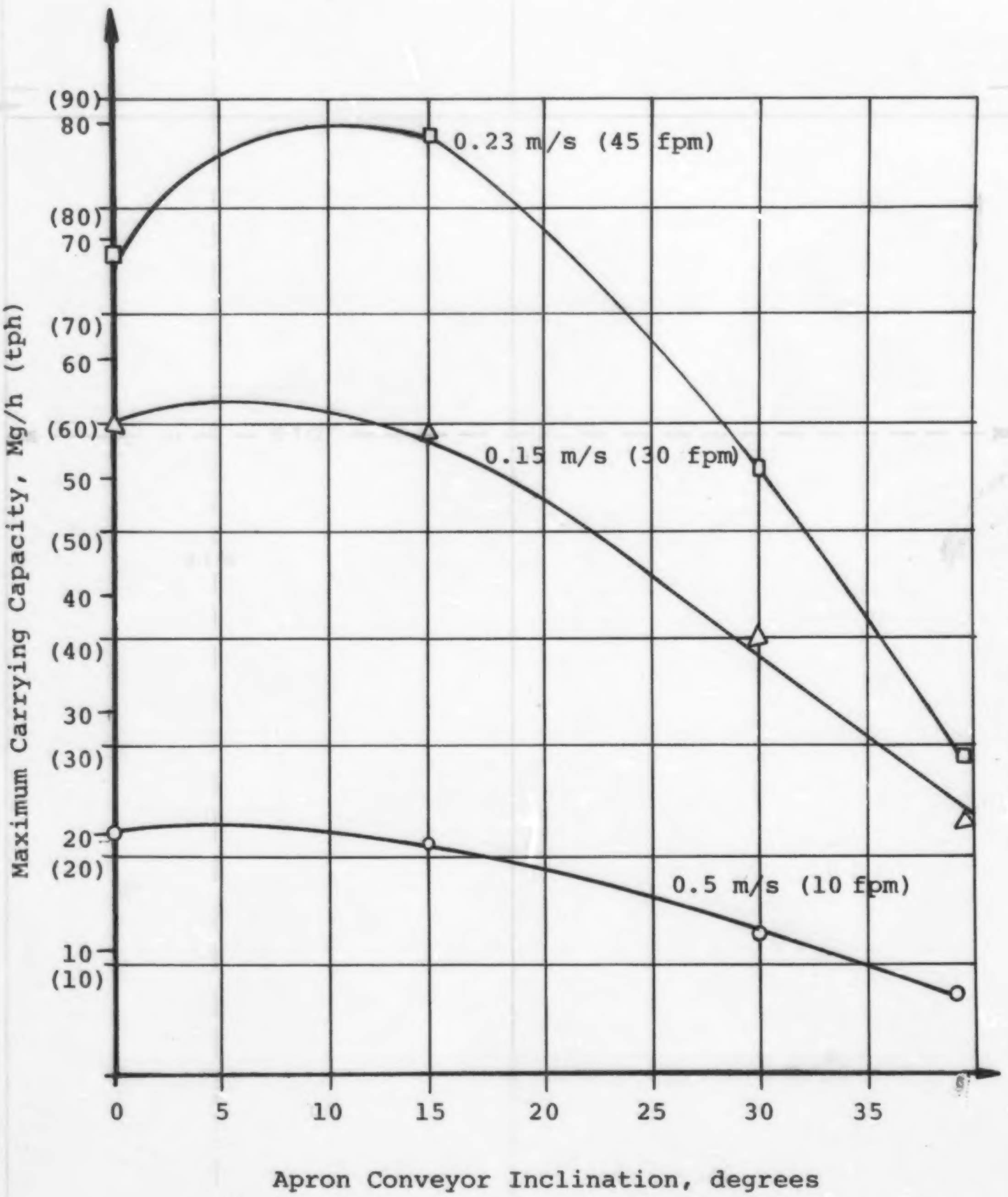

Figure 51. Coal/d-RDF maximum capacity vs. apron conveyor inclination.

BEGIN LAST LINE OF TEXT
BOTTOM OF IMAGE AREA; OUTSIDE DIMENSION FOR TABLES AND ILLUSTRATIONS
3/8"

PAGE NUMBER
EPA-287 (Cin.)
(4-76)

for assessing the maximum angle of inclination is the same as discussed in Appendix A.1, i.e., the inclination at which a pronounced (and intolerable) increase in the fallback and slippage of material occurs. For the d-RDF the angle was 35° (compared to 30° observed on the belt conveyor (see Table 3)) and for the d-RDF/coal blend the angle was 30° compared to 27° on the belt conveyor.

BEGIN FIRST LINE OF TEXT HERE
CENTER OF PAGE
TOP OF IMAGE AREA
DROPPED HEAD: BEGIN SECTIONS HERE
6-1/2"
9-1/8"
BEGIN LAST LINE OF TEXT
3/8"
PAGE NUMBER
BOTTOM OF IMAGE AREA; OUTSIDE DIMENSION FOR TABLES AND ILLUSTRATIONS
EPA Form 2350-4 (4-80)
(PREVIOUSLY CIN. EPA FORM 257)
☆ U.S. GOVERNMENT PRINTING OFFICE: 1981
TYPING GUIDE SHEET

REFERENCES

1. Belt Conveyors for Bulk Materials. Prepared by the Engineering Conference of the Conveyor Equipment Manufacturers Association (CEMA). 2nd. Edition. CBI Publishing Company, Boston, Massachusetts, 1979.

2. Classification and Definitions of Bulk Materials. No. 550. Prepared by the Bulk Materials Classification and Definitions Committee of the Conveyor Equipment Manufacturers Association (CEMA), Washington, D.C., 1970.

3. Johanson, J. R. Know Your Material - How to Predict and Use the Properties of Bulk Solids. Chemical Engineering, Deskbook Issue, October 30, 1978. pp. 9-17.

4. Renard, M. L., and Z. Kan. Design Considerations for Municipal Solid Waste Conveyors. In: Municipal Solid Waste: Resource Recovery. Proceedings of the Seventh Annual Research Symposium, Environmental Protection Agency, Philadelphia, Pennsylvania, March 1981. pp. 30-66.

5. OSHA Safety and Health Standards. No. 2206, Rev. January 1976. U.S. Department of Labor, Occupational Safety and Health Administration, Part 1910, Paragraph 1000, Table 2-3. pp. 504-510.

APPENDIX A

METHODS FOR TESTING WASTE SAMPLES

Method A.1. Angle of Maximum Inclination

Definition - Angle of Maximum Inclination - maximum angle a conveyor belt may be inclined and successfully convey material at a specified feedrate and a belt speed of 0.51 m/s (100 fpm). (The feedrate should be set at a level near but below the maximum capacity established for horizontal operation typically between 70 and 90 percent of this maximum.)

1.0 Apparatus

1.1 Recirculating set of conveyors - controlled throughput.

1.2 Test conveyor - variable speed and incline.

1.3 Angle finder or protractor.

1.4 Tachometer.

1.5 Weighing scale - platform-type with precision of ± 50 g (0.1 lb).

2.0 Sample Collection

2.1 Obtain a gross sample of waste in an amount necessary to maintain the desired feedrate on the test conveyor.

3.0 Test Procedure

3.1 Incline the test belt to an angle at which the material is known to be transported without difficulty.

3.2 Load the pre-weighed material onto the conveyor system and establish desired and constant feedrate.

3.3 Run the conveyor system for approximately 5 minutes.

3.4 Observe and note how material is transported. If the conveyor operates without significant material

BEGIN LAST LINE OF TEXT
BOTTOM OF IMAGE AREA; OUTSIDE DIMENSION FOR TABLES AND ILLUSTRATIONS
3/8"
PAGE NUMBER

fallback, slippage and resulting spillage, increase the angle of inclination by 1 degree.

3.5 Continue the procedure of increasing (or decreasing) the inclination by 1 degree running the system for 5-minute intervals until the angle (or often a range of 2-3 degrees) is reached where there is a pronounced (and intolerable) increase in fallback, slippage and spillage. This angle (or mean of range of angles) is considered the maximum angle of inclination.

4.0 Factors Affecting Results

4.1 Minimum belt sag tension.

4.2 Length of skirt boards.

4.3 Centrally loaded and uniform feed.

BEGIN FIRST LINE OF TEXT HERE
CENTER OF PAGE
TOP OF IMAGE AREA
DROPPED HEAD: BEGIN SECTIONS HERE
6-1/2"
9-1/8"
BEGIN LAST LINE OF TEXT
BOTTOM OF IMAGE AREA, OUTSIDE DIMENSION FOR TABLES AND ILLUSTRATIONS
3/8"
PAGE NUMBER
EPA Form 2350-4 (4-80)
(PREVIOUSLY CIN. EPA FORM 287)
☆ U.S. GOVERNMENT PRINTING OFFICE 1980-660-639
TYPING GUIDE SHEET

Method A.2 Angle of Repose

Definition - The angle of repose is the angle between horizontal and the sloping line from the top of pile to the base.

1.0 Apparatus

1.1 Angle finder or protractor.

1.2 Measuring tape, straight edge.

2.0 Sample Collection

2.1 Obtain a gross sample of approximately 23 kg (50 lbs) from the incoming solid waste fraction.

3.0 Test Procedure (See Figure A-1)

3.1 Cone and quarter the 23 kg (50 lbs) of material.

6-1/2"

3.2 Form a pile of material on a horizontal surface by carefully discharging the representative sample from a hand-held container. The container is held closely to the horizontal surface to start with and is gradually raised as the height of the pile is increased with about 50 mm (2 in) clearance. Final height of the pile to represent load height on belt conveyors at maximum capacity and static conditions. (Determined to be 203 mm (8 in) for tests reported here).

3.3 Measure and record the angle of repose at four equally spaced intervals.

3.4 Repeat steps 3.2 and 3.3 for a total of three piles.

4.0 Calculations

4.1 Calculate and report the average angle of repose for each pile.

$$\alpha_i = \frac{\alpha_1 + \alpha_2 + \alpha_3 + \alpha_4}{4}$$

BOTTOM OF IMAGE AREA; OUTSIDE DIMENSION FOR TABLES AND ILLUSTRATIONS
BEGIN LAST LINE OF TEXT
3/8"

PAGE NUMBER
EPA-287 (Cin.)
(4-76)

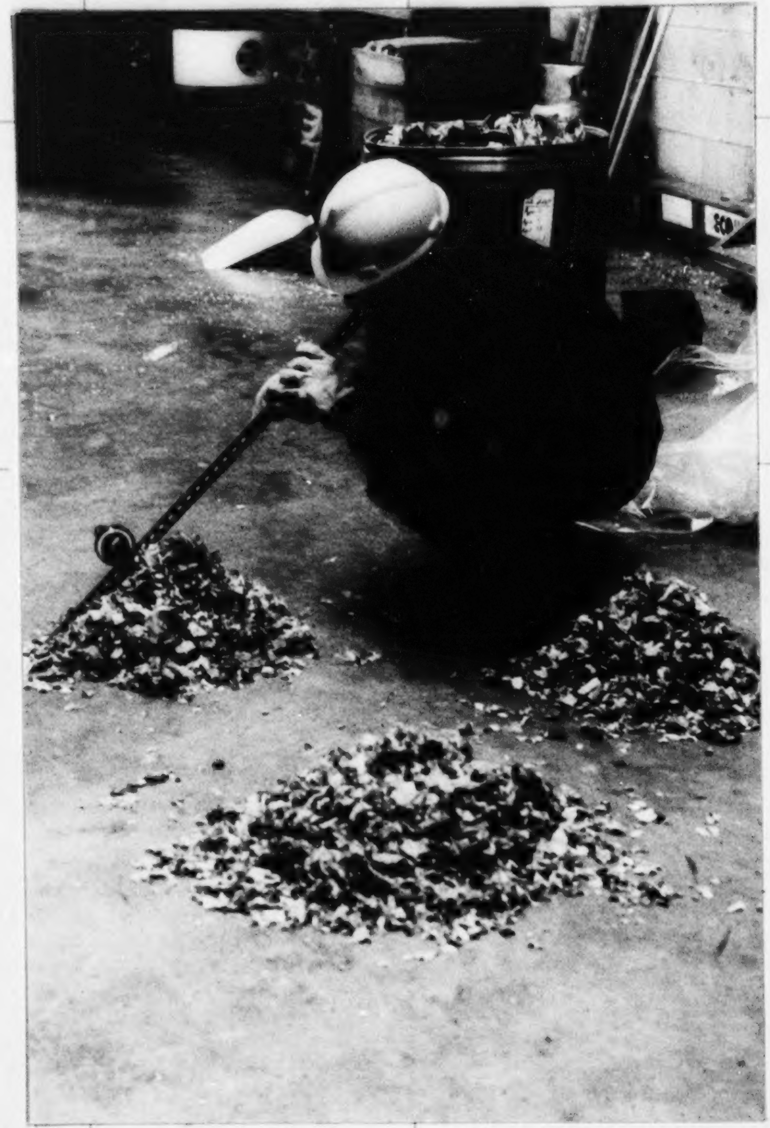

Figure A-1. Angle of repose measurement (Method A.2).

BEGIN LAST LINE OF TEXT
3/8"
BOTTOM OF IMAGE AREA: OUTSIDE DIMENSION FOR TABLES AND ILLUSTRATIONS

Method A.3 Angle of Slide

Definition - Angle of Slide - The angle at which materials on at rest on air inclined surface will begin to slide.

1.0 Apparatus

1.1 Mild steel plate 10 mm (.037 in.) thick having dimensions 1.2 m x 0.9 m (4 ft x 3 ft).

1.2 Rubber sheet (conveyor skirting) mounted on 13 mm (1/2 in.) plywood sheet having dimensions 0.9 m x 0.6 m (3 ft x 2 ft).

1.3 Angle finder or protractor.

2.0 Sample Collection

2.1 Obtain a sample of approximately 0.014 m^3 (0.5 ft^3) from the test material.

3.0 Test Procedure (See Figure A-2)

3.1 Rest one end of the steel plate on the floor with the other end slightly raised and supported on a wooden block. This arrangement facilitates easier lifting of the plate.

3.2 Place the sample on the plate to form a pile approximately 75 mm (3 in.) high.

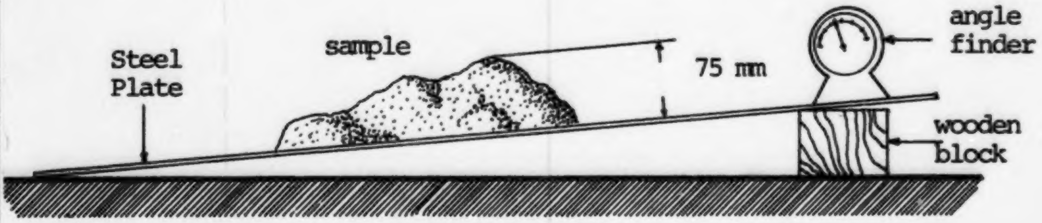

3.3 Slowly raise the plate and record the angle when the material just begins to slide.

3.4 Test three times and report mean angle of slide in degrees.

BEGIN LAST LINE OF TEXT
BOTTOM OF IMAGE AREA; OUTSIDE DIMENSION FOR TABLES AND ILLUSTRATIONS
3/8"

PAGE NUMBER
EPA-287 (Cin.)
(4-76)

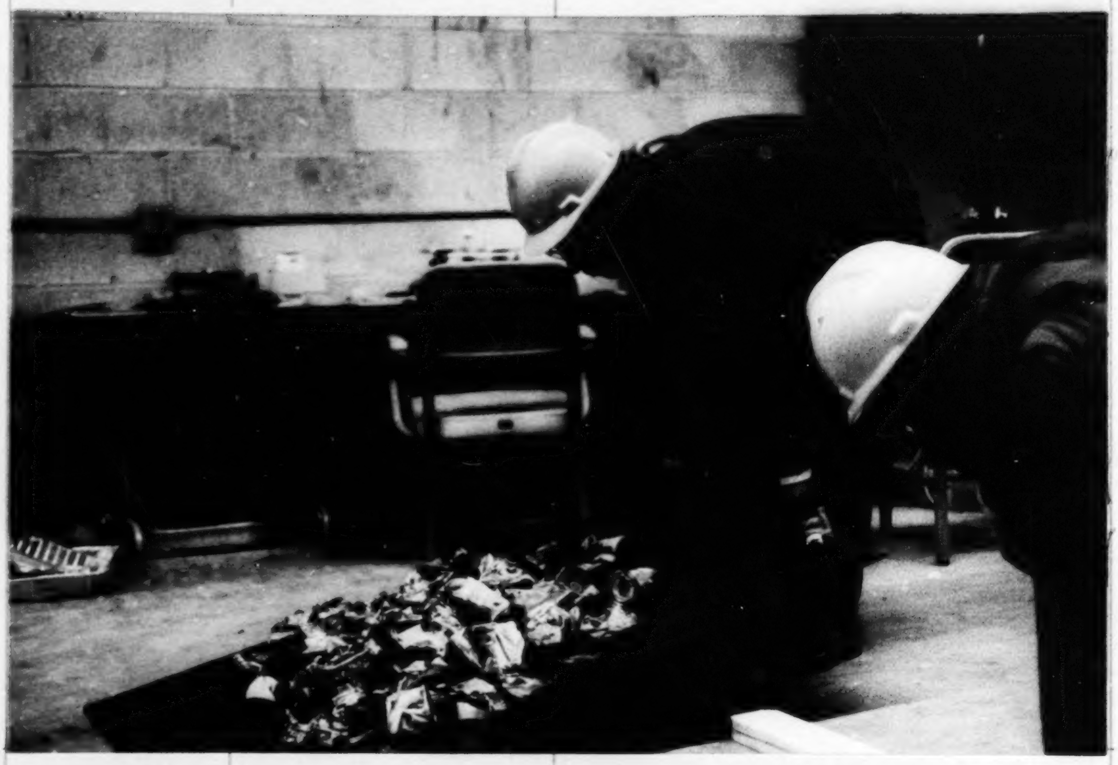

Figure A-2. Angle of slide measurement (Method A.3).

BEGIN LAST LINE OF TEXT
3/8"
BOTTOM OF IMAGE AREA; OUTSIDE DIMENSION FOR TABLES AND ILLUSTRATIONS

Method A.4 Test Procedures for Maximum Angle of Surcharge

Definition - Maximum Angle of Surcharge - The angle made between the slope of material on a fully loaded belt and the horizontal.

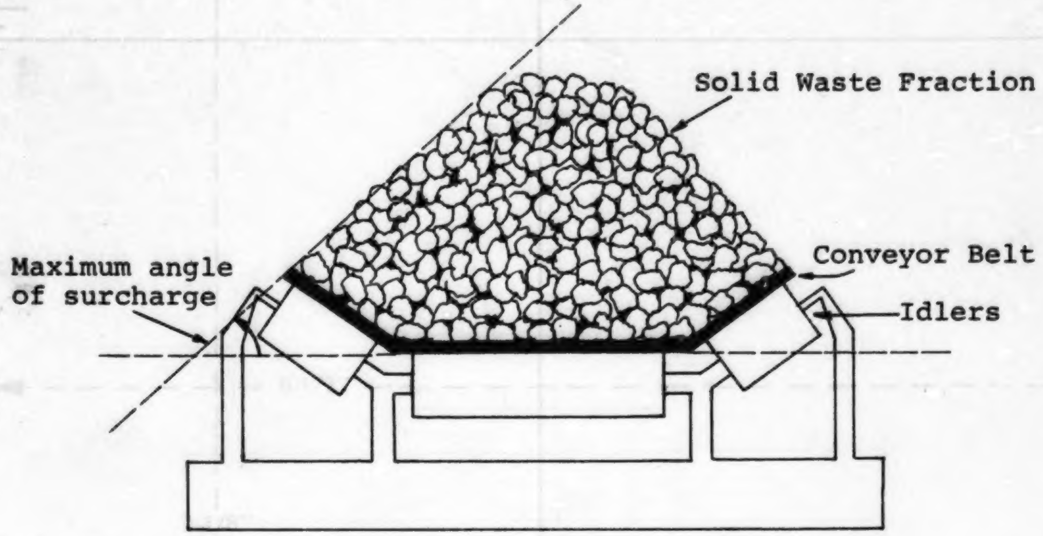

1.0 Apparatus

1.1 Conveyor belt.

1.2 Angle finder or protractor.

1.3 Straight edge.

2.0 Sample Collection

2.1 Obtain a representative sample of waste in an amount required to fully load a 1.5 m length of conveyor belt.

3.0 Test Procedure (see Figure A-3)

3.1 Using a shovel, load a 1.5 m (5 ft) length of the belt with material. The material should be dropped from a height of approximately 150 mm (6 in.) above the top of the pile. The belt is considered fully loaded when the material starts to slip or roll off the belt.

3.2 Place a straight edge against the slope of the pile. Measure and record the angle with an angle finder or protractor.

BEGIN LAST LINE OF TEXT
BOTTOM OF IMAGE AREA; OUTSIDE DIMENSION FOR TABLES AND ILLUSTRATIONS
3/8"

EPA-287 (Cin.)
(4-76)

3.3 Repeat step 3.2 three times (two along each side of the belt) for a total of four readings.

4.0 Calculations

4.1 Maximum angle of surcharge =

$$\frac{\text{Reading 1} + \text{Reading 2} + \text{Reading 3} + \text{Reading 4}}{4}$$

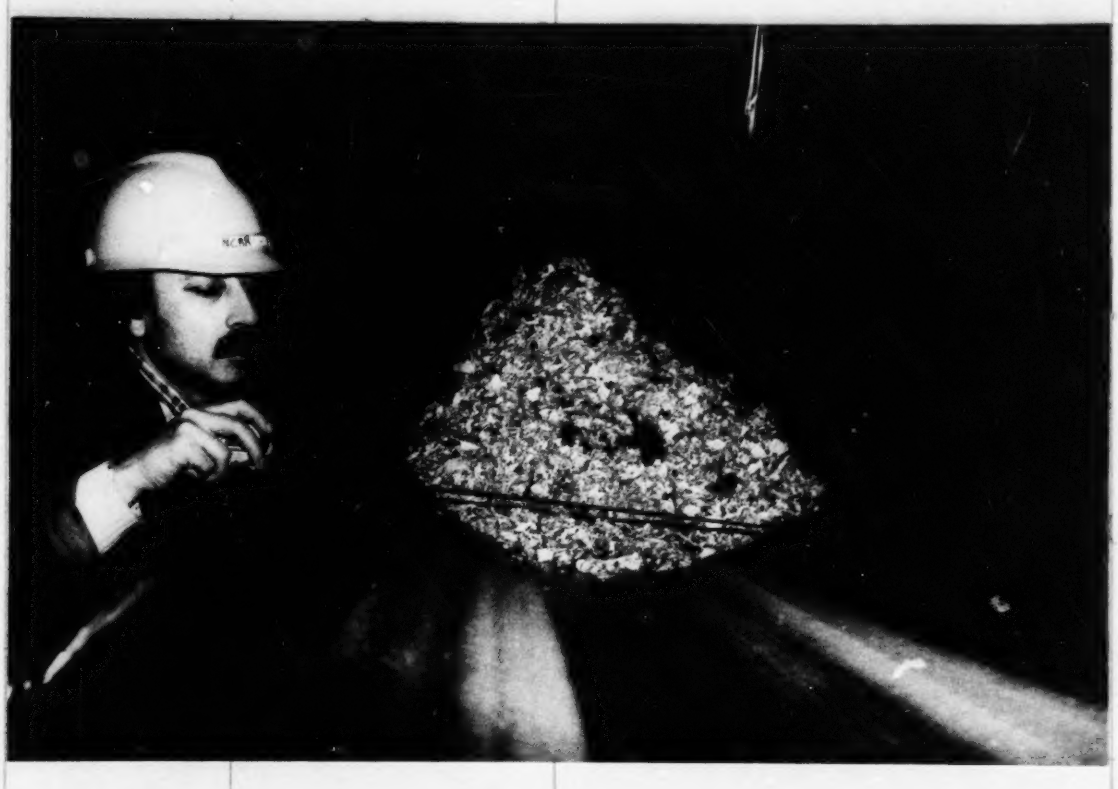

Figure A-3. Maximum angle at surcharge measurement (Method A·4)

Method A.5 Bulk Density ("Loose") by the Cone Method

Definition - The bulk density determination by the Cone Method provides data representative of "as conveyed" bulk density of materials transported on belt conveyors.

1.0 Apparatus

1.1 Weighing scale - platform-type with precision of 50 g (0.1 lb).

1.2 Angle finder or protractor.

1.3 Measuring tape, straight edge.

2.0 Sample Collection

2.1 Obtain a gross sample of approximately 23 kg (50 lbs) from the incoming solid waste fraction.

3.0 Test Procedure (See Figure A-4)

3.1 Cone and quarter the 23 kg (50 lbs) of incoming material. Retain one quarter for measurement of bulk density.

3.2 Form a pile of material on a horizontal surface by carefully discharging the representative sample from a hand-held container. The container is held closely to the horizontal surface to start with and is gradually raised as the height of the pile is increased with about 50 mm (2 in.) clearance. Final height of the pile to represent load height on belt conveyors at maximum capacity and static conditions. (Determined to be 203 mm (8 in.) for tests reported here).

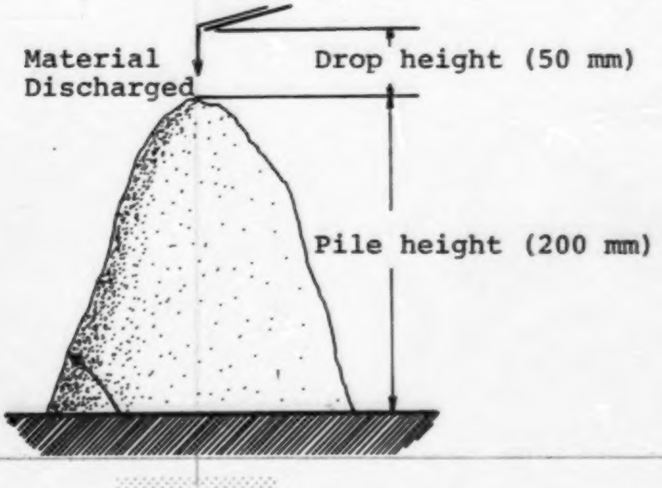

BEGIN LAST LINE OF TEXT
BOTTOM OF IMAGE AREA; OUTSIDE DIMENSION FOR TABLES AND ILLUSTRATIONS
3/8"
PAGE NUMBER

EPA-287 (Cin.)
(4-76)

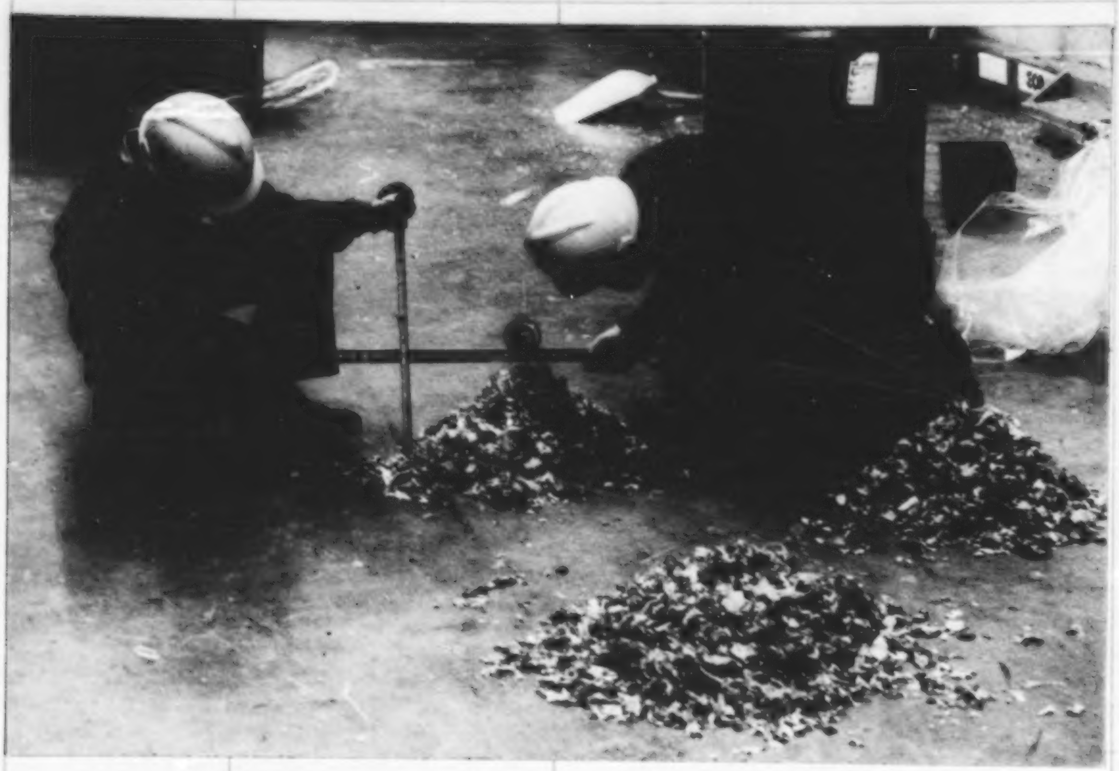

Figure A-4. Loose bulk density measurement (Method A.5).

BEGIN LAST LINE OF TEXT
3/8"
BOTTOM OF IMAGE AREA: OUTSIDE DIMENSION FOR TABLES AND ILLUSTRATIONS

3.3 Measure and record diameter of the base of the pile twice.

3.4 Measure and record height of the pile.

3.5 Weigh and record the weight of material in the pile.

3.6 Repeat steps 3.2-3.5 for a total of three piles.

4.0 Calculations

4.1 Calculate the average diameter of each pile ($D_{\dot{\wedge}}$).

4.2 Calculate the volume (V) of each pile.

$$V(ft^3) = (\tfrac{1}{3})\frac{\pi(D_{\dot{\wedge}})^2}{4}H$$

where: $D_{\dot{\wedge}}$ = average pile diameter

H = height of pile

4.3 Calculate the "as conveyed" bulk density of each pile.

$$B.D. = \frac{W}{V}$$

where: W = weight of pile

V = volume of pile

B.D. = bulk density

4.5 Report average of the three bulk densities.

BEGIN LAST LINE OF TEXT
BOTTOM OF IMAGE AREA; OUTSIDE DIMENSION FOR TABLES AND ILLUSTRATIONS
3/8"

EPA-287 (Cin.)
(4-76)

Method A.6 Bulk Density ("Vibrated") by the Container Method

Definition - The bulk density determination by the Container Method provides density representative of materials constrained and piled upon itself such as in a storage bin.

1.0 Apparatus

1.1 Bulk density sample box - wooden, 30.5 cm x 30.5 cm x 30.5 cm interior. Box is tared.

1.2 Scale - platform-type; precision, 50 g (0.1 lb).

2.0 Sample Collection

2.1 Obtain a sample of approximately 0.06 m^3 (2 ft^3) from the test material.

3.0 Test Procedure

3.1 Fill the container in three increments. After each increment, vibrate the box by lifting and dropping each of the four edges one time.

3.2 Carefully level the top, removing overflow. Weigh and record weight of box and contents. Empty material.

3.3 Repeat steps 3.1 and 3.2 three times, using the remainder of sample for a total of three determinations.

4.0 Calculations

4.1 Bulk density kg/m^3 (lb/ft^3) =

$$\frac{(W_1 - T) + (W_2 - T) + (W_3 - T)}{V}$$

where

W_{1-3} = Weight of sample and box in kg (lb)

T = Tare weight of box in kg (lb)

V = Volume of box in m^3 (ft^3)

BEGIN FIRST LINE OF TEXT HERE
CENTER OF PAGE
TOP OF IMAGE AREA
DROPPED HEAD; BEGIN SECTIONS HERE
BEGIN LAST LINE OF TEXT
3/8"
PAGE NUMBER
BOTTOM OF IMAGE AREA; OUTSIDE DIMENSION FOR TABLES AND ILLUSTRATIONS
EPA Form 2350-4 (4-80)
(PREVIOUSLY CIN. EPA FORM 257)
☆ U.S. GOVERNMENT PRINTING OFFICE: 1980-660-638
TYPING GUIDE SHEET

Method A.7 Moisture Content Determination

Definition - Moisture content is determined on an as-received and dry weight basis.

1.0 Apparatus

1.1 Drying pans 38 cm x 28 cm x 5 cm (15 in x 11 in x 2 in.) having approximatley 0.5 cu ft capacity.

1.2 Drying oven - Freas Model 845 - 0-200°C range, internal volume 0.13 m^3 (4.5 ft^3).

1.3 Balance - precision, 0.1 g.

2.0 Laboratory Sample Collection

2.1 Subdivide gross sample to laboratory samples of 0.014 m^3 (0.5 ft^3); place in sealed polyethylene bag.

2.2 Label sample as to sample number, date, time, contents, and collection point.

3.0 Test Procedure

3.1 Empty content of bag onto clean, tared drying pan, spreading evenly across pan. If required, split sample between two or more pans.

3.2 Weigh and record weight of pan and samples.

3.3 Dry in oven at approximately 105°C ± 1°C. Remove after 24 hours. Record weight of dry sample.

4.0 Calculations

4.1 Percent moisture, dry weight basis = $\frac{A - B}{B} \times 100$

4.2 Percent moisture, as-received basis = $\frac{A - B}{B} \times 100$

where:

A = weight of as-received sample

B = weight of dry sample

BEGIN LAST LINE OF TEXT
BOTTOM OF IMAGE AREA; OUTSIDE DIMENSION FOR TABLES AND ILLUSTRATIONS
3/8"

PAGE NUMBER
EPA-287 (Cin.)
(4-76)

Method A.8 Particle Size Distribution and Largest Lump Size Determination

Definition - This method provides the particle size distribution and largest lump size. (Ref.).

1.0 Apparatus

1.1 Gilson screen (Model TS-2) including the necessary screens and bottom tray (available: 102 mm (4 in.), 76 mm (3 in.), 51 mm (2 in.), 25 mm (1/2 in.) and 6 mm (1/4 in.)).

1.2 Drying oven with capability of maintaining 104°C ±1°.

1.3 Weighing scale with precision of ±1.0 gram.

1.4 Weighing pans.

1.5 Ruler or tape measure.

2.0 Sample Collection

2.1 Subdivide the gross sample to obtain laboratory samples of approximately 0.014 m^3 (0.5 $ft.^3$).

3.0 Sample Preparation

3.1 Place trays containing sample from 2.1 in a drying oven. Dry for 24 hours at 104 ± 1°C. (Ref. Test Method A.7).

4.0 Test Procedure

4.1 Place and clamp appropriate screens onto the Gilson screener. Choice of screen sizes to be used will vary depending on the solid waste fraction.

4.2 Spread dried sample on top screen being careful not to push material through the screen openings. Do not overload the machine. Maximum starting load is approximately 0.014 m^3 (0.5 ft^3). If larger sample is obtained, then batch sieving would be required.

4.3 Screen the material for exactly 10 minutes.

4.4 Observe all but the top screen for blinding or plugging after 1 minute. Blinding is indicated if more than 25 percent of the sample is on any one screen. In case of blinding of a screen, either reject test and re-run the sample with smaller starting load (eg., 0.07 m^3) (0.25 ft^3); or, if available, insert a screen of the next larger size above the blinded screen.

4.5 At end of 10 minutes, remove material from each screen, place their individual contents in tared pans and weigh.

4.6 Weigh and record sample weight of each pan.

4.7 From the fraction retained on the largest screen remove the particle(s) with the largest cumulative dimensions. Measure and record the maximum dimension(s)(largest lump size) and weight (largest lump weight). If necessary, repeat test with the remaining dried sample from 4.2 and/or 4.4.

5.0 Calculations

5.1 Calculate the total weight of material retained on each screen (including the bottom tray).

5.2 Calculate the weight percentage of material retained on each screen.

5.3 Calculate the cumulative weight and percentages of material retained on each screen.

6.0 Result

6.1 The particle size distribution is reported on a moisture-free basis.

6.2 The largest lump size and weight.

6-1/2"
BEGIN LAST LINE OF TEXT
BOTTOM OF IMAGE AREA; OUTSIDE DIMENSION FOR TABLES AND ILLUSTRATIONS
3/8"

PAGE NUMBER
EPA-287 (Cin.)
(4-76)

Method A.9 Dust Concentration Determination

Definition - This test provides measurement of the mass concentration of total suspended particulates per cubic meter of air.

1.0 Apparatus

1.1 Air Sampler - Sierra Instruments Model 305-2000H recording high volume air sampler.

1.2 Filter Media - 203 mm x 252 mm (8 in. x 10 in.) glass fiber.

1.3 Recorder Charts - 102 mm (4 in.) dia.; 4.7 - 31 l/s (10 to 65 CFM) range; 24-hour time scale.

1.4 Balance - precision ± 0.001 g.

1.5 Barometer.

1.6 Thermometer.

1.7 Orifice calibrator and water manometer.

2.0 Test Procedure

2.1 Air Sampler Calibration - Calibrate the air sampler using a special orifice calibrator and a water manometer. For detailed calibration instructions, refer to Sierra Instruments instruction manual series 305.

2.2 Sampler Location - Place the air sampler on a stable platform and away from moving equipment to avoid formation of wind eddies around the sampler.

2.3 Weigh the 203 mm x 252 mm (8 in. x 10 in.) filter. Place and align the filter (rough side up) on the air sampler screen and tighten the hold-down frame clamps, to form an air-tight seal on the outer edges of the filter.

2.4 Set-up Pressure Transducer Flow Recorder - Slip recorder chart under the pan arm and push it flat against dial plate.

2.5 Activate the motor/blower and the flow recorder.

2.6 Record the initial and the final times of the sampling period.

2.7 After the sampling period, remove the filter from the frame, and weigh it.

2.8 Remove the flow recorder chart.

2.9 Record the ambient temperature and the atmospheric pressure.

3.0 Calculations

3.1 Calculate the weight of total suspended particulates (TSP) collected on the filter.

$W_P = W_F - W_I$

W_P = total weight of TSP, (mg)

W_F = final weight of filter and TSP, (mg)

W_I = initial weight of filter, (mg)

3.2 Obtain the sampling flow rate from the recorder chart, Q_R (cfm). If the recorder chart does not show a constant flow rate over the sampling period graphical intigration may be necessary to obtain accurate sampling flow rate.

3.3 Using the Calibration curve (see 2.1) read off the actual sampling flow rate, Q indicated (cfm).

3.4 Calculate sampling flow rate at standard conditions (25^{o}C, 1 atm.):

Q_s = (Pa/Ps) x (Ts/Ta) x Q ind.

Q_s = (Pa/Ta) x 3.156 x Q ind.

where:

Q_s = flow rate in SCFM

$Q_{ind.}$ = flow rate obtained from calibration curve

Pa = Barometric pressure, (in. Mg).

Ps = Standard barometric pressure, (29.92 in. Mg)

Ta = Ambient temperature, degrees Kelvin (^{o}K)

6-1/2"
BOTTOM OF IMAGE AREA; OUTSIDE DIMENSION FOR TABLES AND ILLUSTRATIONS
BEGIN LAST LINE OF TEXT
3/8"

PAGE NUMBER
EPA-287 (Cin.)
(4-76)

T_s = Standard temperature, 25°C = 298°K

°K = Degrees Centrigrade (°C) + 273

3.5 Calculate the mass concentration of TSP:

$C = (W_p/Q_s) \times (1/T_i) \times (SCFM/0.0283\ SCMM)$

where: T_i = Sampling time interval, (min)

C = Mass concentration of TST, (mg/SCM)

3.6 Example of a sample calculation:

Test Conditions:
(1) Sample: Heavy Fraction
(2) Belt Velocity = 200 fpm
(3) Mass flow rate = 15.0 tph
(4) Belt inclination = 14°
(5) Sampler location - 5' perpendicular off mid-print of test belt

6-1/2"

W_F = 3602.3 mg

W_I = 3540.0 mg

9-1/8"

W_P = 62.3 mg

Q_R = 66.0 cfm

Q_{ind} = 68.0 cfm

$Q_S = (29.88/287) \times 3.156 \times 68$

Q_S = 69.25 SCFM

$C = (62.3\ mg/69.26\ SCFM) \times (1/15\ min) \times (SCFM/0.0283\ SCMM)$

C = 2.1 mg/SCM

BEGIN LAST LINE OF TEXT
BOTTOM OF IMAGE AREA; OUTSIDE DIMENSION FOR TABLES AND ILLUSTRATIONS
3/8"

APPENDIX B

EFFECT ON SPILLAGE ON PROPOSED MEASUREMENT

This short appendix examines the effect of the mass spilled during a test on the conveyor circulating loop on the measured spillage rate itself.

A. Spillage Rate over One Cycle.

Figure B-1 schematizes the physical situation studied.

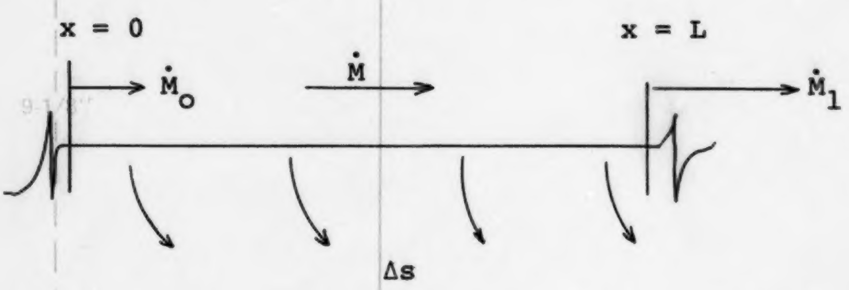

Figure B-1. Spillage, inlet and exit mass flow rates.

On a horizontal or inclined section of belt, of length, L, a "theoretically constant" mass flow rate $\dot{M}_o$ is maintained at the inlet section, x = 0. In actuality, as explained in the body of the text, a given mass M is distributed on the loop. If the time for a cycle around the loop is T_c, $M \simeq M/T_c$.

Let the incoming mass flow rate be $\dot{M}_o$. The measured spillage rate, per unit length of belt, is

$$\dot{s} = \lim_{\Delta t \to 0} \frac{\Delta s}{\Delta t}$$

in which Δs is the amount of material spilled, over a unit length of belt and time Δt.

By definition, $\dot{s}_o = k_s \dot{M}_o$, where $k_s \ll 1$ and is taken to be of order 2 of smallness (10^{-2}, say).

Now, $\dot{M}_1 = \dot{M}_o - \dot{s} \simeq \dot{M}$ to 0 (k_s); $\dot{s}_o = \dot{s}_1 = \dot{s}$ to 0 (k_s). Thus if $k_s = 10^{-2}$, the spillage rate can be measured anywhere along $0 \leq x \leq L$ with an accuracy on the order of 10^{-4}.

B. Measurements Over Several Cycles, No Mass Replacement

Let T_c be the time interval (period) between two successive passages of a particle at x = 0. If the spillage is limited to the section of length L,

$$(\dot{M}_1)_{j = 1} = (\dot{M}_o)_{j = 2} = (1 - k_s)\,\dot{M}_o$$

cycle index

$$(\dot{M}_1)_{j} = (\dot{M}_o)_{j + 1} = (1 - k_s)^j\,\dot{M}_o = [1 - j\,k_s + \frac{j(j - 1)}{2!}\,k_s^2 \ldots]\,\dot{M}_o.$$

The experiment duration is defined by $T_e \equiv j_{max}\,T_c$. It is required that

$$j_{max}\,k_s^2 \ll k_s$$

$$j_{max} \ll \frac{1}{k_s},\text{ or } 10^{-1}\,k_s^{-1}\text{ (say)}$$

Thus if $k_s = 0.01$, $j_{max} = 10$ or $T_e = 10\,T_c$. In the Upper Marlboro test system (see Figure 2), the times spent on the remaining elements of the circuit are: $T_{VIBR.\,CONV.} = 7.7$ sec, $T_{INCL.\,CONV.} = 9.5$ sec, $T_{OTHERS} = 15$ sec for a fixed total of 32.2 sec. If V_B is the belt speed, in m/s,

$$T_c = 32.2 + \frac{7.63}{V_B}\text{ (seconds)}$$

The maximum duration of the test, T_e, or $j_{max}\,T_c$ is represented in Fig. B-2 vs. the belt speed V_B, for $k_s = 0.005$ ($j_{max} = 0.01$ ($j_{max} = 10$). It is seen that at the "target level" of approximately 0.2%, the test duration can be in the range 15 to 30 min without appreciable error due to the material spilled and not replaced on the belt.

BEGIN FIRST LINE OF TEXT HERE
CENTER OF PAGE
TOP OF IMAGE AREA
DROPPED HEAD; BEGIN SECTIONS HERE
BEGIN LAST LINE OF TEXT
3/8"
PAGE NUMBER
BOTTOM OF IMAGE AREA, OUTSIDE DIMENSION FOR TABLES AND ILLUSTRATIONS
EPA Form 2350-4 (4-80)
(PREVIOUSLY CIN. EPA FORM 287)
☆ U.S. GOVERNMENT PRINTING OFFICE 1980-660-539
TYPING GUIDE SHEET

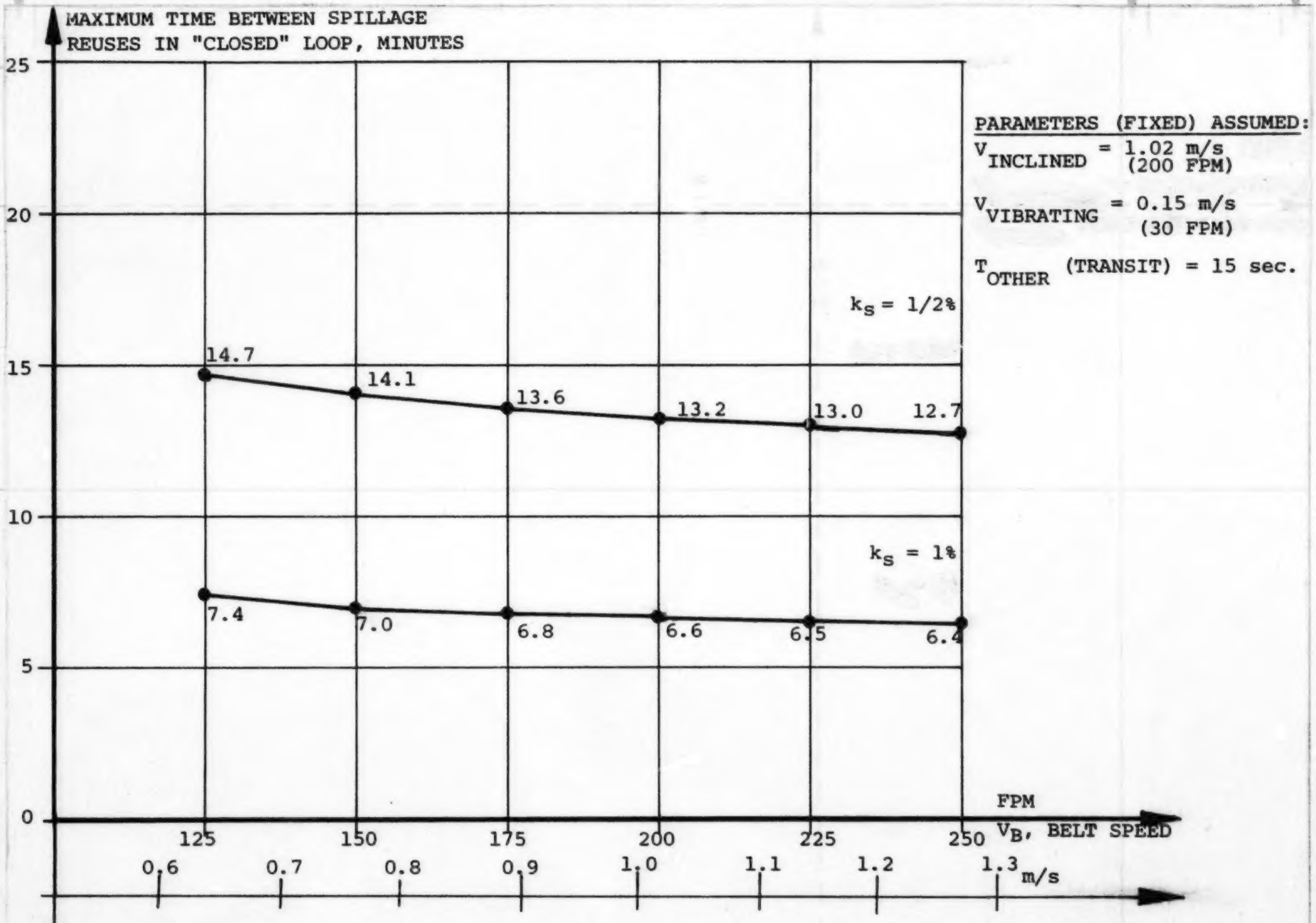

Figure B-2. Maximum time between spillage reuses vs. k_s and speed of belt.